UNIVERSITÀ
DEGLI STUDI
DI PADOVA

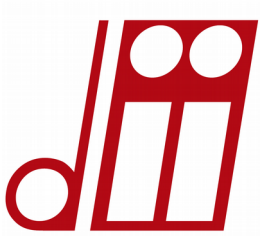

Dipartimento di Ingegneria Industriale

Corso di Laurea Magistrale in Ingegneria dell'energia Elettrica

TESI DI LAUREA MAGISTRALE IN

INGEGNERIA DELL'ENERGIA ELETTRICA

MODEL-FREE PREDICTIVE CONTROL FOR RELUCTANCE SYNCHRONOUS MOTOR DRIVES

RELATORE: Ch.mo Prof. Silverio Bolognani

CORRELATORE: Ing. Davide Da Rù

LAUREANDO: Paolo Gherardo Carlet

ANNO ACCADEMICO 2016/2017

UNIVERSITÀ DEGLI STUDI DI PADOVA

Facoltà di Ingegneria

Dipartimento di Ingegneria Industriale DII

Corso di Laurea magistrale in Ingegneria dell'Energia Elettrica

Model-Free Predictive Control for Reluctance Synchronous Motor Drives

Relatore: Ch.mo Prof. Silverio Bolognani

Correlatore: Ing. Davide Da Rù

Laureando: Paolo Gherardo Carlet Matricola n° 1128895

Anno Accademico 2016/2017

Index

1 Introduction

Model Predictive control techniques are successfully used in three-phase two levels inverters for the current control of ac machines. In particular, the Model Based Predictive control has been successfully applied in the control of a three-phase balanced load connected to the inverter.
This method is based on a simplified discrete model of the electric machine by which it is possible to estimate the future current variations induced by the voltages imposed by the inverter, exploiting both direct measures on the motor and estimated parameters. As a consequence of the simplification of the actual system, the accuracy of the current predictions is affected by many errors introduced by a not perfect model fitting. In addition, this intrinsic error can be further increased in peculiar operative conditions, for example in presence of iron-saturation in the motor magnetic lamination.
Several solutions are proposed in literature to overcome this problem: one of them consists into overcoming the model-based approach for the estimation of the current predictions and the adoption of a Model Free (MF) approach.
This second method is based on the possibility of approximating the eight future current variations generated by each voltage vector imposed by the inverter with the eight more recent measures. A MF predictive current control scheme as the one presented has already been applied for Interior Permanent-Magnet (IPM) Synchronous drives [1].
Since the hypothesis on which is based the MF estimation of the current variations is valid only in a short time window, the Model Free schemes suffer the phenomena of the “stagnation” of the voltage vectors. This phenomena consists in the non application of one voltage vector for a quite long time. One of the first goal of this thesis is the comprehension of the effects of the stagnation on the control stability and performances in the context of a MF predictive current control for a Synchronous Reluctance motor drive. In this different context, in fact, it results difficult to guarantee the stability of the MF scheme and so it is wondered to understand if the instability and the stagnation are related together or if there are other differences between the MF and the MB approaches that justifies the instability observed.
The same authors of the paper [1] have proposed also an improved MF scheme, supported by an anti-stagnation algorithm, able to effectively control a Synchronous Reluctance machine without any stability problem[2]. In particular, the anti-stagnation action consists in a forced application of the unused voltages after a defined time interval. This solution appears suitable for the motor under consideration and so it is interesting to identify which parameters influence more strongly the performances of this method. Since the anti-stagnation action is superimposed to the machine current control, it is determinant to analyze how the two processes interact each other and which weight should be given to each process.
Both the two MF schemes presented are “fully” model-free: it is supposed that the system to control is completely unknown. With a fully MF approach the system is considered as a black-box whose reactions to the input inverter voltages are the output current variations measured in the past.
In case of a Synchronous Reluctance motor drive, the system considered is not a black-box but it is well known. Abandoning the fully MF solutions, it is possible to build alternative MF schemes which exploit partially the knowledge of the controlled system.
These schemes can be still considered model-free since the evaluation of the current predictions does not require the knowledge of the motor’s parameters. In particular, the parameter that should not be used are the resistive and inductive quantities involved in the d – q expressions of the machine equations exploited for the model-based predictions. If this condition is verified, it is possible to decouple the performances of the control from the specific operative condition.
In this category of Model Free schemes it is studied a novel MF method in which the update of the current variations related to the unused voltages is obtained without any forced action but it is a consequence of the normal operation of the motor. This solution is characterized by the

implementation of a reconstructive technique that permits to compute four current variations every switching interval, starting from the measure of other three. The reconstruction is possible only if all the relations between the inverter voltages are known: for this reason the scheme can not be considered a fully model-free one.
In the thesis it is discussed the theoretical hypothesis on which the reconstruction is based and which triplets of voltages can be used. After the theoretical analysis, this second MF solution is implemented for the control of a Synchronous Reluctance motor: this passage would permit to highlight if there are significant differences between the expected and the actual behavior of the control scheme.
Since this scheme needs only three updated current variations for the reconstruction, the possibility that the stagnation occurs could be significantly decreased. With this further improvement of the MF scheme it is wondered to avoid the introduction of a forced anti-stagnation algorithm. A detailed analysis of this control technique would permit to understand if the stagnation problem is completely overcome.

2 Model Based Predictive current control (MBPCC)

2.1 The motor model

The Model-Based Predictive Current Control (MBPCC) is a control technique based on the capability of predict the reaction of a motor to the application of a certain voltage vector.
In order to predict the behavior of the electrical machine, it is required a mathematical model of the machine itself. As a consequence, the precision of the predicted quantities is highly influenced by the accurate knowledge of the motor's parameters that are contained in the model, like the resistance or the inductance of the stator winding.
The motor used for the thesis work is a synchronous reluctance motor (REL). Under the hypothesis of a balanced, three-phase and wye-connected stator winding, the stator voltage equations of a REL machine are:

$$u_a = R_s i_a + \frac{d}{dt}\left(L_{aa} i_a + L_{ab} i_b + L_{ac} i_c\right) \quad (1)$$

$$u_b = R_s i_b + \frac{d}{dt}\left(L_{ba} i_a + L_{bb} i_b + L_{bc} i_c\right) \quad (2)$$

$$u_c = R_s i_c + \frac{d}{dt}\left(L_{ac} i_a + L_{bc} i_b + L_{cc} i_c\right) \quad (3)$$

where u_a, u_b, and u_c are the stator voltages; i_a, i_b, and i_c are the stator currents; R_s is the stator resistance and L_{aa}, L_{ab}, L_{ac}, L_{ba}, L_{bb}, L_{bc}, L_{ca}, L_{cb} and L_{cc} are the self-inductances and the mutual-inductances.
In the proposed model the resistance of the stator winding is assumed constant and so thermal aspects are not taken into account. This assumption does not critically influence the precision of the model, since the voltage drop on the resistance R_s is not so relevant.
Both the self (L_{xx}) and the mutual (L_{xy}) inductances are not constant, because they depend on the relative position of the rotor with the respect to the stator θ_{me}:

$$L_{aa} = L_\Sigma - L_\Delta \cos\left(2\theta_{me}\right) \quad (4)$$

$$L_{bb} = L_\Sigma - L_\Delta \cos\left(2\theta_{me} + \frac{2}{3}\pi\right) \quad (5)$$

$$L_{cc} = L_\Sigma - L_\Delta \cos\left(2\theta_{me} + \frac{4}{3}\pi\right) \quad (6)$$

$$L_{ab} = L_{ba} = -\frac{1}{2} L_\Sigma - L_\Delta \cos\left(2\theta_{me} + \frac{4}{3}\pi\right) \quad (7)$$

$$L_{bc} = L_{cb} = -\frac{1}{2} L_\Sigma - L_\Delta \cos\left(2\theta_{me}\right) \quad (8)$$

$$L_{ac} = L_{ca} = -\frac{1}{2} L_\Sigma - L_\Delta \cos\left(2\theta_{me} + \frac{2}{3}\pi\right) \quad (9)$$

where L_Σ is the mean value between L_d and L_q, the two components of the motor inductance in the d – q reference system, and L_Δ is equal to the half of the difference between L_d and L_q:

$$L_\Sigma = \frac{L_d + L_q}{2} \qquad L_\Sigma = \frac{L_q - L_d}{2}$$

It is chosen to adopt a convention of IPM motor for the REL machine. Under this condition the d-axis is the one on which the Permanent Magnet (PM) works, so the one characterized by the lower reluctance. For a REL machine, since no PM are used, this axis corresponds to the one where are created the magnetic barriers.
Since the aim is to realize a current control of the REL motor, it is convenient to transform the equation of the stator voltages (1), (2), (3) with the Park transformation. The two component of the equation of the stator voltages in this second reference system are the following two expressions:

$$u_d = Ri_d + L_d \frac{d}{dt} i_d - \omega_{me} L_q i_q \qquad (10)$$

$$u_q = Ri_q + L_q \frac{d}{dt} i_q + \omega_{me} L_d i_d \qquad (11)$$

where u_d and u_q are respectively the component d and q of the stator voltage; ω_{me} represents the angular frequency of the electromagnetic quantities; L_d is the direct axis component of the inductance and L_q is the quadrature axis component of the inductance.

Parameter	**Symbol**	**Value**
Pole pair number	p	2
Phase resistance	R_p	4,5 Ω
Direct inductance	L_d	60 mH
Quadrature inductance	L_q	190 mH
Nominal current	I_N	10 A_{pk}
Nominal torque	T_N	19,5 Nm

Table 1: Motor parameters

In the d – q reference system the two inductances of the motor are no more a function of the rotor position θ_{me} and so they are assumed constant in the following analysis. The assumption of two constant inductances implies that it is implicitly neglected also the dependence between their amplitude and the winding current. In particular, the flux-current characteristic of the material used for the lamination is not linear and this fact is not taken into consideration in the model. Unfortunately, this second assumption is much rougher than the previous one. In the two expressions of the motor voltages (10) and (11), the weight of the terms that depend on the inductance is higher than the resistive one and it increases with the rise of the rotor speed. This means that a wrong knowledge of the inductances amplitude produces a higher error in the description of the system. As a consequence, the MBPCC does not perform well when the saturation effect is no more negligible, for example in condition of a high load torque.
Another advantage reached with the Park transformation is obviously that during a steady-state operation the current references are constant.

The MBPCC is a discrete-time control technique with a fixed switching period: for the test performed on the bench it is used a switching period equal to 200μs or 100μs and so a frequency of commutation equal respectively to 5kHz or 10kHz.
In the figure below it is represented a scheme that sum up the measured and predicted quantities needed by a MBPCC scheme to control the machine.

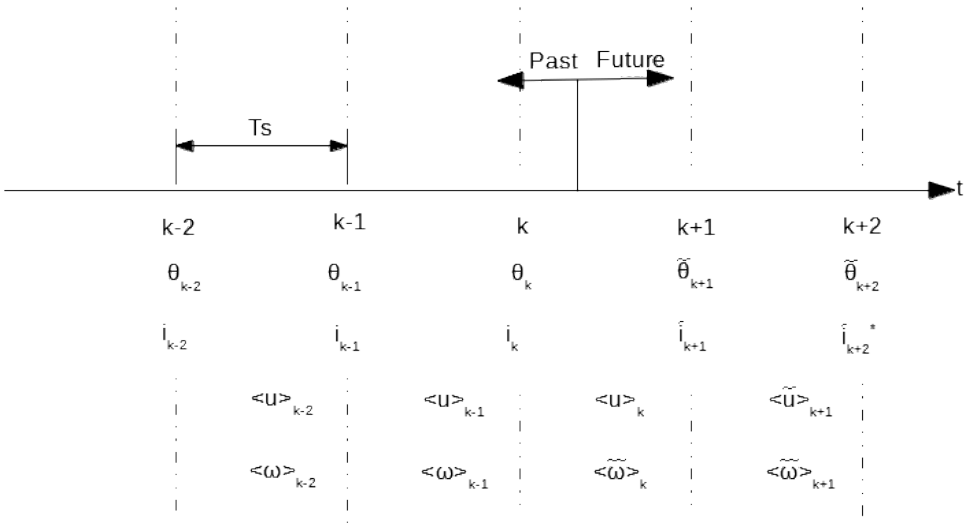

Fig 1 The figure shows the time horizon in which the predictive control scheme works and the most relevant quantities needed for the current predictions in the interval (k+1)st and (k+2)nd

At the beginning of each switching period it has already been decided which voltage vector has to be applied in the following one: for example at the instant t_k it is already known $\bar{u}(k)$ and it is possible to predict $\bar{i}(t_{k+1})$ As a consequence of this statement, the goal of the control action is the identification of the most suitable voltage vector that has to be applied starting from the t_{k+1} time instant and so it is needed a prediction of the motor quantities in two switching periods.
In order to perform a current control at t_{k+2}, it is necessary to rearrange the equations (9) and (10), which are written in a continuous time form, and rewrite them in a discrete form. If we consider, for example, the time interval between t_{k+1} and t_{k+2}, the machine equations can be expressed in a discrete vector form:

$$\bar{u}(k+1) = R\frac{\left(i_{ref,k+2} + \tilde{i}_{k+1}\right)}{2} + \frac{\underline{L}}{Ts}\left(i_{ref,k+2} - \bar{i}_{k+1}\right) + j\,\underline{L}\,\tilde{\omega}_{k+1}\frac{\left(i_{ref,k+2} + \bar{i}_{k+1}\right)}{2} \qquad (12)$$

where $\underline{L}$ is the matrix of the inductances in the d – q system; $i_{ref,k+2}$ is the current reference vector at the instant t_{k+2}; $\bar{i}_{k+1}$ is the prediction of the current vector in t_{k+1}; T_s is the switching period and $\tilde{\omega}_{k+1}$ is the mean velocity of the k+1(st) interval.
The discrete expression of the equations in the (k+1)st interval contains some quantities that are known as the motor resistance and inductances and the switching time. On the other hand many other quantities need to be predicted, such as the speed or the current reached at t_{k+1} because the control scheme works in two future intervals.
Since it is supposed that the measurements of the rotor position and current are performed at the beginning of every switching interval, the last measures that can be used for the prediction are the ones

performed at t_k. In this analysis all the problems related to the acquisition of the measures are neglected.
It is possible to write an equation similar to the (12) also for the k(th) interval: it is sufficient to substitute the index k+1 with k and the index k+2 with k+1.
First of all we consider how it is possible to predict the speed of the motor in the k(th) interval. It is chosen to assume the acceleration in both the k(th) and (k+1)st intervals equal to the acceleration of the (k-1)st interval. This hypothesis is generally not so rough, since the switching period is quite short, too short to observe significant changes of the dynamic of the motor.
On the basis of this hypothesis, the speed of the motor can be predicted directly from the mathematical expression of the acceleration in the discrete form:

$$acc = cost \Rightarrow \frac{\tilde{\omega}_k - \omega_{k-1}}{Ts} = \frac{\omega_{k-1} - \omega_{k-2}}{Ts} \Rightarrow \tilde{\omega}_k = 2\omega_{k-1} - \omega_{k-2} \qquad (13)$$

$$\tilde{\omega}_{k+1} = 2\omega_k - \omega_{k-1} \qquad (14)$$

where $\tilde{\tilde{\omega}}_k$ is the mean predicted speed for the k(th) interval; ω_{k-1} is the mean speed in the (k-1)st interval; ω_{k-2} is the mean speed in the k-2(nd) interval and $\tilde{\tilde{\omega}}_{k+1}$ is the mean predicted speed for the k(th) interval.
Since the prediction of the mechanical quantities is concluded, it is considered now how to compute the prediction of the electric quantities and in particular the currents, that are the controlled quantities.
From the expression of the machine equations referred to the k(th) interval it is possible to express the current at the instant t_{k+1}:

$$\tilde{\bar{i}}_{k+1} = \frac{\bar{u}_k - \left(\frac{R}{2} - \frac{L}{Ts} + j\frac{L}{2}\tilde{\omega}_k\right)\bar{i}_k}{\frac{R}{2} + \frac{L}{Ts} + j\frac{L}{2}\tilde{\omega}_k} \qquad (15)$$

where $\bar{i}_k$ is the current vector built with the currents measured in t_k and $\bar{u}_k$ is the mean voltage vector that is applied in the k(th) interval.
The same equation can be rewritten for the 8k+1)st interval and therefore it is possible to predict the current at the instant t_{k+2}:

$$\tilde{\bar{i}}_{k+2} = \frac{\bar{u}_{k+1} - \left(\frac{R}{2} - \frac{L}{Ts} + j\frac{L}{2}\tilde{\omega}_{k+1}\right)\bar{i}_{k+1}}{\frac{R}{2} + \frac{L}{Ts} + j\frac{L}{2}\tilde{\omega}_{k+1}} \qquad (16)$$

In the two expressions (15) and (16) all the quantities are known or predicted except the magnitude of the voltage vectors imposed to the motor winding $\bar{u}_k$ and $\bar{u}_{k+1}$ that depends on the converter that drives the motor.
On the test bench used in the lab the reluctance motor is driven by a voltage source six-switch two-levels inverter: this means that there are eight possible switch states and so eight voltage vector that can be used to control the machine. This eight states can be represented in the $\alpha - \beta$ reference system by eight fixed voltage vectors, as it is shown in Fig 2: there are six active vectors with the same module and a phase shift of sixty degrees one to the other and two zero-voltage vectors.

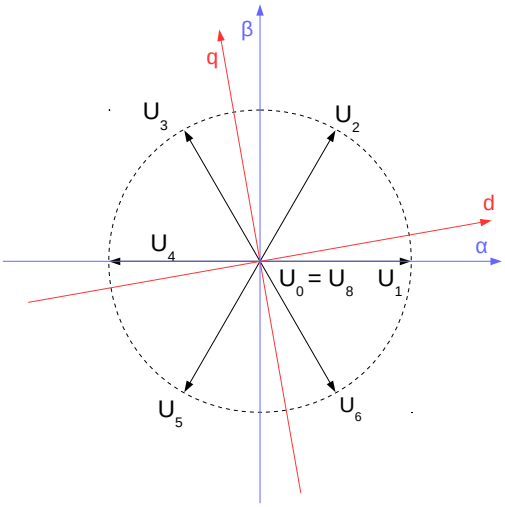

Fig 2: The eight voltage vectors.

Since the control algorithm works in the d – q reference system, it is necessary to transform the eight vectors from the α – β system to the d – q with the Park transformation.
In order to perform this transformation, the knowledge of the rotor position is required almost for all the vectors. The two passive vectors are the only two for which is not needed this knowledge because the same voltage is applied to the three-phase stator winding and so the winding itself is in a short-circuit condition.
Even if in the d – q system exists the complication due to having six non constant voltage vectors, this system is preferred to the α – β because of the advantages underlined before.
Since the speed of the rotor has already been predicted with the equations (13) and (14) supposing a constant acceleration, it is possible to adopt the same hypothesis to predict the rotor position, needed by the Park transformation:

$$\begin{gathered} acc = cost \Rightarrow \frac{\tilde{\omega}_k - \omega_{k-1}}{Ts} = \frac{\omega_{k-1} - \omega_{k-2}}{Ts} \Rightarrow \\ \Rightarrow \frac{\frac{\tilde{\theta}_{k+1} - \theta_k}{2} - \frac{\theta_k - \theta_{k-1}}{2}}{Ts} = \frac{\frac{\theta_k - \theta_{k-1}}{2} - \frac{\theta_{k-1} - \theta_{k-2}}{2}}{Ts} \Rightarrow \\ \tilde{\theta}_{k+1} = 3\,\theta_k - 3\,\theta_{k-1} + \theta_{k-2} \qquad \tilde{\theta}_{k+1} = \theta_k + \tilde{\omega}_k\,T_s \end{gathered} \tag{16}$$

The estimation of the rotor position is the only one that requires the storage of a quantity related to the (k-2)nd interval: it consist actually in a parabolic extrapolation of the point.
The amplitude of the voltage vectors were the last unknown of the equation (16) and so now it is possible to predict the eight current vectors at the end of the (k+1)st switching interval, which is the interval in which the control action is performed.
The control action consists into choosing the most suitable voltage vector in order to achieve a predefined target at the end of the (k+1)st interval. This aspect involve the introduction of a criteria on the basis of which one of the eight possible vector have to be selected: the criteria is represented by the minimization of a cost function, whose expression is related to the type of control has to be performed (in this case a predictive current control). Of course, there are many different criteria that can be used

for selecting the voltage vector and each criteria produces different dynamic behavior of the motor: for his reason the topic is treated separately.

2.2 The choice of the cost function

The influence of the cost function on the dynamic behavior of the machine is the result of the interaction between the type of control that is desired to perform, the parameters used in the cost function and the mathematical expression of the cost function itself.
Since the MBPCC is a current control technique, it is reasonable to adopt a cost function that contain an expression of the current error between a reference and a predicted current at the end of (k+1)st interval.
As a first possible solution, it is chosen a cost function J, found in literature [1], which is essentially an expression of the absolute current error:

$$J = \left|i_{d,k+2} - i_{d,k+2,ref}\right| + \left|i_{q,k+2} - i_{q,k+2,ref}\right| \qquad (1)$$

The evaluation of the cost function requires a prediction of the current, that can be computed with the method described in the previous section. Instead of considering the amplitude of the current at the instant t_{k+2}, it is possible to analyze the expressions of the current variations during a whole switching period. It is reported, for instance, the general expression of the d – q components of the variations during the k(th) interval:

$$\Delta i_d(k) = \frac{T_s}{L_d} u_d(k) + \frac{T_s}{L_d} \left(-R i_d(k) + \omega_{me} L_q i_q(k)\right) \qquad (2)$$

$$\Delta i_q(k) = \frac{T_s}{L_q} u_q(k) + \frac{T_s}{L_q} \left(-R i_q(k) - \omega_{me} L_d i_d(k)\right) \qquad (3)$$

The magnitude of the two variations is strongly influenced by the motor anisotropy: adopting an IPM convention, the d-axis inductance L_d is always lower than the d-axis one.
As a consequence of this peculiarity, the current variations on the d-axis are higher than the q-axis ones, in fact the amplitude of the inductances appears at the denominator of both the expressions (2) and (3).
In order to better highlight the effect of the anisotropy in the selection of the vectors, it is considered a steady state operation of the machine at not so high speed and under a low load torque. In these conditions the contribution of the active vectors to the current variations has the most relevant weight.
It is analyzed now a common transient that can be required to the machine: an acceleration from zero speed to a positive speed reference, for example 100rpm (Fig 3). During this transient, the speed loop ask the motor to express its maximum (nominal) torque, which means that the machine tries to reach quickly its base point.

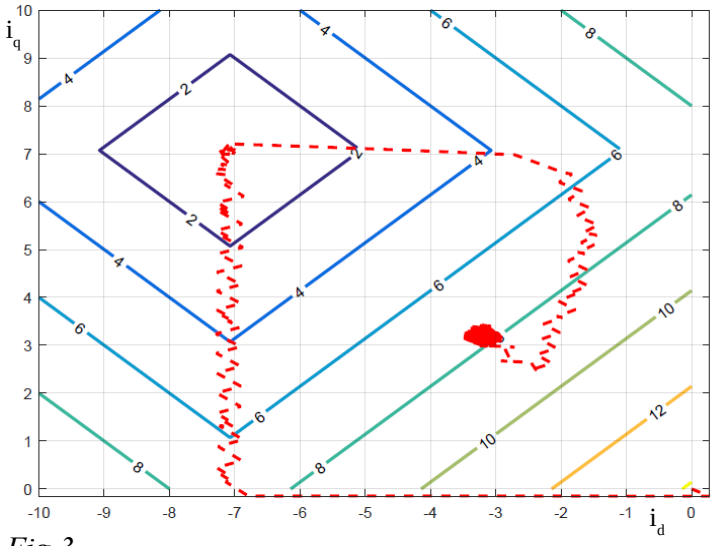

Fig 3

Since the d-axis current variations are higher, the minimization of the cost function gives intrinsically priority to the voltage vectors that can increase the d-component of the current, because it is the fastest process to reach the base point.
The cost function (1) is characterized by contour lines with a square shape because of the adoption of an absolute value expression. Since the weight given to the two variation's components is the same, the d-axis direction would always be preferred in the dynamic transients, because of the larger amplitude of the d-axis variations.
This aspect produces a non-optimal current dynamic, that is reported in the first picture of Fig 4. The interaction between contour lines of the cost function and current variation causes a first decrease of d-current without any increase of the q component. Only after the achieve of the d-current reference the rise of the q-current begins.
This behavior is non optimal because in the meaning while the d-current increases, the torque of the machine remains zero because the q-current remain almost nil. One possible expression of a REL motor torque is, in fact, the following:

$$M = \frac{3}{2} p(L_d - L_q) I_d I_q \qquad (4)$$

It is relevant to underline that this expression is valid only under the assumption of no iron saturation, when L_d and L_q represents the actual flux-current relationship.
In Fig 4 this effect can be easily observed in the first 5ms, which corresponds to the first twenty switching periods. As a consequence of this delay of the q current rise, the machine is not able to express a significant torque in the first instants of the acceleration transient, when the q-current remains very low. Also at the end of the accelerating transient, when the torque required is minor, the decrease of the current components happens in two different moments: at first an increase of the d-current and after that the decrease of the q component.
The trajectory described by the operative points during the acceleration is not the MTPA line but some horizontal and vertical segments (Fig 3).
In conclusion there is evidence that the delay of the q-current rise causes a worsening of the performances in terms of current tracking. In addition, a collateral effect of this fact is also a worsening of the torque response and an increase of the time required for the accelerating or decelerating transients.

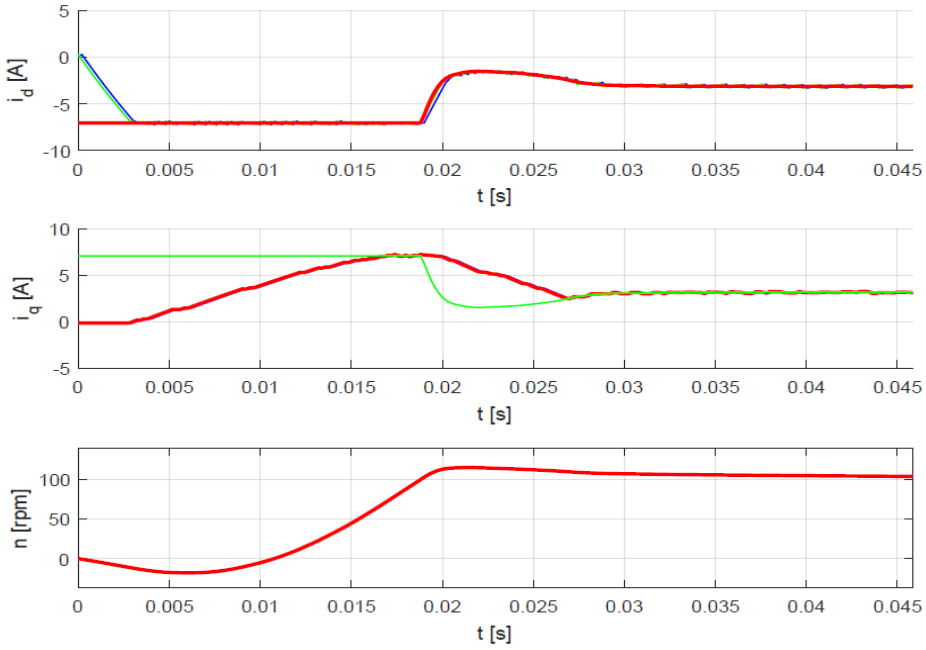

Fig 4: It is evident the different behavior on the two axis.

Since the amplitude of L_d is slightly lower from the one of L_q (for the REL motor under analysis their ratio is almost one third), all the d-current variations generated by the eight voltage vectors are wider than the q-ones. For this reason, in all the dynamic transient, when the two currents are quite far from their references, the control scheme finds that the fastest method to reduce the current error consists into working only on the d-axis. As a consequence, during the transients, the q axis control has a secondary role with the respect to the d-axis one and the q current error is not reduced.
In order to avoid that the q current remains so far from its reference and to obtain a faster torque response, it is wondered to compensate this different behavior that the control scheme manifests on the two axis.
One of the most interesting advantage of a predictive control consists in the possibility of modifying the dynamic behavior of the motor changing the expression of the cost function J. The change of the mathematical expression of the cost function permits, in fact, to produce different contour lines in the $i_d - i_q$ plane and so the selected vectors may be different.
Many different cost functions are investigated to improve this undesired behavior. In order to not have two delayed rises of the two current components, it is needed to anticipate the q-current rise. A possible solution to reach this goal consists into adding a higher weight coefficient to the q-current error: the weight should be chosen properly, because a bad compensation would be completely useless, since one of the axis continues to be preferred.
If we neglect the inductive and resistive contributes to the current variations, the exact compensation is obtained multiplying the q-axis error per the ratio between the two inductances L_d and L_q (from the expressions (2) and (3)):

$$J = \left|i_{d,k+2} - i_{d,k+2,ref}\right| + \frac{L_q}{L_d}\left|i_{q,k+2} - i_{q,k+2,ref}\right| \qquad (5)$$

A similar result could be obviously reached decreasing the d-variations weight with a coefficient equal to the inverse of the precedent inductances ratio.

This ratio does not introduce any other unknown in the problem because the amplitude of the each inductance has already to be measured in order to permit the current predictions (Chapter 2.1). The adoption of a constant weight coefficient is based on the simplifying hypothesis that the ratio is almost the same in all the different operative condition: if the hypothesis is not verified, this technique is no more effective. Later on this theme is going to be discussed.
In Fig 5 it is reported the trajectory described by the operative points with the actual compensated cost function and the new contour lines for the same transient described before.

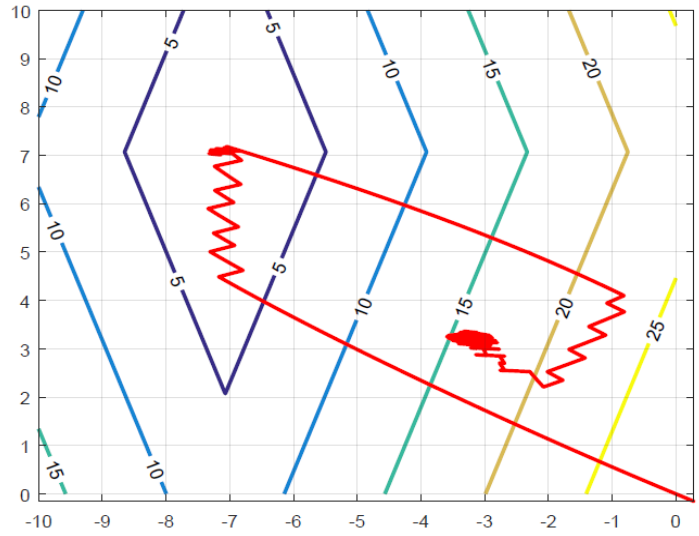

Fig 5

The trajectory described by the operative points is totally changed. Since the two component of the variation are retained equal to the cost function, even if thy are physically different, the operative point describes a trajectory normal to the contour diamonds lines, which is the shorter path to reach the nominal point. From this point of view, the horizontal and vertical movements along the diagonals of the diamonds, observed in the previous case, are disadvantageous.
A second possibility that has be taken under under consideration is the use of a second order cost function instead of the expression of the absolute current error: this means that J represents the difference between the magnitude of the reference current vector and the current vector that we are able to produce at t_{k+2}.
In particular in Fig 6 and Fig 7 are shown the contour lines and the trajectories of the operative points produced by the two following quadratic cost functions:

$$J = \sqrt{\left(\left(i_{d,k+2} - i_{d,k+2,ref}\right)^2 + \left(i_{q,k+2} - i_{q,k+2,ref}\right)^2\right)} \qquad (6)$$

$$J = \sqrt{\left(\left(i_{d,k+2} - i_{d,k+2,ref}\right)^2 + \left(\frac{L_q}{L_d}\right)^2 \left(i_{q,k+2} - i_{q,k+2,ref}\right)^2\right)} \qquad (7)$$

The first expression is very similar to the (1), so it does use any weight coefficient, but it produces ellipse shape contour lines, which does not contain the sharp edges that characterize the previous diamonds.
On the other hand, the second expression is an expression that permits to gain both the advantages of the axis compensation and the ellipse shape contour lines.

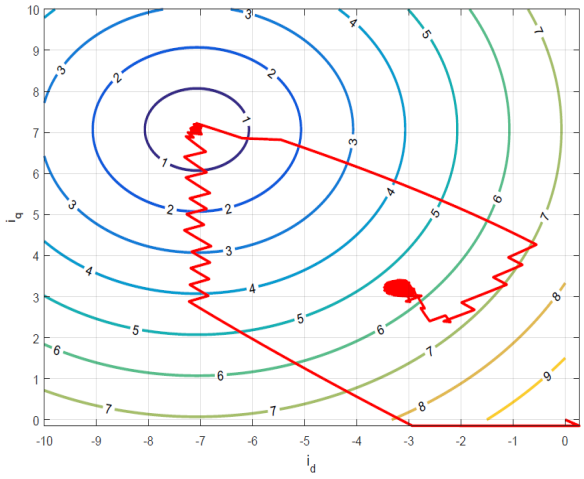

Fig 6: Second order cost function

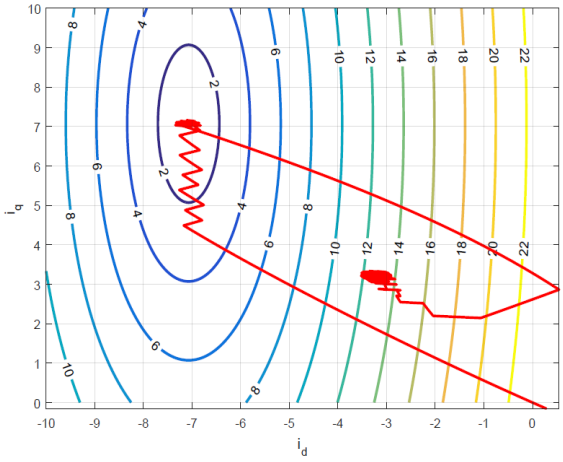

Fig 7: Second order cost function and compensation of the inductances

The most relevant advantage gained with a second order cost function is the parabolic decay of the two components of the current error. If we consider the same accelerating transient, at the beginning the error is high for both the axis, so the higher amplitude of the d-variation originates the horizontal part of the trajectory: the anisotropy of the machine dominates.
After this tract, when the d-current error start to be significantly minor than the q-component, the difference is amplified by the elevation to the second power and so the role of the q error increases more and more. When the amplification due to the second power permits assume the dominant role, the minimization of the cost function gives vectors that increase the q-current component (Fig 6). In conclusion, the adoption of the second order cost function guarantee a partial resolution of the delay of the two rises, without the introduction of any compensation.
Anyway, also for the second order function, a compensation of the anysotropy permits to prevent the delay of the q-current rise, if the weight coefficient is correct. The trajectory obtained with the compensation of the axis is represented in Fig 7. Although the contour lines are different than the case of the expression (5) the direction of the trajectory is almost the same: also in this case it is not possible to obtain an exact compensation for the same reason of the first order function that adopt the compensation.
Even if the saturation problem has not been studied yet, it is interesting to make some consideration about its effect on the presented cost functions.
The saturation of the iron changes the magnitude of the inductances, especially the q-axis one (in the IPM convention).
All the cost functions that adopt the compensation of the difference between the two inductances may not be so advantageous because the ratio L_d /L_q is not well estimated and so the compensation would be wrong: for sure a constant compensation is not adoptable. It appears very difficult to taking into account the saturation of the iron in the expression of the cost function: the ratio of the inductances should be extrapolated from the current measures and updated step by step.
As a consequence, if the machine saturates, the cost functions (1) and (6) are probably the best choice since they both have the advantage of being not influenced by the saturation of the iron as the others.
In conclusion the cost function that is used for the MBPCC scheme is the expression (6), because it is able to partially resolve the delay of the current rise.
Since also the other predictive controls analyzed are based on the minimization of a cost function, the analysis performed in this chapter can be extended also for the other schemes: the expression of the quadratic error will be used also for in the Model Free control schemes.

2.3 Steady state operation

After the choice of the most suitable cost function, it is interesting to study the behavior of the motor during a constant speed operation.
As a first hypothesis, we attribute to the iron a linear B-H curve, neglecting the saturation phenomena: this approximation is verified in the test performed on the bench when the load torque is very low, for example in no-load tests.
It has already been discussed the fact that the eight voltage vectors are not constant in the d – q system in fact they are expressed by the following two equations:

$$u_d = \frac{2}{3} U_{dc} \cos\left(\theta_{me} + k\frac{2}{3}\pi\right) \qquad (1)$$

$$u_q = \frac{2}{3} U_{dc} \sin\left(\theta_{me} + k\frac{2}{3}\pi\right) \qquad (2)$$

where U_{dc} is the available voltage on the DC-bus; t is the time instant considered and k is the index of the voltage vector.
The amplitude of the two voltage components changes in a periodical way both on the d and q axis. In particular, in a steady state operation the vectors' periodicity is fixed and so it is easier to understand which vectors would be chosen in each rotor position by the process of minimization of the cost function.
First of all it is interesting to observe that there are two particular vectors between the eight, which are the two zero-voltage vectors $\overline{U}_0$ and $\overline{U}_7$. To understand this statement, it is reported the current variation produced by one of this vector:

$$\Delta i_d(0) = \frac{T_s}{L_d}\left(-R i_d(k) + \omega_{me} L_q i_q(k)\right) \qquad (3)$$

$$\Delta i_q(0) = \frac{T_s}{L_q}\left(-R i_q(k) - \omega_{me} L_d i_d(k)\right) \qquad (4)$$

These are the only two current variations that do not depend on the rotor position but only on the speed of the machine and the load torque, that influences the amplitude of the two currents i_d and i_q. In addition this two components are contained also in all the other six expressions of the variations as an adding term:

$$\Delta i_x(n) = \frac{T_s}{L_x} u_x(n) + \Delta i_x(n) \qquad (5)$$

where "x" represents the general d or q component and "n" the vector index.
The two zero components produce a shift of the sinusoidal term due to the voltage vectors: the weight of the shift on the two axis is different since in the d and q expressions of the variations the sign between the resistive and inductive contributes are different.
Since the zero variations are just a part of the total variations produces by an active voltage vector, this means that they could have a quite low amplitude with the respect to the other, depending on the specific operative conditions.

The study of the high load torque operations requires the introduction of the iron saturation effect and so we analyze at first the influence of the velocity and we keep the load torque equal to zero.
Considering an IPM convention, if the speed of the motor is positive, the machine operates in the second quadrant of the d – q plane, so the regime d-current is negative and the q one is positive.
In the expression (3) both the terms that form the variation have the same sign (positive); on the opposite in the expression (4) they have different signs. If we add to this consideration the difference between the two inductances, we can state that $\Delta i_d(0)$ is always positive (for positive speeds) and much higher than $\Delta i_q(0)$.
Even if the sign of $\Delta i_q(0)$ could not defined ex ante, the resistive component is commonly dominant at low speed and so the variation results negative. Assuming a MTPA operation, the speed ω_{sign} for which $\Delta i_q(0)$ changes it sign is the following one:

$$\omega_{me,sign} = \frac{R}{L_d} \quad \Rightarrow \quad n_{sign} = \frac{60\,R}{2\,\pi\,L_d\,p} \tag{5}$$

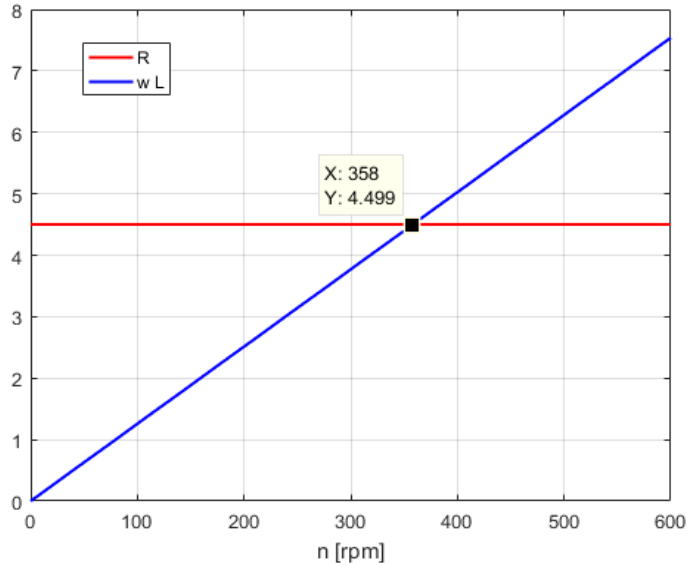

Fig 8: Estimation of the speed for which the q current variation changes its sign.

In the case of the motor under analysis, this speed is equal to 358rpm (Fig 9): from the expression (5) it is evident that the speed depends only on the motor parameter.
When the motor reaches the reference speed, it produces a constant torque in order to compensate mechanical and electrical losses, and the possible load torque. This means that the d – q current components should fluctuate around the respective constant references.
The minimization of the cost function obviously is obtained when the applied vectors are the ones that minimize these current ripples.
Since all the current vectors are formed by the sum of the zero component and the voltage term, the zero-vectors $\overline{U}_0$ and $\overline{U}_7$ are the two that produces the minimum fluctuation, considering both the axis.
Because of the previous considerations, the application of these vectors cause an increase of the d-axis current and a decrease of the q-axis one. As it has already been notice, the two variation have a very different amplitude, in particular the q one is quite small. As a consequence of this fact, an application of an active vector that causes a large change of the q-current is not the optimal choice.

In conclusion, the active vector that is able to keep the current closer to the references is the one that produces a consistent decrease of the d-current and maintains almost constant the q one: this requirements are verified by the vector closest to the d-axis direction. Because of the rotation of the d – q system, this second vector depends on the rotor position and it changes every one sixth of the electromagnetic period.
Under the hypothesis of no load torque and speed lower than n_{sign}, both (3) and (4) assume values that are lower with the respect to the variation of the current due to the voltage vectors that are:

$$\Delta i_d(\bar{u}_k) = \frac{T_s}{L_d} u_{d,k} \qquad (6)$$

$$\Delta i_q(\bar{u}_k) = \frac{T_s}{L_q} u_{q,k} \qquad (7)$$

In particular, the amplitudes of this values depends on the voltage of the DC-bus, which is kept over 200V for all the simulations and the tests performed.
The decrease of d-current caused by the selected active vector is so high that it is often not completely compensated by the zero one: another active vector would be chosen by the minimization of the cost function. This second active vector has to produce obviously a positive d-current variation and a q-current variation slightly positive, in order to counteract the low decrease caused by $\overline{U}_0$.

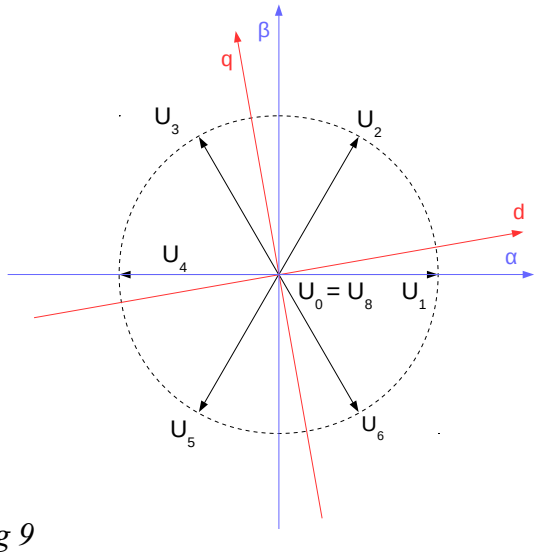

Fig 9

To understand the behavior that we have just explained, we can consider the example reported in Fig 9. Since the rotor position is almost aligned with α-axis, the first active vector selected is $\overline{U}_4$, which produce a fall on the d-axis and a quasi-zero variation on the q-axis. The second active vector selected is $\overline{U}_2$, since it is the one able to compensate $\overline{U}_4$ and increase slightly the i_q.
After a rotation of sixty electromagnetic degrees of the d-axis, the role of $\overline{U}_4$ is replaced by $\overline{U}_5$ and $\overline{U}_2$ is substituted by $\overline{U}_3$, on the other hand $\overline{U}_0$ is the only vector that continuous to be applied: the only vector that is applied in all the electromagnetic period is the zero one.

In the end, the behavior of the motor under the specified hypothesis is characterized by a periodical repetition of three voltage vector, with a periodicity that is equal to the periodicity of electromagnetic quantities.
This behavior is proved by both the simulations performed with MATLAB Simulink and the tests on the bench: in the following figures it can be observed a comparison between the vector's sequence obtained with the Simulink model (Fig 10) and the sequence obtained in a test performed on the bench (Fig 11), both in case of a speed 300rpm and a load of 2Nm.
The scheme is implemented on the bench using the platform DSPACE.

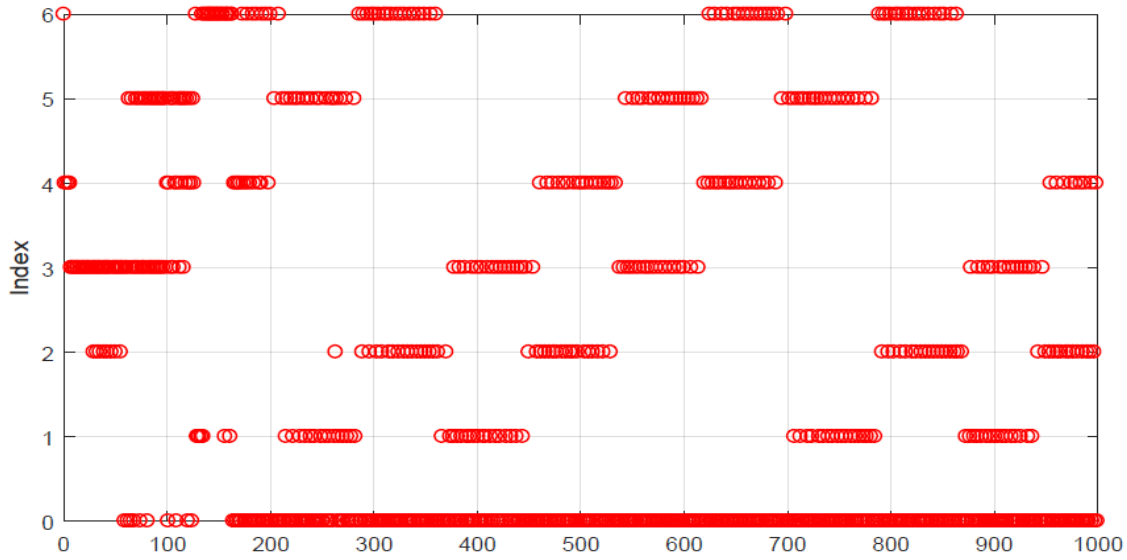

Fig 10: Sequence of voltage vectors obtained in the simulation performed with MATLAB Simulink

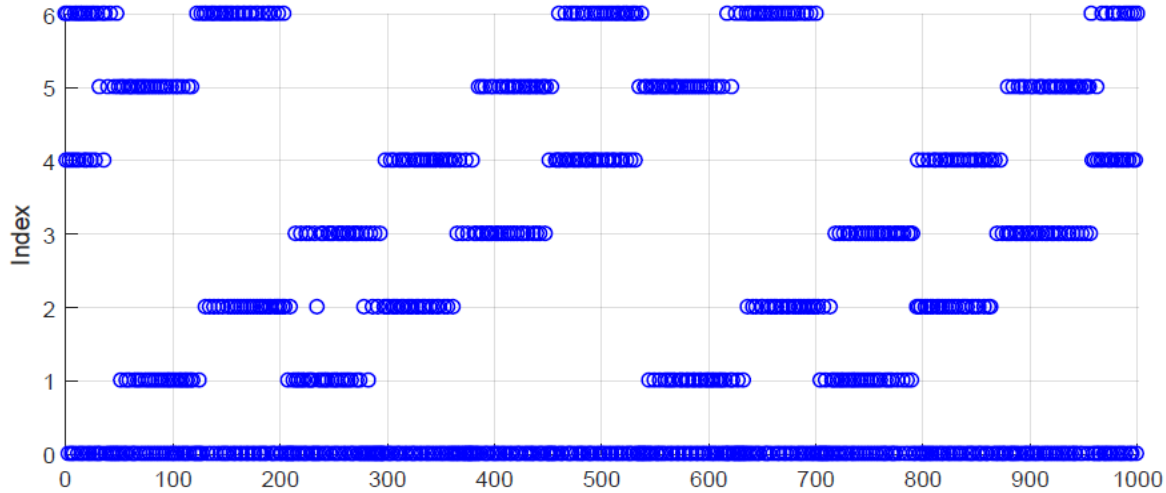

Fig 11:Sequence of voltage vectors applied to the motor winding during the test on the bench

In order to find other evidences of the process of the selection of the vectors, it is possible to extrapolate the speed of the motor from the periodicity of the sequence, which is similar in both the cases, and compare it with the reference speed of the test:

$$T_{em} = n^{\circ}_{intervals}\, T_s = 500 \cdot 200 \cdot 10^{-6} = 0{,}1\,s \;\Rightarrow\; T_m = p\, T_{em} = 0{,}2\,s \;\Rightarrow$$
$$n = \frac{60}{2\pi}\,\frac{2\pi}{T_m} = 300\,rpm \tag{8}$$

The increase of the speed above n_{sign} does not change significantly the choice of the vectors, even if the inversion of the sign of $\Delta i_q(0)$ occurs. Even though the second active vector of the triplet changes, because it is required a Δi_q of opposite sign to compensate the zero variation, the sequence that can be observed is the same.
If we consider the example of Fig 9, the application of $\overline{U}_2$ is substituted, at speed higher than n_{sign} by $\overline{U}_6$: this means that the triplet applied is $\overline{U}_0$, $\overline{U}_2$ and $\overline{U}_6$. This situation is the same that would occur in the case of a speed lower than n_{sign}, when the d-axis rotates of an angle equal to 270°: it is impossible to distinguish the different criteria used for the choice of the second active vector using only the plot of the vectors applied. Only if it is known the rotor position, the change could be noticed.
In addition, it is quite difficult to find the exact speed for which this change of the $\Delta i_q(0)$ sign occurs, because its expression (5) depends only on the motor parameters. Under the hypothesis of MTPA operation and ideal machine, it is possible to find n_{sign} splitting the resistive component from the inductive one. On the other hand, when the iron saturation occurs and the nominal data of the motor are modified, the speed changes: this change, anyway, it is not so relevant since the sequence observed would not change.
A more accurate study of the high speed performances will be done during the study of the Model Free schemes, since the Model Based control scheme presented does not manifests significant problem, from the point of view of the stability.
The operation that it is just described represents the one we would like to achieve for the REL motor operating at constant speed in the MTPA regime, independently from the type of predictive control adopted. In fact, as it has already been noticed, this is the solution that guarantees the minimum fluctuations of the current components from their respective references: this fact reduces the torque ripple and so also the speed ripple. The key-aspect that permits to reach this goal is a frequent application of the zero-voltage vectors, which is the one that generates the minimum current variations.
The iron saturation, unlike the speed, is a parameter that can not be neglected in the study of the MB schemes because it is able to dramatically change the behavior of the machine. In the case of the motor under analysis, this effects of this phenomena can be noticed for very low load torques, with the respect to the nominal value, and so it must be taken into analysis.

2.4 Iron saturation effects

The performances of a predictive control scheme are strictly influenced by the capability of the predictive technique of estimate the future quantities, with an acceptable accuracy, in a wide range of operative conditions. In a Model Based predictive approach, the correspondence between the machine equations and the real behavior of the motor should guarantee this requirement.
Since the equations are obtained thanks to several simplifying hypothesis, some phenomena that commonly can occur in the motor are neglected: one of the most rough approximation is due to not considering the effects of the iron saturation.
In the analysis performed in the previous chapters, the flux-current curve of the machine is approximated with a linear function for both the axis: this means that the two inductances L_d and L_q are considered two constant parameters. If we consider the B-H curve of motor's magnetic lamination, this hypothesis is acceptable only in case of a low load.

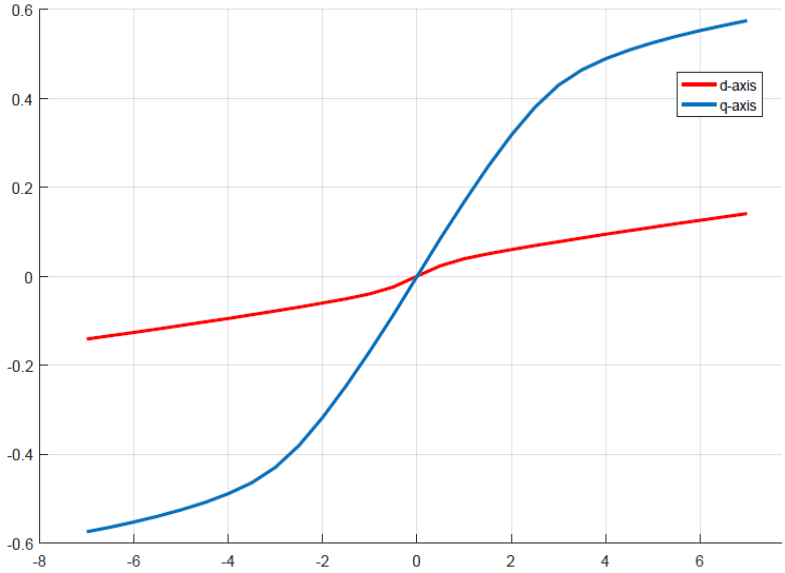

Fig 12: The curves represent the real flux-current characteristic of the motor

In Fig 12 it is reported the flux-current curve measured for the REL motor under analysis: the d-axis curve is quite well approximated by a linear model, on the other hand a linear function is not able to describe with a good precision the flux-current curve on the d-axis. Neglecting the cross saturation, a more accurate expression of the machine equations would be:

$$u_d(t) = R\, i_d(t) + \frac{d\lambda_d(i_d(t))}{dt} - \omega_{me}\, \lambda_q(i_q(t))$$

$$u_q(t) = R\, i_q(t) + \frac{d\lambda_q(i_q(t))}{dt} + \omega_{me}\, \lambda_d(i_d(t)) = R\, i_q(t) + \frac{d\lambda_q}{di_q}\frac{di_q}{dt} + \omega_{me}\, L_d(i_d)\, i_d \quad (1)$$

where λ_d and λ_q are the d and q components of the flux linkage.

The different behavior of the two axis is justified by the geometric and electromagnetic anisotropy of the REL machine: the axis that is characterized by a longer iron path, so the axis with the lower reluctance, is the one more affected by the change of the inductance. The higher is the geometrical anisotropy of the motor, the higher is its torque and the more different are the effects of the iron saturation on the two axis.
Since the two machine equations on the d and q axis are coupled, both the current predictions are influenced by the change of inductance. In order to highlight this aspect, we can rewrite the q-current variation due to the application of the k-th vector:

$$\Delta i_q(k) = \frac{T_s}{l_q(i_q)} u_q(k) + \frac{T_s}{l_q(i_q)} \left(-R i_d(k) - \omega_{me} L_d i_d(k)\right) \qquad (2)$$

where $l_q(i_q)$ represents a compact expression of the term $d\lambda_q/di_q$ in the previous formula (1).
From the expression (2) it is evident that the d-inductance, whose amplitude is more influenced by the iron saturation, compromises also the predictions on the other axis.
Since a linear model overestimates the magnetic flux produced in the machine in a saturated condition, also the inductance's amplitude is overestimated, in particular the d-axis component. This fact causes an underestimation of all the current variations because the inductances' amplitudes appear at the denominator of both the terms that forms the whole variation.
As a result, the first consequence of the iron saturation is an increase of the prediction error. A not nil error characterizes the MB scheme also in not saturated conditions of the machine because of the simplifying hypothesis introduced to build the model of the REL motor and because of the disturbs that affect the measures. An analysis of this error has been performed on the motor in order to quantify the amplitude of this error.

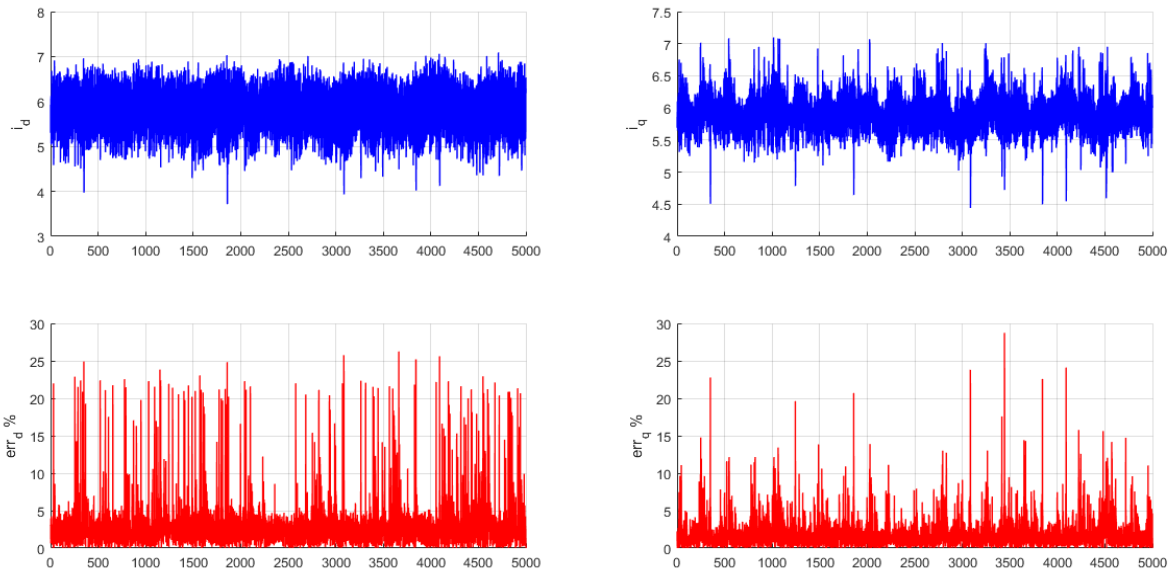

Fig 13: On the top are represented the two component of the measured current, on the bottom the two figures represent the percentage prediction error committed in the prediction

The previous figure (Fig 13) reports the measures related to a test performed at a constant speed of 100rpm and a torque load of 12Nm. In this particular conditions the prediction error assumes a peak

amplitude around 30% of the actual current: this prove that the model previously described becomes partially inadequate when the saturation modifies the inductances of the machine.
A direct consequence of the inaccurate predictions of the current variations is observable in the increase of the current ripple. It is supposed that the two current references are constant, as happens in a steady state test. If in the instant t_k the d-current is slightly lower than its reference, it will be chosen a vector able to induce a current rise during the k-th interval, with the process of the minimization of the cost function. If we are in a saturated condition, the prediction at the instant t_{k+1} is underestimated and so it will be induced a higher current variation: the result could be a current significantly higher than the reference. As a consequence, in the following interval it is required a decrease of the current, but also the evaluation of the decrease will be underestimated and so the current will be much lower than its reference.
This underestimation of the absolute amplitude of the variations amplifies obviously the natural ripple of the current due to the tracking of the two references. An increase of the ripple is evident in particular in the simulations performed with the software MATLAB Simulink.
In the simulations the saturated behavior of the motor is approximated with a modification of the machine's model. In stead of adopting a constant value for the two inductances, it has been used the non linear characteristic reported in Fig 12.
The reported simulation (Fig 14) is related to another test performed at a constant speed of 100rpm with a load torque of 3Nm: it is reported the behavior of the axis where the error is higher. Even if the load is not so high, it is possible to notice a significant difference between the predicted current (red line) and the measured current (blue line). It is reminded that the prediction of the current variations is obviously computed before the measurement, this is the reason why the two curves are shifted.
A wide current ripple induce also a higher oscillation of the torque and so a consequential increase of the speed ripple.

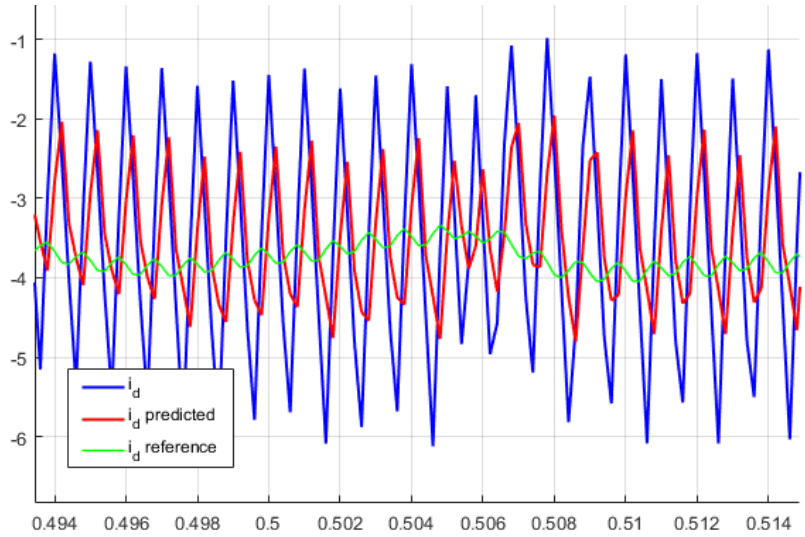

Fig 14: A zoom of the current ripple caused by the wrong estimation of the d current variation.

Another aspect that has to be analyzed is the eventual influence of the iron saturation on the criteria used for the selection of voltage vectors during a constant speed regime. In particular, since the current ripple is increased, it is expected that other sequences of vectors would be adopted.
A critical operating condition is identified: if the amplitude of the ripple is larger than the current variation induced by the application of the zero-voltage vector, an active vector could substitute the role of the zero. In Fig 15 it is reported an extract of the applied vectors for a constant speed of

300rpm and a 14Nm load torque: it is interesting to compare this sequence with the one that is reported in Fig 10 (or Fig 11), which represent a test performed at the same speed but with a minor load torque.

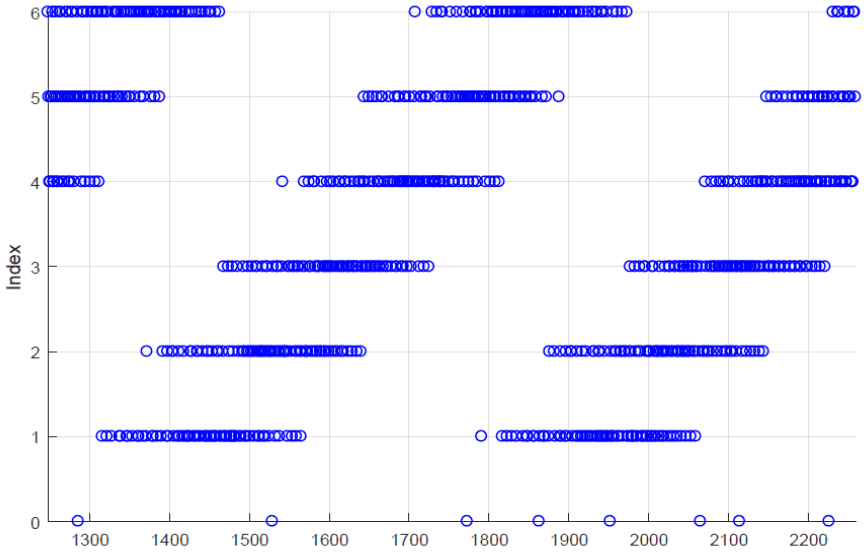

Fig 15: The zero voltage vector is almost never applied to the motor's winding

First of all, the comparison highlights that the frequency of application of the zero voltage vector decreases significantly in a saturated regime. Since the current ripple is increased, the zero current variations could be considered not wide enough to compensate the ones induced by the active vectors.
On the other hand, a higher load torque requires also a higher current load of the machine and so the zero component of the current variations increases its relative weight. A reduction of the frequency of application of this vector is expected also for this reason, neglecting the contribute due to the increase of the prediction error.
It is difficult to understand which of the two phenomena is dominant in this particular case or if other vectors should substitute $\overline{U}_0$ because it is needed a more accurate predictive technique: a more detailed analysis is possible with the MF predictive schemes.
In addition it is noticed that, without the saturation effect, considering a speed of 300rpm, only two active vectors are used in one sixth of the electromagnetic period, that corresponds to 83 switching periods (Fig 11). On the other hand, if the machine is saturated (Fig 15), in the same time interval three active consecutive vectors are used and so it is evident that in a saturated regime the sequence of vectors changes.
In conclusion, an incorrect knowledge of machine parameters, or a change of these parameters because of different operating conditions, compromise always the performances of a MBPCC: the increase of the prediction error in presence of iron saturation is an evident probe of this statement. It is expected that also the change of the stator resistance R, due to an overheated, can reduce even more the performances.
One possible solution to solve this is problem consists into changing the model of the motor according to the operative conditions. It is possible to build an adaptive model of the machine using in a smart way the consistent number of measures that are performed on the motor in different time intervals.
An alternative solution consists into designing a predictive control scheme that does not require the knowledge of all this variable parameters: this second solution is the one that is going to be analyzed.

2.5 Appendix: The Simulink Model

For both the predictive schemes that are going to be studied the quantity of the REL motor that is controlled is the speed: this is possible on the bench using the slave inverter. As a consequence, the most external loop of the scheme is a speed loop that compares the reference speed to the one that is measured on the motor with an encoder.
A PI controller converts the speed error in the module of the current reference: since at first it is considered only the MTPA operation, the d – q components of the working points are always collocated on the same operative line, in particular the bisector of the second quadrant (in case of a IPM convention). When, in a second phase, it is used also a the voltage loop for the flux weakening operation, the evaluation of the current reference is more complicated and it is influenced by other variables.

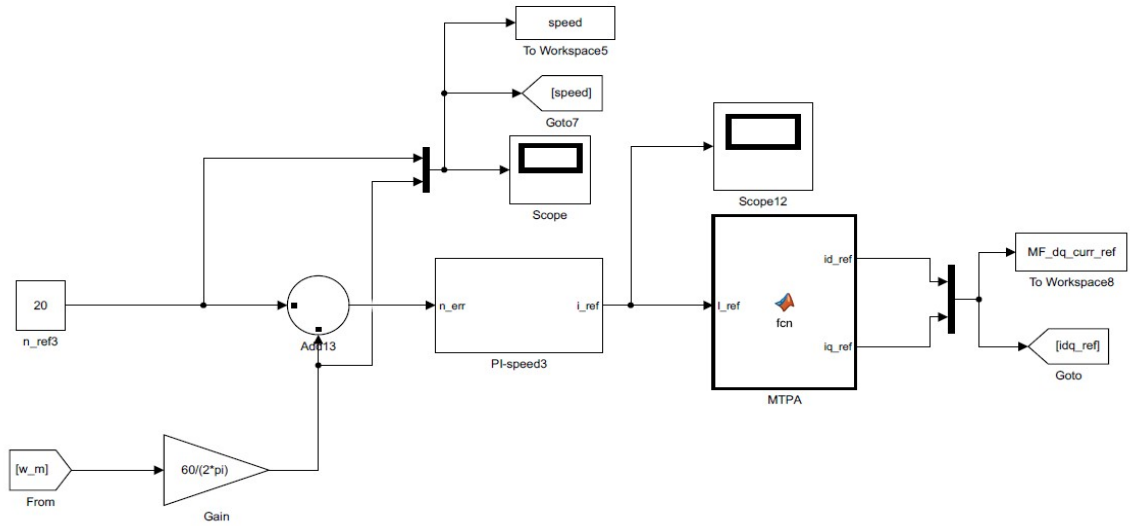

Fig 16:Speed loop of the scheme and generation of the current references.

The two current references that are generated by the block MTPA (Fig 16) represent the current that we would like to achieve in a future time instant.
In order to reach this reference it is needed a predictive algorithm, able to estimate the evolution of the motor quantities on the bases of some hypothesis. In particular, since the speed loop gives a current reference, one of the most influencing predicted quantities are the two d – q components of the current or the current variation produced by a voltage vector in a switching period, depending on the specific scheme. The predictive algorithm is the core of the scheme and it is contained in a specific Matlab Function.
In the case of the MB scheme, the input variables of the block are the ones involved in the expression of the current predictions, in particular the electromagnetic speed, the two d – q components of the current related to the previous interval and of the voltage vectors, the current reference generated by the speed loop and all the parameters of the REL motor.
The Matlab Function permits at first to compute all the current predictions in the (k+2)nd interval and in a second moment to evaluate the amplitude of the cost function for the seven voltage vectors, in order to choose the most suitable vector.

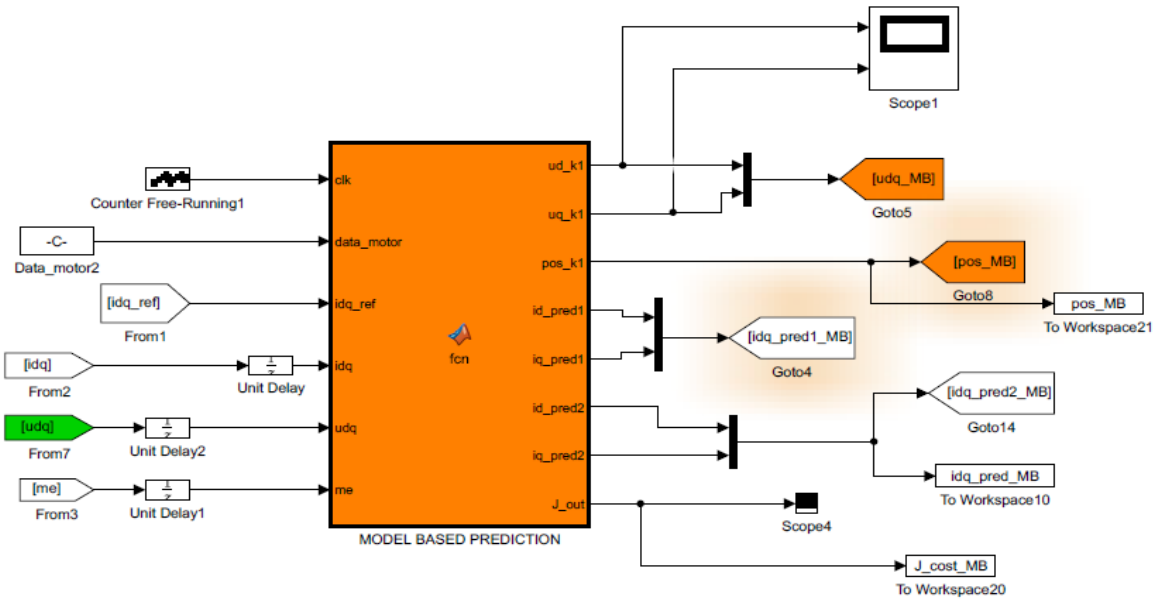

Fig 17: Block in which is insert the model-based predictive algorithm

The vectors chosen are applied to the model of the REL motor: the model represents the d – q components of the motor equations. In order to take into account the modification of the rotor parameter, there are two possibilities for the choice for the amplitude of the inductances. It is possible to impose a constant amplitude of the inductance, introducing a linear flux-current characteristic. On the other hand, it can be imported the measured non-linear characteristic.

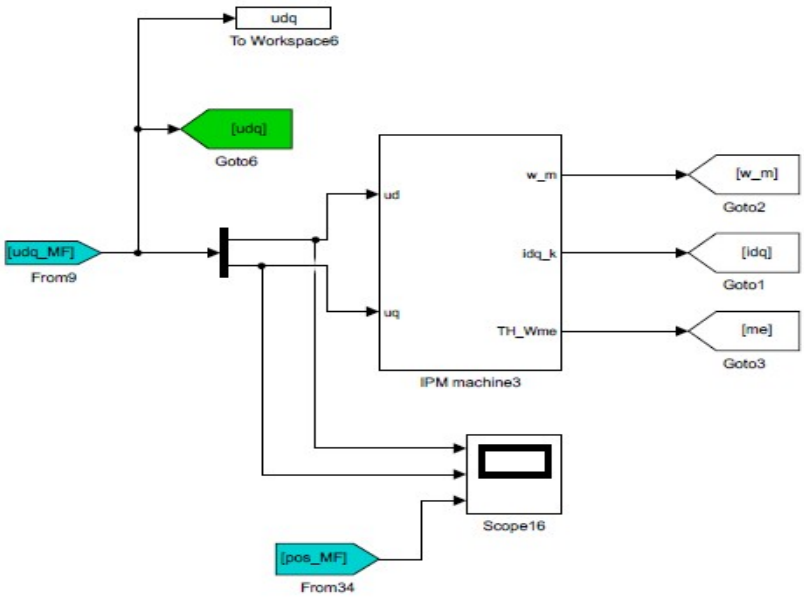

Fig 18

In the first case, the model adopted perfectly fits the behavior of the motor because the inductances' amplitudes are the same, in the second case it is possible to simulate the presence of an error in the motor's model, as in presence of iron saturation.

3 Model Free Predictive Current Control (MFPCC)

3.1 Introduction

The Model Free Predictive Current Control is a predictive control scheme that does not require the knowledge of motor mathematical model thanks to a different use of the measurements performed on the machine.
In the case of MBPCC, the current variation predictions are directly estimated from the d – q equations of the machine, expressed in a discrete-time form. These computations need several information of the motor: the measures or the prediction of mechanical quantities, like the position or the speed of the rotor and the measures or the prediction of electrical quantities, like the currents or the voltages.
At first, we focus the attention on all the measures that are required to perform the predictions every switching period, which are implicitly expressed in the Chapter 2.1.
The information of the rotor position at the beginning of (k-1)st step and k(th) step are both needed, in order to estimate the rotor position and speed for the next time interval. Secondly, it is necessary a measure of the current components at the beginning of the k(th) step, which represent the two starting points for the d – q current predictions. In conclusion, it is required at least to keep stored all the measurements related to the beginning of the (k-1)st time interval and obviously the ones related to the beginning of the k(th) interval.
In order to understand the working principle of a MFPCC, it is introduced the following example: the n(th) voltage vector is applied in the (k-1)st interval and the same vector it is considered the optimum to be applied also for the (k+1)st time interval, after the minimization of the cost function.
A MBPCC scheme would predict the current variations due to this vector for two intervals, using both the measures and the motor's parameters:

$$\Delta i_{d,n}(t_k, t_{k-1}) = \frac{T_s}{L_d} u_{d,n}(t_k) + \frac{T_s}{L_d} \left(-R i_d(t_k) + \omega_{me} L_q i_q(t_k)\right) \quad (1)$$

The accuracy of the predictions is highly influenced by unknown quantities, in particular L_d, L_q and R because the change of these parameters in different operating condition is neglected in the Model Based predictive approach: many hypothesis are introduced to simplify the system.
An alternative consists into using only the current measures related to the beginning of the (k-1)st interval and to the beginning of the k(th) interval. With only this two information it is possible to reconstruct the two components of the current variation produced by the n(th) voltage vector:

$$\Delta i_{d,n}(t_k, t_{k-1}) = i_d(t=t_{k-1}) - i_d(t=t_k) \quad (2)$$

$$\Delta i_{q,n}(t_k, t_{k-1}) = i_q(t=t_{k-1}) - i_q(t=t_k) \quad (3)$$

We wonder to use these values also to predict the current variation caused by the same vector in the (k+1)st interval, if the approximation is not too rough.
At first it is essential to understand which conditions change in the motor between the two time intervals. The machine equations (1) and also the q expression contains all the parameters that we have to take into consideration.

Since the intervals are separated only by a switching period (100-200μs are the period used on the bench), it is possible to neglect the change of the speed ω_{me}, because the inertia of the machine is able to maintain almost constant the speed in a so short time step.
Secondly, thermal phenomena are not fast enough to change the value of the resistance R, which amplitude can be supposed constant. Also the inductive parameters L_d and L_q of the motor should not change significantly, because the currents i_d and i_q remain close to their references, in particular in a steady state regime, and so the level of saturation of the machine is almost the same.
In the end, the two components of the voltage vectors, u_d and u_q, do not change relevantly: they are not constant in the time, because of the rotation of the machine, but the angular motion of the rotor is not so wide in a switching period. The validity of this hypothesis is strongly influenced by the amplitude of the rotor speed since the higher is the operation speed the wider is the rotation of the d-axis.
As a conclusion of this analysis, we can assume that a sufficiently accurate current prediction can be obtained using only the current measures that are performed every switching period.
This prediction technique can be even more precise than the one adopted by the MBPCC if the approximations introduced are not as rough as a wrong knowledge of the machine model. The MF approach, in fact, does not need any estimation of the motor parameter, as expressions (2) and (3) show and so their change do not influence the performances of the scheme.
The method used in the example can be extended also for the other voltage vectors: since the two zero vectors should produce the same variations, it is chosen to use only one of the two, in particular $\overline{U}_0$.
In order to implement this control strategy, it is required a memory of all the seven current variations produced by the voltage vectors: for each vector is built a Look Up Table (LUT) that contains the d – q components of the variation.

Volt. Vect.	**LUT 0**	**LUT 1**	**LUT 2**	**LUT 3**	**LUT 4**	**LUT 5**	**LUT 6**
d-axis	$\Delta i_{d,0}$	$\Delta i_{d,1}$	$\Delta i_{d,2}$	$\Delta i_{d,3}$	$\Delta i_{d,4}$	$\Delta i_{d,5}$	$\Delta i_{d,6}$
q-axis	$\Delta i_{q,0}$	$\Delta i_{q,1}$	$\Delta i_{q,2}$	$\Delta i_{q,3}$	$\Delta i_{q,4}$	$\Delta i_{q,5}$	$\Delta i_{q,6}$

Table 2: Current LUT

As a consequence of the need of the knowledge of this table, a new problem appears for the MFPCC schemes: when the drive is initialized all the LUT are empty and so it is required to find a solution to fill them. Since this problem can be solved in different ways, the topic will be discussed separately (Chapter 4.4).
The current variations stored in the tables are the ones that are insert in the expressions similar to (2) and (3) in order to predict the current variations at the end of the k(th) and of the (k+1)st time intervals. As in the case of a MBPCC scheme, the current at the end of the k(th) interval depends on the k(th) voltage vector, so the control action involves also the prediction of the (k+1)st current variation (Fig 19).

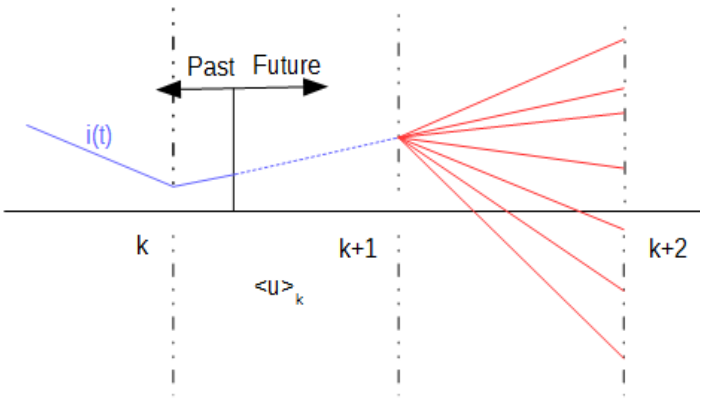

Fig 19: The current prediction interests two intervals

The choice of the most suitable vector is made on the basis of the minimization of a cost function, that can be, for example, the one used for the MBPCC and so the quadratic expression of the current error.
In conclusion, the MFPCC is a current control predictive scheme that uses only the current measures, instead of the whole motor model, to evaluate the predictions.
Since the approximation of using the measured current variations is valid only for a few switching intervals, it is required to maintain updated the information of the LUT: a possible solution consists into refreshing one LUT every switching period. If the n(th) vector is selected for the (k+1)st interval, the difference between the currents that will be measured in the t_{k+1} and t_{k+2} is overwritten in the n(th) LUT since it represents the update of the old value.
In literature it is suggested to analyze another key-aspect of this control technique, which is denominated “stagnation”. This phenomena consists in the repetition of the same voltage vector or a couple of voltage vectors for a long time interval, so five or six vectors are not applied.
In the example reported before, it is highlighted the fact that the high accuracy of the predictions is reached only if the time between two applications of the same vector is very short. If some vectors become stagnant, the LUT of all the other vectors are no more updated.
It is important to underline the fact that, for the MFPCC described, there is an intrinsic problem that affects the update of the current variation LUT. Since seven voltage vectors can be applied and the current variations are computed directly from the current measures, the oldest LUT contains the variations measured seven switching interval before. Fortunately also the amplitude of this time interval is not so wide and so this intrinsic stagnation does not compromise significantly the accuracy of the predictions.
Many simulations performed with different reference speeds or load torques revel the fact that a MFPCC scheme as the one presented always manifests a stability problem and so it can not be implemented.
The typical behavior of the motor in a speed step test is usually the one shown in Fig 20.
At first the dynamic of the motor is quite good: it accelerates and quickly reaches the reference speed value (200rpm). After the accelerating transient, it follows the reference speed for a certain time interval and finally, in all the simulation analyzed, the motor suddenly looses the speed reference and, if a load torque is present, it continues to decelerate.

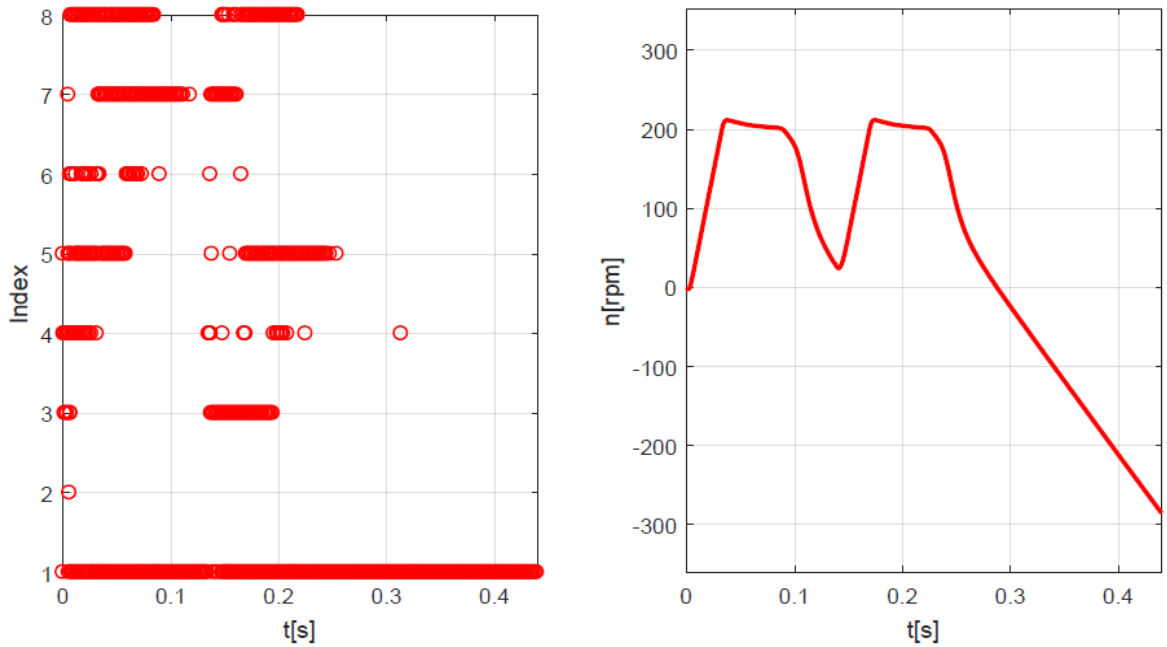

Fig 20: On the left are represented the vectors applied to the machine and on the right the loss of the speed control.

In Fig 20 it is possible to observe that after 0,3s only one voltage vector is applied: this proves that the stagnation is anyway one of the possible causes of the instability.
In order to understand the phenomena, it is considered the case of a constant speed operation of the motor, with the d-axis aligned with the α-axis. It is also assumed that all the current variations contained in the LUT at the beginning are accurate, as in the ideal case.
Since the information of the LUT permits to predict correctly the behavior of the motor, the sequence of the chosen voltage vectors is exactly the same of a MBPCC scheme. The expected sequence is the one of the not saturated case, because the MF approach should decrease the influence of the saturation and so the current variations are known with a good precision. In particular the sequence that should be observed is: $\overline{U}_0$, $\overline{U}_2$ and $\overline{U}_4$; $\overline{U}_0$, $\overline{U}_3$ and $\overline{U}_5$; $\overline{U}_0$, $\overline{U}_4$ and $\overline{U}_6$; $\overline{U}_0$, $\overline{U}_5$ and $\overline{U}_1$; $\overline{U}_0$, $\overline{U}_6$ and $\overline{U}_2$; $\overline{U}_0$, $\overline{U}_1$ and $\overline{U}_3$ (as in it is explained in Chapter 2.3).
The following analysis is based on the signs of the current variations that are produced by the sequence of the vectors, for a positive speed operation. We consider the rotation between two positions distant more than a half of an entire rotation of the d-axis: the mechanical rotation of the motor depends obviously on the number of pole pairs, which is equal to two for the REL machine under analysis.
In the following table are reported the signs of all the variations that are stored in the current LUT. From the analysis of the MB scheme it is known that there is an almost cosinusoidal dependence between u_d and the position θ_{me}, on the other hand u_q has a sinusoidal dependence. The variations due to $\overline{U}_0$ are omitted because their amplitude do not depend on the rotor position, but only on the speed and on the load torque. All these considerations permits to roughly predict the behavior of the drive.
When the sign of the variation stored is different from the expected one, in the table it is reported in red the sign that the variation should have.

Triplet	**0-2-4**		**0-3-5**		**0-4-6**		**0-1-5**		**0-2-6**	
Vector	Δi_d	Δi_q	Δi_d	Δi_q	Δi_d	Δi_q	Δi_d	Δi_q	Δi_d	Δi_q
1	> 0	≈ 0	> 0	≈0 (<0)	>0 (<0)	≈0 (<0)	< 0	≈ 0	< 0	> 0
2	> 0	> 0	> 0	>0 (≈0)	> 0	>0 (<0)	>0 (<0)	>0 (<0)	< 0?	...
3	< 0	> 0	> 0	> 0	> 0	>0 (≈0)	> 0	>0 (<0)	>0 (<0)	...
4	< 0	≈ 0	< 0	> 0	> 0	> 0	> 0	>0 (≈0)	> 0	...
5	< 0	> 0	< 0	≈ 0	< 0	> 0	> 0	> 0	> 0	...
6	> 0	< 0	>0 (<0)	< 0	< 0	≈ 0	< 0	> 0	> 0?	...

Table 3: Reconstruction of the signs of the current variations

From the table it is evident that a MFPCC scheme is not able to predict correctly the signs of the current variations: only for the first triplet of vectors the predictions are correct.
The problem that afflict this control technique is the fact that the change of the rotor position is completely ignored and this fact introduces a significant prediction error. Even if in the expression (1) the position is not directly highlighted, it appears in the expression of u_d, in fact the d – q system is a rotating system.
As a consequence, in the actual example, the two active variations of the triplet are the only two that are correctly estimated. With the actual solution, in fact, the only process that permit an update of the current LUT is the application of the voltage vector on the motor winding. The moment in which the system is better known is when there is the change of the triplet in fact four variation are updated.
If we look at the second triplet of the table, there are already two wrong predictions of the q components, for example it is not taken into consideration that $\overline{U}_1$ begins to induce positive q variations. The MFPCC could be able to maintain the control of the machine because the d-axis variations, whose amplitude are larger as it has been discussed in the analysis of the MBPCC, are almost correctly estimated: only $\Delta\bar{i}_6$ is bad evaluated.
We could even suppose that the machine is able to complete a half of the electromagnetic period and consider the fourth triplet: after this further rotation, the situation becomes even worst. Since three of the seven q-axis variations are not correctly estimated, it is not possible to find an active variation able to reduce the q current. The two negative active variations, in fact, are retained positive because they were measured in a previous position.
Also in this situation it is still possible to maintain for a while the control of the motor exploiting the zero variation, which is negative: its amplitude, anyway, is lower than an active one. As a consequence, the q current tracking is compromised, in particular the current starts slowly to increase and diverge from its reference (Fig 21). It is reminded that the amplitude of these variations is lower: this is the reason why the control has not been lost yet.
The d-axis reference continues to be tracked in the first instants since the relative current LUT still contain variation of both the signs. If we observe the last two columns of the tables, which are related to the fifth triplet of vectors we notice that also d-axis tracking is almost compromised: it depends on the application of $\overline{U}_2$. The non application of this vector, in fact, brings to a situation in which the d-axis is characterized by five LUT with the same sign. When the last negative variation becomes positive the d-current begins to increase (Fig 21) and the control of the motor is definitely lost.
All the simulations realized with Simulink evidence this peculiar behavior: at first the loss of the q current reference and then the loss of the d reference. One of the possible solution of the stagnation could consist in the prevention of the occurrence of this two conditions, in particular the loss of the d-axis control, that is characterized by wider the current variations, should be always prevented.

The dynamic of the machine from this point is difficult to predict, it is the results of the interaction between a permanent repetition of the zero and the load torque. The zero voltage vector, in fact, is the vector that produce the minimum modification of the current and so it is continuously chosen to minimize the cost function.

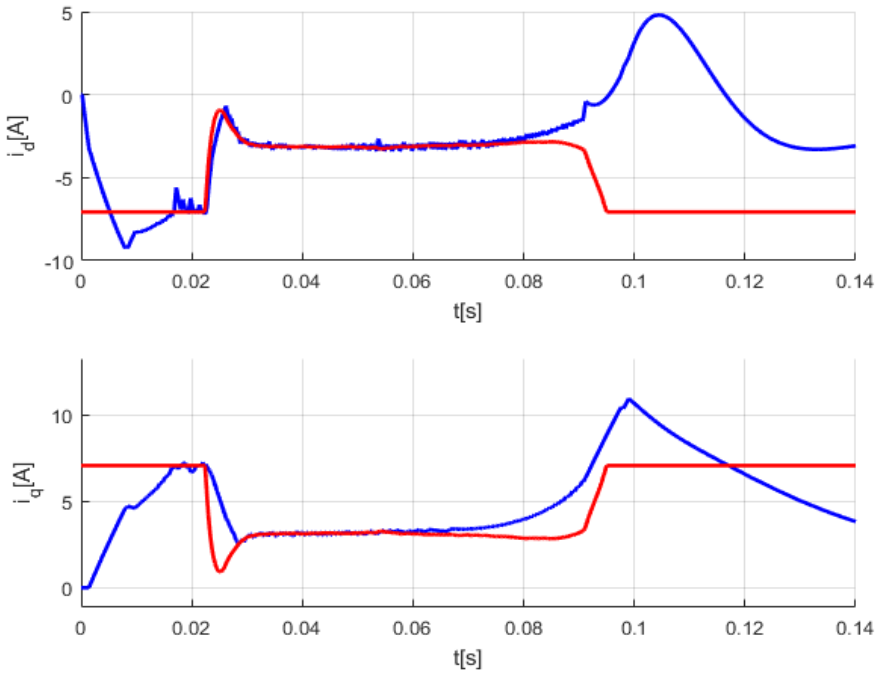

Fig 21: The red lines represent the reference current and the blue lines the measured currents. The q current reference is lost before than on the other axis.

For a constant speed regime the described phenomena always occurs, the higher is the speed reference and the earlier the control of the machine is lost. Also in case of a negative speed reference the stagnation occurs, in fact the phenomena is generated by the periodic application of the voltage vectors.
A solution of the stagnation problem is required in order to stabilize the control of the motor. Different solutions are proposed to solve this problem adopting different techniques to update frequently the current variations. We will focus in the analysis of three possible solutions:

- a forced update of the current variations;
- an anti-stagnation driven by the choice of a smart cost function;
- an indirect update technique.

3.2 Forced anti-stagnation

The easiest solution for the instability of the machine consists into prohibiting that a vector become stagnant, trying to keep sufficiently updated all the current variations.
With the actual Model Free scheme, the update of the stored variations is obtained directly from the current measures, so it is realized only when a voltage vector is applied to the winding of the motor. As a consequence of this statement, if the information contained in a certain LUT is considered old, we have to apply the related voltage vector, even if the process of minimization of the cost function would have chosen another one. In the interval in which the update is performed it is often not applied the optimal vector and the current could diverge from its reference bur we have to accept this fact if we want to guarantee the stability.
In order to implement this algorithm, it is needed the choice of a parameter able to quantify how old are the information stored in the seven current LUT: this parameter can be, for instance, the number of switching period n_{old} for which a vector has not been applied.
This means that for each vector is introduced a counter that is incremented by one unit every switching period in which the vector is not applied. If the vector is chosen by the minimization of the cost function before that it reaches the threshold value, the counter is simply reset. On the other hand, if the counter reaches the value n_{old}, at first the vector is forced to be applied and then the counter is reset.
In literature [2] it is suggested that a fixed number of fifty switching period should be sufficient to prevent the stagnation problems and so to maintain the stability in a wide range of operative conditions.
In Fig 22 it is reported on the left the speed of the machine during a constant speed operation at 100rpm and a load torque equal to 2Nm, adopting an n_{old} equal to 50; on the right it is zoomed an electromagnetic period in order to understand the weight of the anti-stagnation process on the choice of the optimal vector.

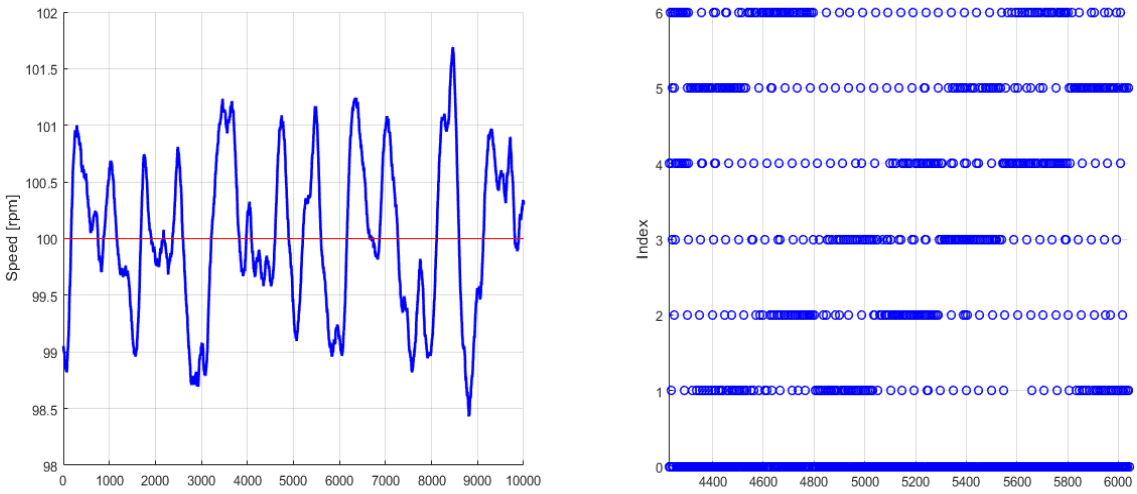

Fig 22: On the left it is reported the measured speed of the machine and on the right the vectors applied to the motor. In the second figure it is particularly evident the anti-stagnation action.

The figure shows that the anti-stagnation algorithm permits to solve effectively the instability but also to guarantee a quite good speed ripple, so that the solution is very interesting also from the point of view of the speed control performances.
In the representation of the chosen vectors it is evident how the algorithm works and in particular when the non-optimal vectors are applied. The main trend shown in the figure is very similar to the one of Fig 9, so a periodical repetition of two active vectors and the zero-vector. Superimposed to the periodic sequence, some random vectors are applied: this is the effect of the update of the LUT with the forced anti-stagnation algorithm. If we consider $\overline{U}_2$, for instance, it is possible to notice that it is applied almost every fifty step when it is not the optimal choice, which corresponds exactly to the frequency of the update.
The forced update of the voltage vectors is obviously an undesired requirement of a Model Free scheme, because it is wondered to adopt apply always the vector found by the minimization of the cost function, that maintain the current as close to the reference as possible.
In particular, if we consider the previous example, in one sixth of the electromagnetic period, which is $200T_s$ long, there should be applied only three vectors (Chapter 2.3). The other four should not be used to control the motor and they are applied at least sixteen times, with a n_{old} equal to fifty. Unfortunately, since all the non optimal vectors are active, they produce a quite large current variation on both the axis and so sometimes, after the update of one of them, it is required the application of another one to adjust the current trend. This fact further increase the number of undesired vectors that are applied in the considered interval.
In order to understand if the frequency of the current LUT update is sufficient to describe correctly the system, it is possible to analyze the prediction error: it is considered firstly a n_{old} equal to 50 and secondly a n_{old} equal to 300.
The error is no more caused by the iron saturation, as for the MB scheme, but by the change of the current variations due to the rotation. It is reminded that the current variations are characterized by a sinusoidal dependence to the rotor position: this means that every time that the a voltage vector is forced to be applied, the consequent prediction error should present a peak.
Despite this fact, the accuracy of the predictions in case of a n_{old} equal to 50 (Fig 23) has the same order of magnitude of the one that characterize the Model Based scheme in a saturated regime (Fig 13).

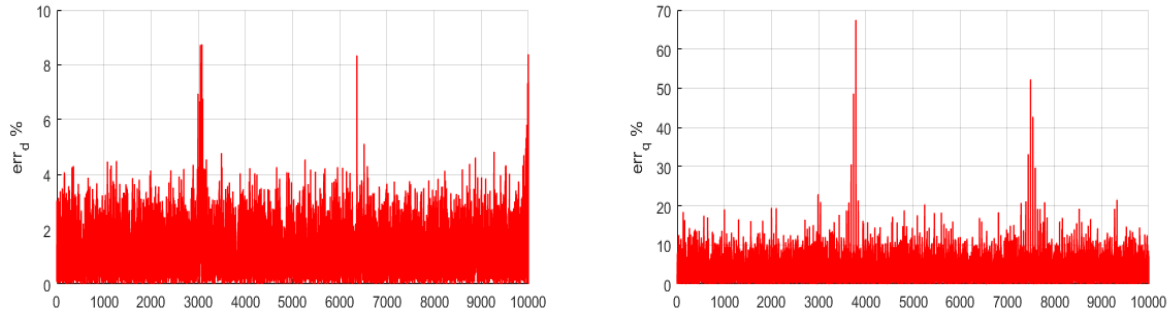

Fig 23: The update is forced after a maximum number of switching intervals equal to 50.

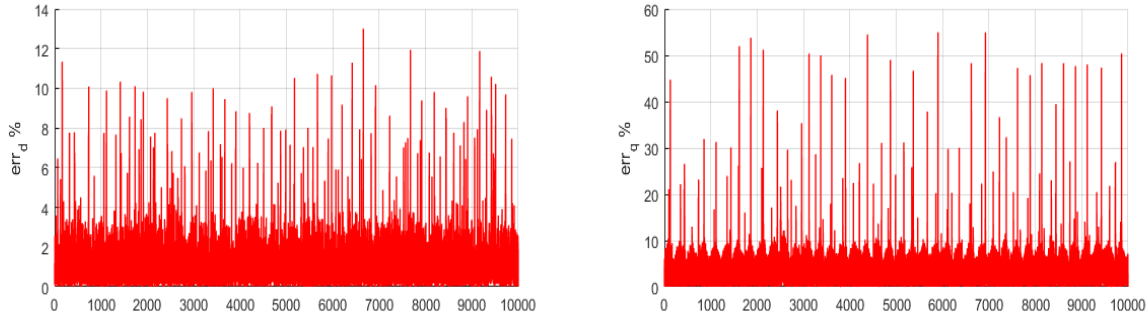

Fig 24: The update is forced after a maximum number of switching intervals equal to 300.

The comparison between the amplitude of the error for the two different n_{old} highlights that the more frequent are updated the current LUT related to the voltage vectors, the higher is the frequency of the error peaks but the lower is their maximum amplitude.
A frequent update, in fact, guarantees a precise knowledge of the change of the voltage components u_d and u_q caused by the rotation of the d – q system and so a very low prediction error. In Fig 23 it is very difficult to distinguish the intrinsic prediction error due to the hypothesis introduced to estimate the future current variations, from the one caused by the forced updates of the current LUT: it is impossible to understand from the frequency of the peaks which value of n_{old} has been used.
On the contrary, Fig 24 underlines that a less frequent update generates more evident peaks of the prediction error, so it is much easier to detect when the forced update is realized. Also in this second case, in the intervals in which there are no forced updates the prediction error is inferior to the 10%: an increase of the amplitude of n_{old} should be possible.
The reduction of the amplitude of n_{old}, in order to achieve a lower prediction error, could not always be the most convenient choice, because a too high frequency of update can compromise as well the stability of the scheme.
An equilibrium has to be found between the frequency of update, the amplitude of the prediction error and the prevention of the instability intrinsically caused by the stagnation. Since it is well known the system that is controlled, it is possible to find an upper and a lower constrain for the choice of a more convenient value of n_{old}.
The first constrain comes from the analysis of the constant speed operation of the REL machine that has been already done for the MBPCC scheme in case of not saturated machine. In particular, it is reminded that in a sixth of the electromagnetic period only three voltage vectors are applied.
As a consequence of this fact, we understand that all the non-optimal vectors applied in this interval are not required to control the motor: from this point of view, it is wondered to apply the minimum number of non optimal vectors that is possible. Since the application is anyway needed in order to update the amplitude of the stored variations and to prevent the stagnation (and the consequent instability), each vector should be applied no more than once during one sixth of the electromagnetic period.
This condition can be defined with a mathematical expression:

$$\frac{1}{6}T_{em} < n_{old}T_s \Rightarrow \frac{1}{6}\frac{2\pi}{p\omega_m} < n_{old}\frac{1}{f_s} \Rightarrow \frac{1}{6}\frac{2\pi 60}{p 2\pi n} < n_{old}\frac{1}{f_s} \Rightarrow n_{old} > \frac{10 f_s}{p\, n} \qquad (1)$$

where n is the speed of the motor expressed in rpm.

The equation shows that there is an inverse dependence between the minimum number of n_{old} and the speed of the rotor, so that it should be chosen a different value of n_{old} for each operating speed. Before discussing the possibility of adopt a variable amplitude for n_{old}, it is found also the second constrain.
The second constrain that can be detected for n_{old} is an upper constrain and it is needed in order to prevent the stagnation. Also this constrain is obtained from the analysis of the behavior of MBPCC scheme and, in particular, from the table that highlights the wrong estimation of the predictions of the current variation signs.
A possible way to guarantee the stability consists into updating the current LUT with a frequency that permit to maintain a correct knowledge of the signs of the variations on both the axis. For a constant speed operation this constrain is verified if the vectors are updated at least once every fourth of the electromagnetic period.
Also this constrain can be expressed mathematically with a similar process used for the expression (1) and the result is the following:

$$\frac{1}{4}T_{em} > n_{old}T_s \Rightarrow \frac{1}{4}\frac{2\pi}{p\omega_m} > n_{old}\frac{1}{f_s} \Rightarrow \frac{1}{4}\frac{2\pi 60}{p2\pi n} > n_{old}\frac{1}{f_s} \Rightarrow n_{old} < \frac{15f_s}{p\,n} \qquad (2)$$

This second value could be probably increased, from the point of view of the stability. In the periodical sequence in which the vectors are applied, the two applications of the same vector are separated by an electromagnetic angle equal to 180°. As a consequence, even if the signs of the two variations components change every 90°, there are no negative effects of the error for a quarter of the electromagnetic period.
The expressions (1) and (2) define an interval of values in which it is possible to select n_{old}. Since the amplitude of the prediction error decreases with the increase of the frequency of update, it should be preferred the adoption of the values closer to the lower constrain (1).
As the previous expression, also this constrain depends on the speed of the motor: this fact supports the thesis that the choice of an optimal value of n_{old} should always take into account this parameter. On the other hand, an alternative solution to guarantee the stability could be the utilization of the minimum value for n_{old}, the one that permits to stabilize the control of the machine till the nominal speed of the drive. This is the reason why, at first, it was used a n_{old} equal to fifty (according to the value proposed in [2]), which is one of the lowest value that can be selected.
It is interesting to study if the adoption of a fixed number of intervals influences positively the dynamic performances of the scheme, thanks to a more frequent update of the current predictions and the lower predictions error.
In the following figures is reported the comparison between two tests realized in the same operative conditions, in particular a constant speed of 100rpm and a load torque of 2Nm, but with two different n_{old}. In the first one it is used a n_{old} equal to 50, in the second a n_{old} equal to 200, so the value that can be obtained from the expression (1).

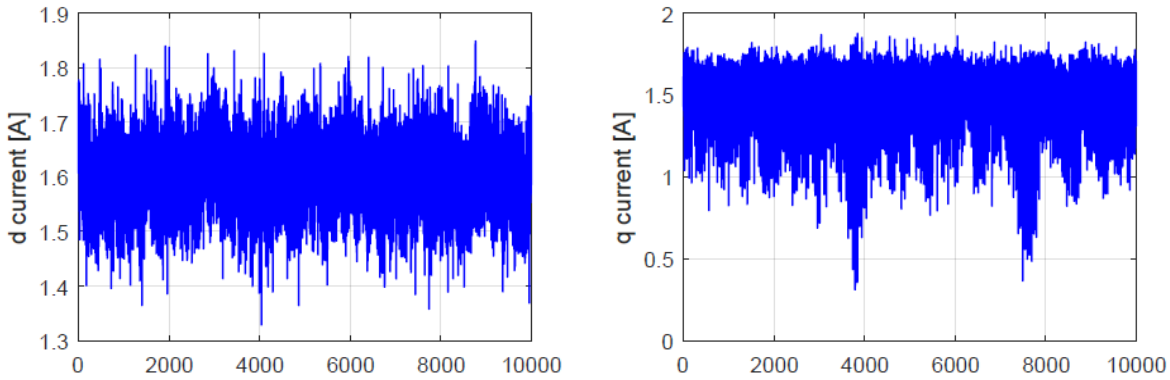

Fig 25: n_{old} equal to 50

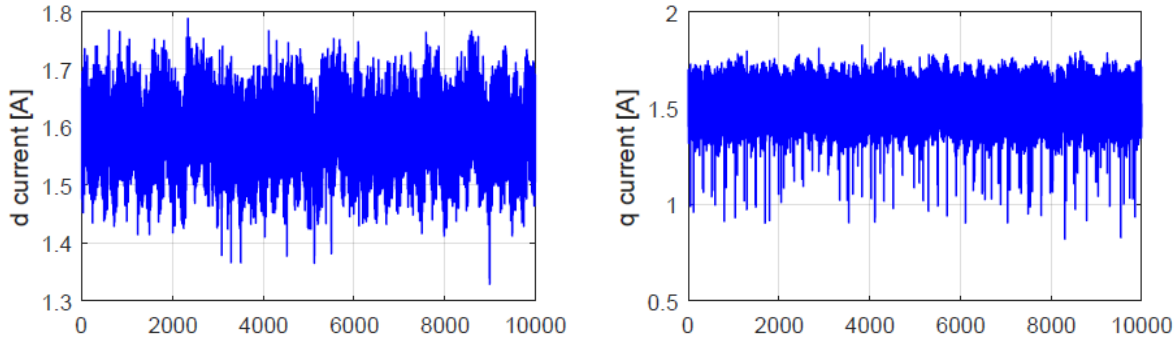

Fig 26: n_{old} equal to 200

The comparison of the current ripple on the two axis between the two cases evidences no relevant differences: the choice of a higher n_{old} produces even a slight reduction of the ripple. This fact proves that it is possible to increase the number of n_{old} without compromising the performances of the scheme. The tests on the motor demonstrates that, in general, the less frequent application of non optimal vectors is the most influencing parameter in the reduction of the amplitude of the current ripple. On the other hand, the reduction of the prediction error and the consequent more accurate description of the system has only a secondary role. It is obvious that the error can not be too high, in order to preserve the stability. If the error is already acceptable, a further reduction of the error is not effective to increase the performances of the scheme: the aim of the control scheme is not the perfect reconstruction of the reactions of the system.
The most relevant advantage of the MFPCC is that the iron saturation does not influence the performances of the control scheme because the current variations are directly measured and not computed with a model. With the MF approach, in fact, it is built an adaptive model of the motor because the reactions of the motor to the input voltage vector are continuously updated
Unfortunately other problems can occur for some particular ranges of speed, in particular for very low speeds or quite high speeds: the MBPCC scheme, on the contrary, is not so influenced by the change of the speed.

3.3 Low speed operation

In case of very low speeds, it is no more convenient to work with a constant value of n_{old}, since this value is the optimal only for a high speed operation. The point is that each non-optimal vector is applied several times in one sixth of the electromagnetic period, even if after the first application the signs of its current variations is updated in the relative LUT and the instability due to the stagnation should not occur.
If the frequency of update is too high, the role of the anti-stagnation process becomes more relevant than the minimization of the cost function, whose results guarantee the tracking of the current references with the lower ripple that is possible. It is reminded, in fact, that the introduction of the forced update is necessary in order to prevent the instability but the lower is its impact on the choice of the vectors, the higher should be the performances of the control scheme.
The effects of a too high current ripple are evident also in the tracking of the speed reference. In Fig 27 and Fig 28 it is shown the speed ripple that characterize the simulations of a 20rpm regime of the motor: in the first it is used a n_{old} equal to 30, in the second the optimal n_{old} that can be obtained by the expressions (1) and (2).

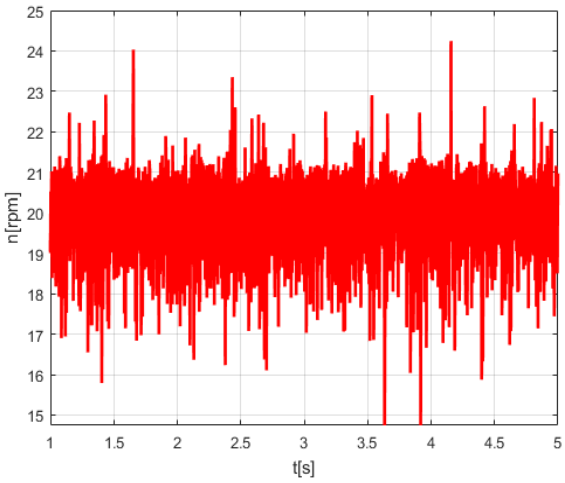

Fig 27: n_{old} equal to 30

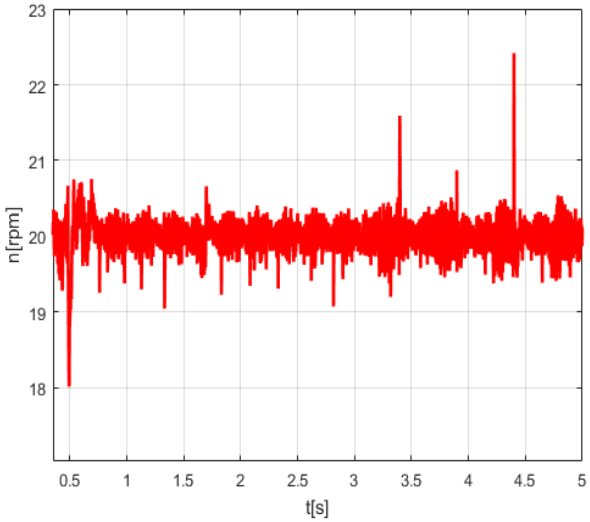

Fig 28: n_{old} equal to 1250

In a low speed operations the amplitude of the speed ripple becomes quite high with the respect to the reference speed because the high current ripple produces also a significant torque ripple. One of the most interesting aspect of this anti-stagnation solution is that the stability can be maintained for a very large range of speeds, accepting the reduction of the performances.
In order to reduce the speed ripple, the most immediate solution consists into respecting the two constrains that are defined by (1) and (2) and so adopting a different number of n_{old} for each operative speed: the lower limit in this case indicates that n_{old} could be even 1250, much higher than the value used in the simulation represented in Fig 27.
If the motor has to work only at low speeds, it is possible also to choose a constant number of intervals, optimized for the particular range of speeds. Unfortunately this second solution does not permit to reach higher speeds because when (2) is no more verified the stability of the scheme can be compromised.
Another possible upgrade of the actual method for this operative conditions consists into introducing other conditions when a non-optimal vector has to be updated, instead of verifying only the two

constrains. Even if we are using a model-free approach, it is convenient to exploit also other considerations that come from the REL machine equations.
It is considered now the zero-component of the current variation: since the inductive component is directly proportional to the speed, its amplitude is negligible in these particular conditions. This means that the zero-variations are not so high, in particular in the conditions when also the load torque is quite low. As a consequence, the zero voltage vector is chosen very frequently by the cost function when the currents are close to their references. For a low speed operation, we could state that the zero-vector does not suffer of the problem of the stagnation.
If one of the vector counter reaches the threshold value n_{old} in the same interval when an active vector is selected by the minimization of the cost function, it is not convenient to update the old current LUT. The choice of an active vector, in fact, suggests that the current components are already quite far from their references. In this particular condition the update could further increase the distance of i_d and i_q from their references and so it could increase the amplitude of the current ripple.
If it is not used any other supporting criteria, the effect of the update is completely random, because the forced update does not take into consideration which will be the currents variations produced.
In order to reduce the current ripple, it is possible to introduce a second simple condition that has to be verified the variation whose relative counter reaches the threshold n_{old}: the update of the old LUT is forced only if the related voltage vector substitutes $\bar{U}_0$, otherwise it is postponed. With this strategy it is eliminated the possibility that it has been previously presented. The forced updates are realized only when the current is very close to the reference and so, after the application of the non optimal vector, the two current component are still not so far from their references.

```
for i=1:nn+1
   if flag_MF(i)>= soglia_old
%        if id_k2(pos_k1)<id_ref; %
       if pos_k1==1  pos_k1==8
       pos_k1=i;
       no_opt_flag=1;
        else
       pos_k1= pos_k1;
       no_opt_flag= no_opt_flag+1;
       end
   end
end
```

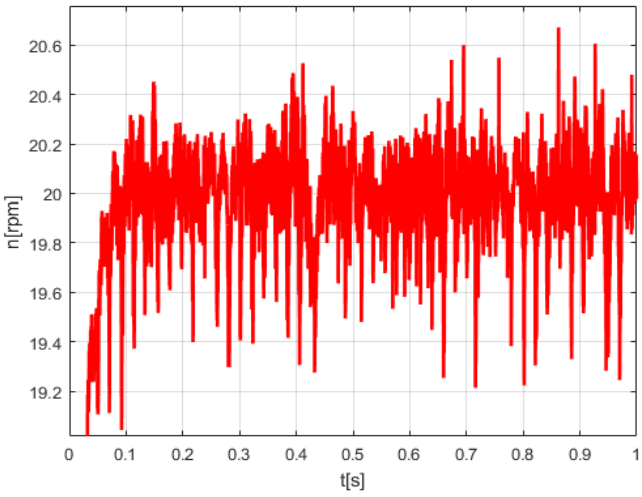

Fig 29: Speed of the motor with the adoption of n_{old} equal to 100 and the smart utilization of $\bar{U}_0$.

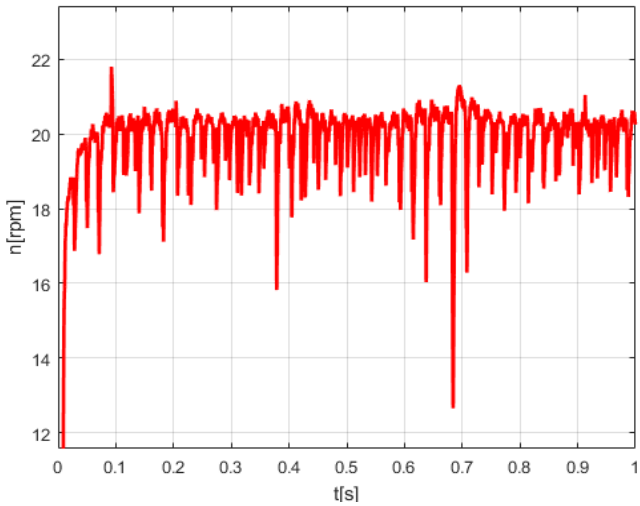

Fig 30: Speed of the motor with the adoption of n_{old} equal to 100.

One of the most interesting advantages of this solution is the fact that it is possible to adopt a not so high amplitude of n_{old}, with the respect to the optimal value, without reducing too much the performances in terms of speed ripple. In the two previous figures are compared two simulations of the REL machine at a quite low speed: in the first one it is observable the speed ripple generated by using the substitution of the zero vector and a n_{old} equal to 100, in the second it is represented the case of the adoption of n_{old} equal to 100, without any other condition.
The performances of the first solution are almost comparable to the ones that could be reached with an optimal selection of n_{old}. If it is adopted an anti-stagnation action with a constant amplitude of n_{old}, the correct use of the zero vector can increase the range of speed for which the motor can be controlled with acceptable performances.
In addition, it is possible also to combine the strategy of a variable frequency of update with the substitution of the zero vector: this represent the best solution found for the forced anti-stagnation scheme in case of a low operative speed (Fig 31).
The improvement of the performances obtained combining the two strategies is not so high, since the increase of n_{old} reduces the number of forced updates, so the number of intervals in which it is possible to exploit the advantages of the supporting condition on the zero vector.

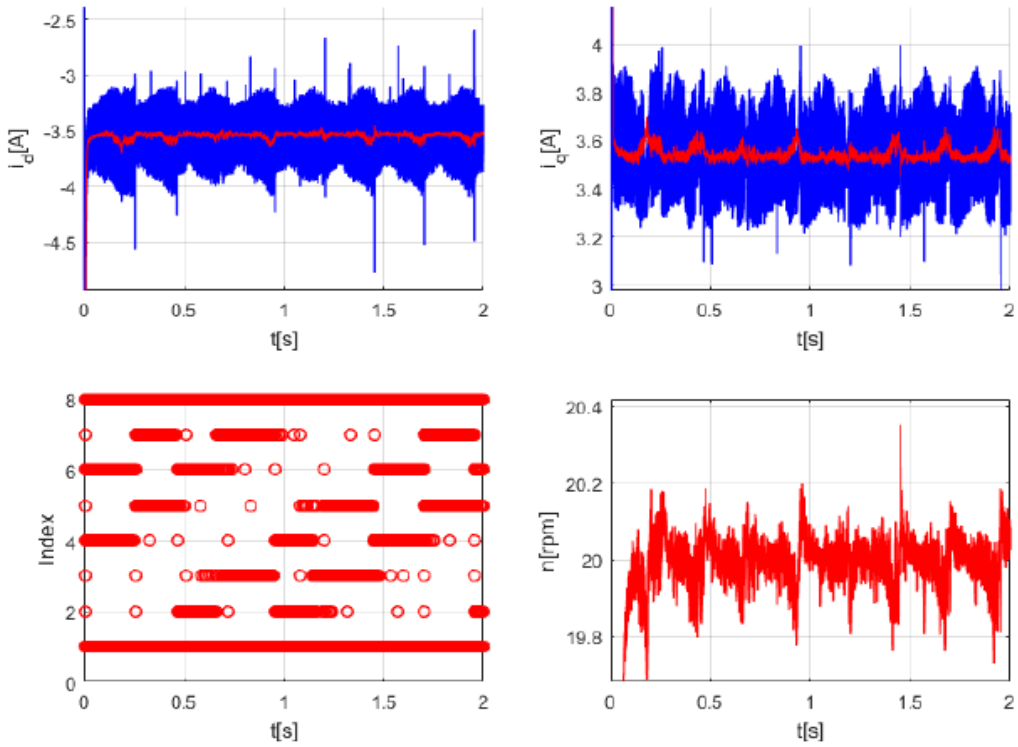

Fig 31: n_{old} equal to 1000 and smart utilization of the zero vector

Unfortunately, the described method can not be extended till the nominal speed of the drive.
In general, in all the operative conditions in which the frequency of application of the zero vector is not so high. The hypothesis on which this solution is based is the fact that there is a so frequent update of the zero current variation that the substitution of one of the many applications is not so relevant. If the minimization of the cost function does not give the zero vector, the update of the old vectors is delayed without any constrain and so the vector that should be updated becomes stagnant.
A different problem appears when the motor has to operates at high speed, in particular when the optimal number of n_{old} is lower than fifty and so for speed higher than 500rpm.
The problem actually is similar to the one that is observed for the low speed operation. In these conditions a sixth of the electromagnetic period is covered in a number of step that is quite low: it could be even lower than fifty step. As a consequence, every application of one of the four non-optimal vectors has a significant weight in a so short time interval. The weight of the anti-stagnation process is quite relevant with the respect to the current tracking, as in the case of a low speed operation with a too high amplitude of n_{old}.
Even if the expressions (1) and (2) permits to impose an optimal frequency of update from the point of view of the current signs, the current references tracking can not be neglected. The two constrains, in fact, are introduced only to preserve a sufficiently accurate knowledge of the current variations. It is difficult to find which is the minimum value of n_{old} that is able maintain the stability of the control, because many parameters must be taken into consideration, like the amplitude of the switching period, the load torque and the nominal speed of the motor. For the motor under analysis, many simulations and tests suggest that it is hazardous to adopt a n_{old} minor than thirty: other control schemes should be used in these conditions.
The problem of the high-speed stability will be better discussed for the improved MFPCC, since the maintaining of the stability becomes even more critical.

Although the application of random vectors is a rough solution to the instability of the control scheme, it is anyway particularly strong from the point of view of the stability.

3.4 An anti-stagnation driven by a smart cost function

A second anti-stagnation solution consist into trying to exploit directly the expression of the cost function to guarantee an intrinsic stability of the scheme. With this approach, the cost function has to cover simultaneously two roles and so it can not be simply the expression of the current error: other variables have to be considered in its minimization.
The principle on which this method is based is the same of the forced anti-stagnation solution: when a voltage vector is not applied for too many intervals, it should be applied in order to correct the wrong information of the rotor position that it contains. On the other hand, the main difference between the two schemes is the fact that, with this second solution, the vector chosen by the cost function is always the one applied in the following interval, without any other complication in the implementation.
As for the previous solution, the indicators used to evidence how old is the information of the rotor position contained in each current variation are seven counters, indicated with $flag_{old}$. These counters are directly insert in the expression of the cost function of the n(th) vector:

$$J(n)=f(\Delta i_d(n),\Delta i_q(n),flag_{old}(n)) \qquad (1)$$

It is evident that the performances and the stability of the control scheme are strongly dependent on the adoption of a suitable cost function.
We can start the analysis of this anti-stagnation solution considering a cost function of the second order, in particular an expression of the module current error, very similar to the one used in the Chapter 2.2:

$$J = (i_{d,k+2}-i_{d,k+2,ref})^2+(i_{q,k+2}-i_{q,k+2,ref})^2 \qquad (2)$$

There are many possibilities to modify this expression with the counters previously introduced: the expression of J should be an arrangement between two different requirements.
If we consider a time window of a few switching interval, the effect of the $flag_{old}$ on the cost function should be almost negligible. In this time horizon, in fact, the change of the rotor position is not so wide and so the minimization process should find the voltage vector that guarantees the best tracking of the current reference. The amplitude of J, in this case, should be, with an acceptable approximation, equal to the one given by the expression (2). Actually the amplitude could be also different, the key element is that the voltage vector found must be the same of the previous one: the imposition of having the same amplitude helps to research a mathematical role for the $flag_{old}$.
On the other hand, when one vector is not applied for several intervals, the current expression of the current error could be completely changed since the cost function should assume the role that was covered by n_{old} in the Chapter 3.2.
In this second case J should become an inverse expression of n_{old}, because it is reminded that the chosen vector is the one that minimize J and it is desired to apply the oldest vector.
In conclusion, the possible expressions of the cost function could be the ones where the mathematical effect of the counters $flag_{old}$ is represented by a decrease of the amplitude of J with the increase of the age of the vectors.

Since in the analysis of the forced MF scheme we have noticed that the dynamic performances are reduced all the times that a non optimal vector is applied, the anti-stagnation effect should have a secondary role.
All these requirements could be verified by a cost function with $flag_{old}$ as the denominator of the current error:

$$J = \frac{\left(i_{d,k+2} - i_{d,k+2,ref}\right)^2 + \left(i_{q,k+2} - i_{q,k+2,ref}\right)^2}{flag_{old}^{k}}, \qquad 0<k<1 \qquad (3)$$

When the counter of a voltage vector is not so high the numerator of the expression, which is the current error has a dominant weight, and so it is optimized the tracking of the current reference. If a vector become stagnant the denominator assumes the highest weight and so the minimization of the cost function gives the oldest vector.
In order to prevent the application of too many old vectors, the weight of $flag_{old}$ is reduced by the exponent k, that must be minor than one. If k is equal to one, in fact, the effect of $flag_{old}$ is so strong that a non optimal vector is chosen almost once every two or three intervals.

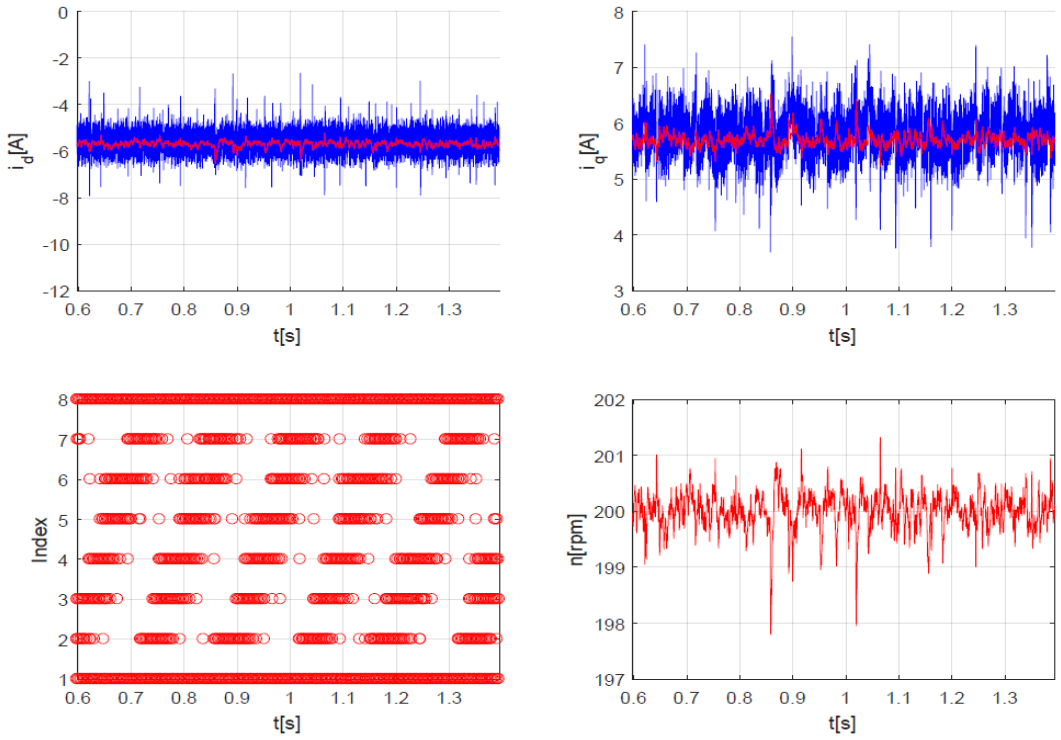

Fig 32

In the simulations performed with MATLAB Simulink it is used an exponent k equal to 0,4 which represent a good compromise between the stabilization and good dynamic performances, in terms of current ripple and current ripple.
This cost function permits to reach interesting results in particular at medium and low speeds and medium and low load torques: in Fig 32 it is reported a simulation at a speed of 200rpm and a load torque of 4Nm.

The evident weak point of this scheme is that it does not take into account the fact that a correct anti-stagnation based on the application of non optimal vectors is influenced by the rotor speed. In particular, the weight of the anti-stagnation role of the cost function should increase with the rise of the speed. On the other hand, the expression used works almost in the same way in all the operative conditions.
One of the disadvantages of this expression of the cost function is the fact it is quite difficult to include also the information of the speed, with the respect to the forced anti-stagnation solution. It is possible to modify the weight of the two roles trying to find a balance between the exponent of the current error and the one of the $flag_{old}$. In order to simplify the problem it is possible to maintain constant the exponent of the cost function and work only on the parameter k, the exponent of the vector counters.
We can consider, for example, a constant speed of operation at 400rpm. Since a k equal to 0,4 is suitable for a speed of 200rpm (Fig 32), it is expected that a reduction of the exponent would be convenient. In the following figures are compared the different dynamics produce by the cost function (3) with an exponent k equal to 0,4 (Fig 33) and 0,25 (Fig 34).

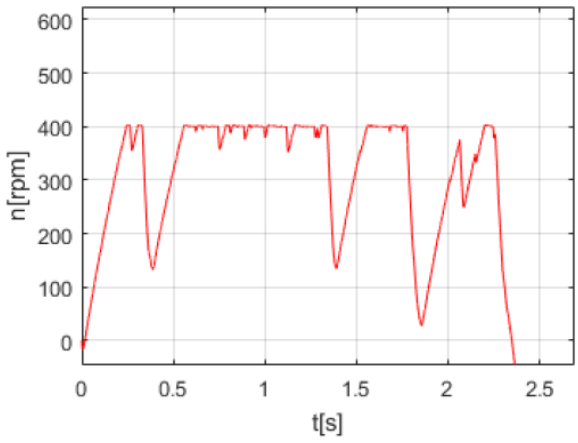

Fig 33: k equal to 0,4

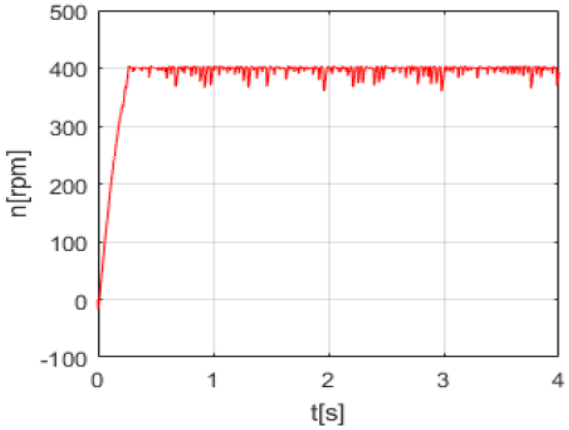

Fig 34: k equal to 0,25

It is evident that a k equal to 0,4 does not give a significant weight to the anti-stagnation process in fact the stability of the control scheme is compromised. On the other hand, a reduction of k does not produce the improvement expected since the speed ripple is very high with the respect to the one observed both for the MB scheme or the MF scheme with a forced anti-stagnation.
The point is that the modification of the exponent of the function is not suitable for the linear change of the frequency of update that it is required: the change of the exponent accelerate too fast the update. A further variable could be introduced to obtain better performance but, anyway, it is difficult to impose a desired behavior working on the exponents of the functions and so it is convenient, at first, to look for other expressions of the cost function with a single variable.
The same effect obtained with the adding of the term at the denominator of the cost function can be generated also by an exponential function, where the exponent is related with the age of the voltage vectors:

$$J = \left(\left(i_{d,k+2} - i_{d,k+2,ref}\right)^2 + \left(i_{q,k+2} - i_{q,k+2,ref}\right)^2\right) \cdot e^{\frac{k}{flag_{old}}} \qquad (4)$$

Similarly to the previous expression, the anti-stagnation role is assumed by a function of the vector counters. In this case the balance between the current error and the anti-stagnation term is reached

choosing a proper value for the constant k in order to that give to the current error a dominant role, delaying the anti-stagnation effects: the weight of the parameter k is determinant, as for the previous expression of the cost function. In the simulations performed on MATLAB Simulink it is used a k equal to 0,01.
The adoption of an exponential function is justified by a faster decrease of the amplitude of J. Even if k is optimized for intermediate values of speed, a faster reduction of J permits a sufficient anti-stagnation effect also for higher speeds (Fig 35).

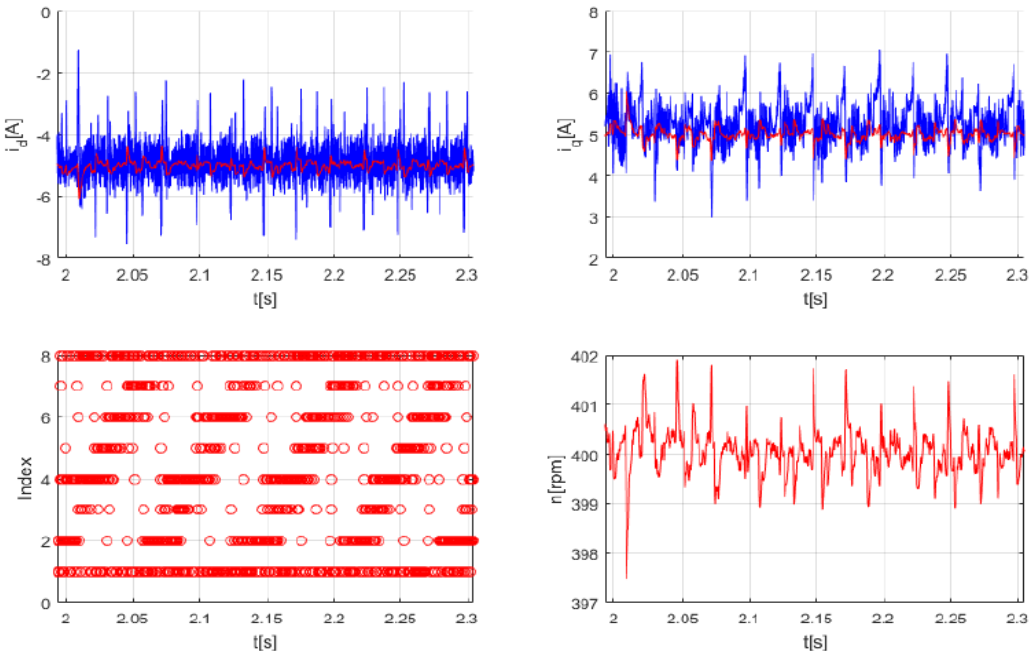

Fig 35

This second cost function permits to extend the range of speed for which the motor can be controlled but it manifests some problems: it is evident that both the current ripple and the speed ripple have a significant amplitude.
One of the reasons of this reduction of the performances can be found in the choice of the voltage vectors. In Fig 35 we can notice that not all the vectors have the same frequency of application in the periodical sequence that characterize a constant speed operation: the vector $\overline{U}_3$, for example, is applied for a much shorter time than $\overline{U}_4$.
These contractions and extensions are a direct consequence of the non linearity of the anti-stagnation action of the cost function. In addition, also this second expression of J does not take into account the relation between the frequency of update and the speed and this generates, at low speeds, the increase of the current ripple observed in the Chapter 3.2: the anti-stagnation action is not optimized.
Also for this cost function it is possible to exploit a variable amplitude of the parameter k but, similarly to the previous case, the non linearity of the problem complicates the association of a specific value of k for each operative speed. In particular, it is difficult to identify a range for the selection of k, as for the parameter n_{old} of the forced anti-stagnation algorithm. The utilization of an exponential function is characterized by completely different dynamic responses also with a change of the parameter k of a factor ten per cent.
This first analysis of the opportunity of solving the stagnation of the vectors working directly on the expression of the cost function of the predictive scheme evidences that a consistent number of solutions could permit the stabilization of the MF approach. In particular, the key factor in the

optimization of the performances of these schemes consists into finding a correct balance between the two roles that the cost function has to cover simultaneously.
In this work it has been analyzed only the possibility of introduce just one parameter to quantify how old is a vector for sake of simplicity, but other parameters could support the minimization process, for example the speed. The speed, in fact, permits to create a relation between the cost function and the frequency of update required to guarantee the stability.
An alternative to the adoption of the speed could be the utilization of the rotor position, as an indicator of the position error that characterize a current variation. When the speed is high the position change faster and, consequently, the position error assume a more relevant weight in the cost function: the anti-stagnation action would be intrinsically related to the speed, as it is obtained in the previous case.
With the introduction of other variables the numbers of different expressions that could be adopted further increase and also the behavior of J becomes more complicate to be understood.
On the other hand, the utilization of just one variable and not linear expressions of the current error does not seem the most suitable choice: it is very difficult to control completely the anti-stagnation action, from the point of view of the frequency of update. Unfortunately, the non-linear expressions are required in order to separate in the time the current tracking from the necessity of keeping a frequent update of the current variations.
The utilization of a smart cost function does not solve, anyway, the essential weak point of a MF scheme stabilized with forced updates, so with the application of non optimal vectors, from the point of view of the current tracking. In fact, there is always a contribute of the current ripple induced by the anti-stagnation action.
In this second case it is even more difficult to maintain acceptable performances, with the respect to the forced MF scheme, since the cost function could never be an expression of the current error. This is the reason why it is chosen to find a solution to the stagnation using a totally different approach.

3.5 Appendix: The Simulink model

The model used to simulate the behavior of the MFPCC is very similar to the one used for the MBPCC. In particular, there are two parts that are exactly the same for the two methods that are the d – q model of the REL motor and the generation of the current references with the speed loop: also in this case it is considered only the MTPA regime.
The difference between the two predictive schemes is the technique of prediction of the current variations. For the MF solution the current predictions are estimated with two different Matlab functions: the first compute the first prediction in the k-th interval (Fig 36) the second the prediction in the (k+1)st interval (Fig 37).
In the second function there is the actual selection of the voltage vector and the process of minimization of the cost function. This is the block modified for the optimization of the parameter n_{old} discussed in the Chapter 3.2 and for the smart utilization of the zero vector in case of a low speed operation considered in the Chapter 3.3.

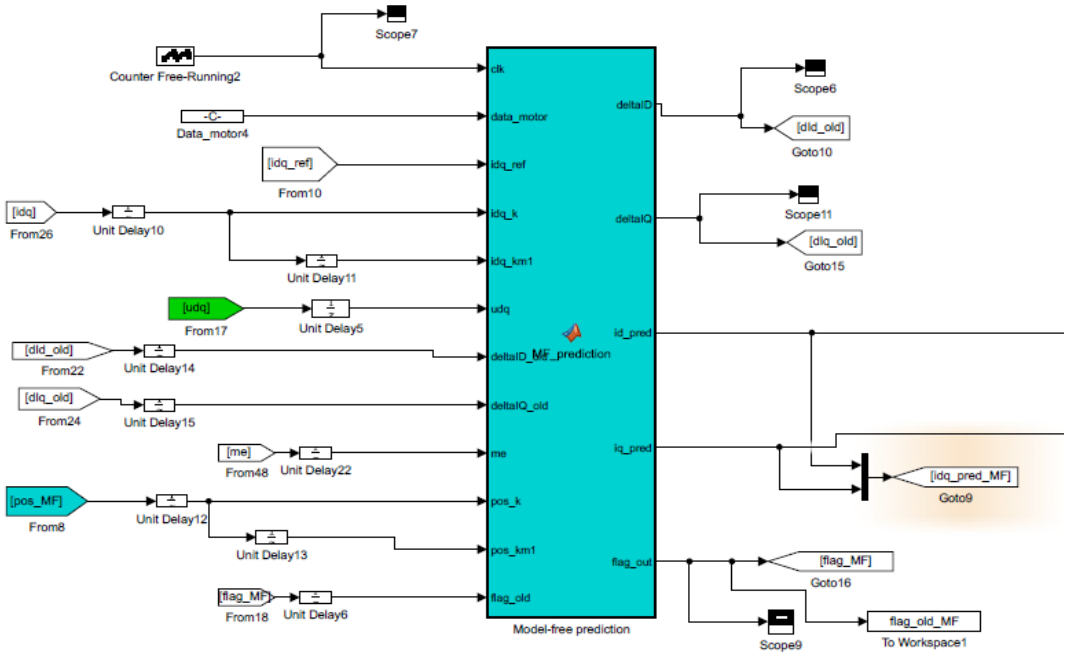

Fig 36: Current prediction in the k-th interval

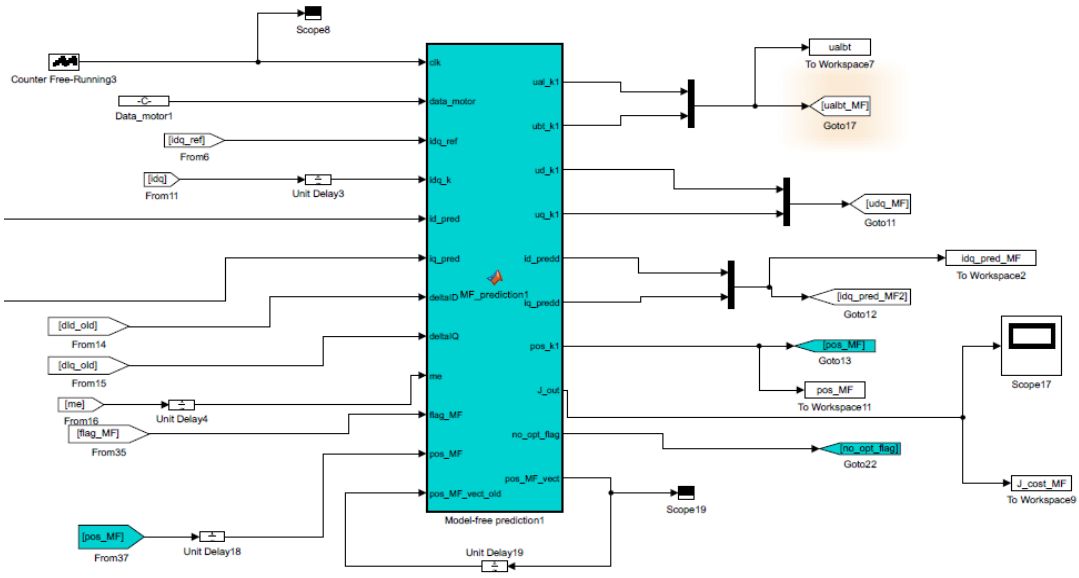

Fig 37: Current prediction in the (k+1)st interval and selection of the voltage vector

4 Improved Model Free Predictive Current Control

4.1 Description of the reconstructive technique

The current ripple introduced by a forced anti-stagnation algorithm or by the one that exploit a smart cost function, analyzed in the previous chapters, can be partially reduced but can never be completely eliminated, since it is required in order to stabilize the operation of the REL machine. In particular, the current ripple represents the direct effect of a "physical" update of the currents variations related to each voltage vector. With the expression "physical" it is underlined the fact that, when a vector is considered old, this vector is directly applied to the winding of the machine, by-passing the optimization process. As a consequence, the only way to obtain an update of a stagnant current variation is its application.
From this considerations, it has been investigated a new way of implementing the MFPCC that does not require the application of non-optimal vectors. It is evident that another solution has to be found in order to prevent the stagnation of the voltage vectors.
If the vectors are not directly applied to the winding of the motor, their update should be obtained indirectly with some mathematical computations. In order to maintain the good performances that characterize a MFPCC scheme when the iron saturation occurs, the predictions of the current variations should be realized without the utilization of the inductive and resistive parameters of the REL motor.
First of all we illustrate the hypothesis adopted to permit the reconstruction of the current variations produced by the voltage vectors imposed by the inverter.
If we look at the machine d – q equations for a specific rotor position, seven are the current variations that the voltage vectors can induce and each of them has two fixed projections on the d-axis and the q-axis. Since the seven current variations are mathematically related, it is possible to use only some of them to reconstruct all the others.
The sum of the six current variations vectors is not zero because a zero-component is contained in each of them, in particular this component is the contribute of the zero-vector:

$$\Delta \bar{i}_k = \Delta \bar{i}(\bar{U}_0) + \Delta \bar{i}(\bar{U}_k), \qquad k = 1,2,3,4,5,6 \qquad (1)$$

The six active vectors current variations without the zero component describe a regular hexagon: the edges of this hexagon are translated by the zero current vector from the origin of the d – q system. As a consequence of this statement, only three currents vectors are required in order to compute the amplitude of all the others: one defines the origin of the hexagon and the other two the relative position between all the active vectors.
Not all the possible triplets of current variations can be used to reconstruct the others, because of the mathematical relations between the vectors. We present now which triplets can be used and which are the mathematical expression that permits the reconstruction of the current variations
It is possible to identify five main groups of triplets from which the reconstructive process can begin:

- three consecutive active vectors;
- two opposite vectors and another active vector;
- two consecutive vectors and the zero vector;
- two non consecutive active vectors and the zero vector,
- three non consecutive active vectors.

In the category of the two non consecutive vectors and the zero not all the combinations are useful, in particular the two active vectors can not be opposite one to the other. The sum of two opposite variations, in fact, gives the zero vector variation, whose amplitude is already known because it is already contained in the triplet:

$$\Delta\bar{i}_1+\Delta\bar{i}_4 = \Delta\bar{i}(\bar{U}_1) + \Delta\bar{i}(\bar{U}_0)+\Delta\bar{i}(\bar{U}_4) + \Delta\bar{i}(\bar{U}_0) = 2\Delta\bar{i}(\bar{U}_0) \qquad (2)$$

Fig 38: The sum of the two active variations of the triplet does not produce any information of the other other variations

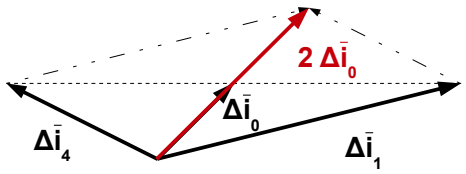

This kind of triplet is totally useless for the reconstruction and so it can be neglected for the ideal reconstructive process. On the other hand, when this Model Free scheme is implemented, this statement is no more true, because the situation is slightly different from the one that we are now considering.

Three consecutive active vectors

Since there are six possible combination of this type, it is presented only one of them: the other five are almost similar from the point of view of the mathematical computations.
A triplet of consecutive vectors is, for example, the one that is composed by the first three current variations related to the active voltage vectors $\bar{U}_1$, $\bar{U}_2$ and $\bar{U}_3$.
The missing active vectors, in this case, are all the vectors that are opposite to the triplet: it is possible to use this geometrical property for the reconstruction after the estimation of the zero component.
Since the six active components define a regular hexagon, it is possible to use the geometrical properties (Fig 41) of the figure to compute the current variation due to $\bar{U}_0$:

$$\Delta\bar{i}_0 = \Delta\bar{i}_1 + \Delta\bar{i}_3 - \Delta\bar{i}_2 = \Delta\bar{i}(\bar{U}_0) + \Delta\bar{i}(\bar{U}_1) + \Delta\bar{i}(\bar{U}_0) + \Delta\bar{i}(\bar{U}_3) - \Delta\bar{i}(\bar{U}_2) - \Delta\bar{i}(\bar{U}_0) \qquad (3)$$

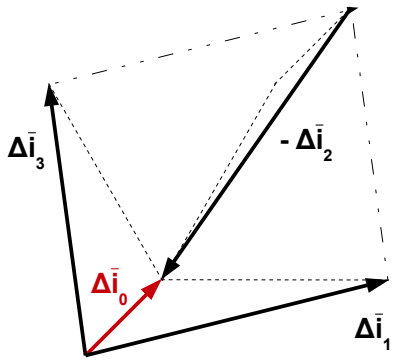

Fig 39: Reconstruction of $\Delta\bar{i}_0$ (3)

The opposite vectors are computed using the symmetry from the origin:

$$\Delta\bar{i}_4 = 2\Delta\bar{i}_0 - \Delta\bar{i}_1 = 2\Delta\bar{i}_3 + \Delta\bar{i}_1 - \Delta\bar{i}_2 \quad (4)$$

$$\Delta\bar{i}_5 = 2\Delta\bar{i}_0 - \Delta\bar{i}_2 = 2\Delta\bar{i}_3 + 2\Delta\bar{i}_1 - 3\Delta\bar{i}_2 \quad (5)$$

$$\Delta\bar{i}_6 = 2\Delta\bar{i}_0 - \Delta\bar{i}_3 = 2\Delta\bar{i}_1 + \Delta\bar{i}_3 - \Delta\bar{i}_2 \quad (6)$$

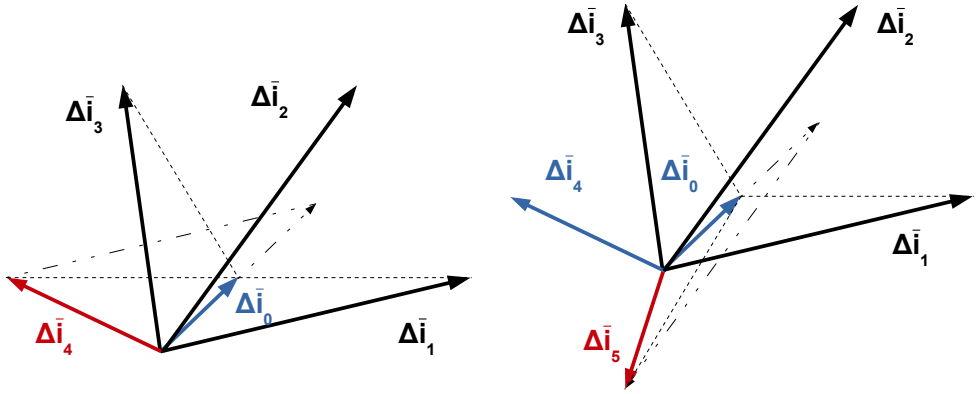

Fig 40: On the left it is represented the reconstruction of $\Delta\bar{i}_4$ (4) and on the right the reconstruction of $\Delta\bar{i}_5$ (5). The black vectors are the one of the original triplet, the blue are the ones already reconstructed and the red is the one that is desired to obtain. The zero variation is amplified in order to highlight the passages of the reconstruction.

For this category and also for the others, the expression of all the current variations are re-elaborated in order to highlight the fact that only three current vectors are required for the reconstruction: this is the reason why all the variations are expressed as functions of the triplet $\overline{U}_1$, $\overline{U}_2$ and $\overline{U}_3$.

Two opposite active vectors and another active vector

For this sequence it is presented the case of the triplet of current variations related to $\overline{U}_1$, $\overline{U}_2$ and $\overline{U}_4$, that is again one of the six element of this group.

As the previous case, it is computed at first the zero vector contribution, using the two opposite variations produced by $\overline{U}_1$ and $\overline{U}_4$ (Fig 41), like in the expression (2):

$$\Delta\bar{i}_0 = \frac{\Delta\bar{i}_1 + \Delta\bar{i}_4}{2} = \frac{2\Delta\bar{i}(\bar{U}_0) + \Delta\bar{i}(\bar{U}_1) + \Delta\bar{i}(\bar{U}_4)}{2} \quad (7)$$

Thanks to the knowledge of another active current variation and not the zero vector, as in the triplet of the expression (2), it is possible to continue the reconstruction. Since we have just obtained the amplitude of the variation induced by $\overline{U}_0$, it is possible to compute the one related to $\overline{U}_5$, which is the opposite of $\Delta\bar{i}_2$, exploiting again the symmetry from the origin:

$$\Delta\bar{i}_5 = 2\Delta\bar{i}_0 - \Delta\bar{i}_2 = \Delta\bar{i}_1 + \Delta\bar{i}_4 - \Delta\bar{i}_0 \quad (8)$$

At this point the two variations due to $\overline{U}_3$ and $\overline{U}_6$ are the only two missing: a possibility to reconstruct them consists into computing the one caused by $\overline{U}_3$, using the sum of the two caused by the application of $\overline{U}_2$ and $\overline{U}_4$ and then exploit again the symmetry from the origin to evaluate the last one.

$$\Delta\bar{i}_3 = \Delta\bar{i}_2 + \Delta\bar{i}_4 - \Delta\bar{i}_0 = \Delta\bar{i}_2 + \frac{\Delta\bar{i}_1}{2} + \frac{\Delta\bar{i}_4}{2} \qquad (9)$$

$$\Delta\bar{i}_6 = 2\Delta\bar{i}_0 - \Delta\bar{i}_3 = -\Delta\bar{i}_2 + \frac{\Delta\bar{i}_1}{2} + \frac{\Delta\bar{i}_4}{2} \qquad (10)$$

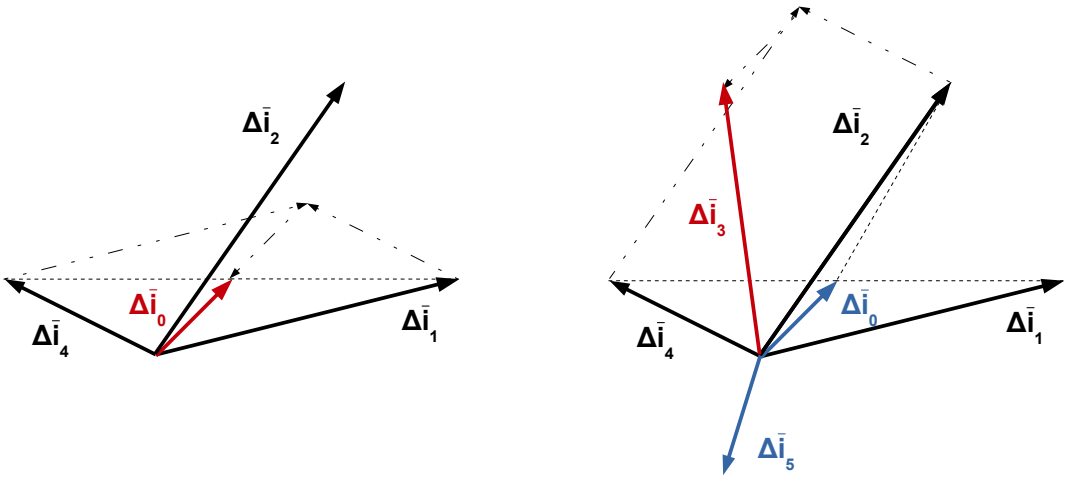

Fig 41: On the left it is represented the reconstruction of the zero variation (7), on the right the reconstruction of $\Delta\bar{i}_3$ (10). The conventions are the same of the previous figures.

Two consecutive active vector and the zero-vector

It is possible, for example, to consider the triplet of current variations due to $\overline{U}_0$, $\overline{U}_1$ and $\overline{U}_2$ to show how to reconstruct all the others.

The main difference between this kind of triplet and the previous two is the fact that the contribution of the zero is already known. As a consequence of this, we can obtain immediately the two opposites to $\overline{U}_1$ and $\overline{U}_2$,which are $\overline{U}_4$ and $\overline{U}_5$, with the symmetry:

$$\Delta\bar{i}_4 = 2\Delta\bar{i}_0 - \Delta\bar{i}_1 \qquad (11)$$

$$\Delta\bar{i}_5 = 2\Delta\bar{i}_0 - \Delta\bar{i}_2 \qquad (12)$$

Fig 42: On the left it is represented the reconstruction of $\Delta\bar{i}_4$ (11), on the right the reconstruction of $\Delta\bar{i}_5$ (12).

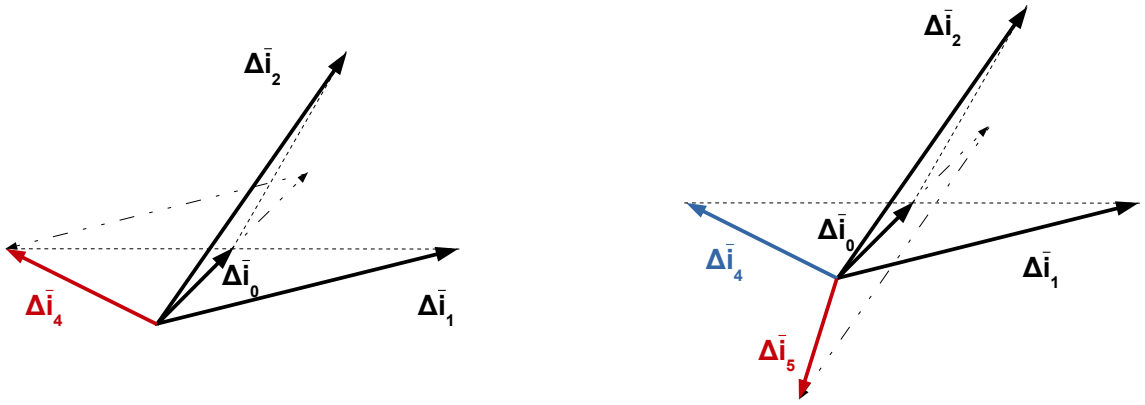

It is noticed that in this situation the known variations are exactly the same of the previous type of triplet considered: it is possible to reuse the same geometrical property of the expressions (9) and (10) to compute the current variations due to $\bar{U}_3$ and $\bar{U}_6$. Since the three starting vectors are different, the expressions of these two missing variations are different:

$$\Delta\bar{i}_3 = \Delta\bar{i}_2 + \Delta\bar{i}_4 - \Delta\bar{i}_0 = -\Delta\bar{i}_1 + \Delta\bar{i}_2 + \Delta\bar{i}_0 \qquad (13)$$

$$\Delta\bar{i}_6 = 2\Delta\bar{i}_0 - \Delta\bar{i}_3 = \Delta\bar{i}_1 - \Delta\bar{i}_2 + \Delta\bar{i}_0 \qquad (14)$$

Two non-consecutive and non-opposite active vectors and the zero-vector

For this category of triplet it is presented the case of $\bar{U}_1$, $\bar{U}_3$ and $\bar{U}_0$, in order to compare this case to the previous one.

When the zero-vector is one of the triplet, it is always convenient to use the symmetry from the origin to compute the opposite variations to the two already known active vectors:

$$\Delta\bar{i}_4 = 2\Delta\bar{i}_0 - \Delta\bar{i}_1 \qquad (15)$$

$$\Delta\bar{i}_6 = 2\Delta\bar{i}_0 - \Delta\bar{i}_3 \qquad (16)$$

At this point two vectors one opposite to the other are missing, as for the previous two kinds of triplets. Also for this situation it is reused the same geometrical reconstruction used in the previous case, so (13) and (14), but with two different vectors, in particular the variations caused by $\bar{U}_2$ and $\bar{U}_5$:

$$\Delta\bar{i}_2 = \Delta\bar{i}_1 + \Delta\bar{i}_3 - \Delta\bar{i}_0 \qquad (17)$$

$$\Delta\bar{i}_5 = 2\Delta\bar{i}_0 - \Delta\bar{i}_2 = 3\Delta\bar{i}_0 - \Delta\bar{i}_1 - \Delta\bar{i}_3 \qquad (18)$$

Three non consecutive and non opposite active vectors

The triplet composed by three non consecutive and non opposite active vectors is a triplet where the three known vectors have a phase shift of $2\pi/3$ one with the respect to the other. This kind of triplet comprehends only two possible combinations, instead of six: we will focus on the triplet of current variations produced by $\bar{U}_1$, $\bar{U}_3$ and $\bar{U}_5$.

Since the zero vector represents the omopolar component, it is computed from the sum of the three already known active vectors:

$$\Delta\bar{i}_0 = \frac{\Delta\bar{i}_1 + \Delta\bar{i}_3 + \Delta\bar{i}_5}{3} \qquad (19)$$

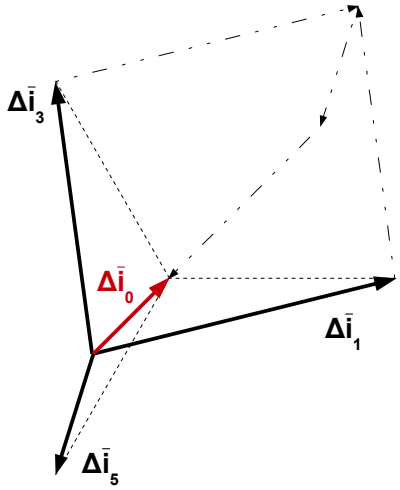

Fig 43: Reconstruction of $\Delta\bar{i}_0$ (19)

The reconstruction of the three missing active current vectors is quite simple since the they are the opposites of the starting triplet. Using the symmetry from the origin, the expressions of these three current variations are:

$$\Delta\bar{i}_2 = 2\Delta\bar{i}_0 - \Delta\bar{i}_5 = \frac{2}{3}\Delta\bar{i}_1 + \frac{2}{3}\Delta\bar{i}_3 - \frac{2}{3}\Delta\bar{i}_5 \qquad (20)$$

$$\Delta\bar{i}_4 = 2\Delta\bar{i}_1 - \Delta\bar{i}_5 = \frac{2}{3}\Delta\bar{i}_3 + \frac{2}{3}\Delta\bar{i}_5 - \frac{2}{3}\Delta\bar{i}_1 \qquad (21)$$

$$\Delta\bar{i}_6 = 2\Delta\bar{i}_0 - \Delta\bar{i}_3 = \frac{2}{3}\Delta\bar{i}_1 + \frac{2}{3}\Delta\bar{i}_5 - \frac{2}{3}\Delta\bar{i}_3 \qquad (22)$$

With the presentation of this last type of triplet we have shown all the possible methods of reconstruction of four of the seven current variations, whose inputs are three different current variations.

This improved Model Free scheme exploits the same technique of the previous MFPCC to choose the optimal vector for the (k+1)st interval. Seven current predictions are estimated for the k(th) interval and other seven for the (k+1)st interval: the voltage vector that minimize the cost function at the end of the (k+1)st interval is the one applied to the motor winding.
Since a Model Free approach is used for the estimation of the current variations, the measured currents are directly used to predict the future behavior of the REL machine. For this improved MF scheme it is not true that the model of the motor is not used, because the reconstruction process is based on the knowledge of the relations between the current vectors, which are given by the machine equations.
All the expressions used up to now are valid only if it is considered a specific time instant, characterized by a specific speed of the rotor and a specific position of the d – q system. This fact means that also the three current variations used for the reconstruction must be measured at the same time instant. Since it is obviously impossible to verify this hypothesis, it is evident that some approximations are introduced when this technique is actually implemented to solve the stagnation problem.
A first intrinsic error in the current predictions is introduced by the fact that there is a rotation of the d-axis during the switching period that separates the last current measure, which is preformed at the beginning of the k(th) interval, and the end of the (k+1)nd interval, where it is chosen the most suitable voltage vector. It is reminded that the only condition that permits a perfect reconstruction of the variations is the knowledge of three current variations all related to the k(th) interval. Since the switching period is quite short, the delay of one switching interval is not so relevant.
A more rough approximation is introduced by the fact that the three variations used for the reconstruction are the three most recent generated by three different voltage vectors. Of course, the current variation measured between t_{k-1} and t_k is always used for the reconstruction but it is not always possible to use the two previous variations.
When three different vectors are applied in a row, the reconstruction should be very precise and so the prediction error should be minimum: this is the best approximation of the ideal case that can be obtained by the actual scheme.
On the other hand, if only one vector of the triplet is quite old, the reconstruction of the current variations could be affected by a significant error. In this second case the only two accurate variations are the other components of the reconstructive triplet.
Since every vector of the triplet is measured in a different interval, the time order of the elements of the triplet assumes a relevant role, because it is a useful criteria to qualify the accuracy of the information carried by each variation.
Every switching period we must know which is the oldest component of the triad in order to establish if it is possible to insert the last measured current variation in the reconstructive triplet. Of course, since three current variations related to three different voltage vectors are required for the complete reconstruction of the LUT, it is not possible to substitute the oldest variation of the triad with one related to a voltage vector that is already present in the reconstructive triplet.
From this point of view, it is wondered that the operation of the machine can keep updated at least three vectors, without introducing a forced update action, that could be, for example, the one produced by the forced algorithm of anti-stagnation analyzed in the Chapter 3.
Another consequence of the fact that every variation contains implicitly an information of the rotor position is that every type of triplet of can support the reconstruction. In the previous analysis it has been noticed that a triplet of two opposite vectors and the zero is completely useless: this is no more true for the actual scheme. As it has already been proved, it is still not possible to update the four current LUT that are not in the triplet but it could be done an update of the oldest member of the reconstructive triplet. Two are the reconstructions that can be computed with this triplet, depending on the oldest vector.
If the oldest member variation is the one generated by $\overline{U}_0$, the difference between the two active opposite variations gives an update of the zero component itself.

On the other hand, if the oldest element is one related to one of the two active vectors, it is possible to update it using the opposite active variation and the zero one, with an expression similar to the (15). This second update possibility is quite interesting from the point of view of the prevention of the stagnation. If a voltage vector is not updated for a half of the electromagnetic period, this construction permits to correct the signs of its current variation and prevent the beginning of the process that causes the loss of the speed control (Chapter 3.1).
In the implemented scheme it is decided to not exploit this possibility and so all the reconstructive processes permit always the update of four current LUT.
In the following figure it is reported how the two components of the current variations are reconstructed by the algorithm during a test performed at a constant speed of 300rpm and a load torque of 4Nm.

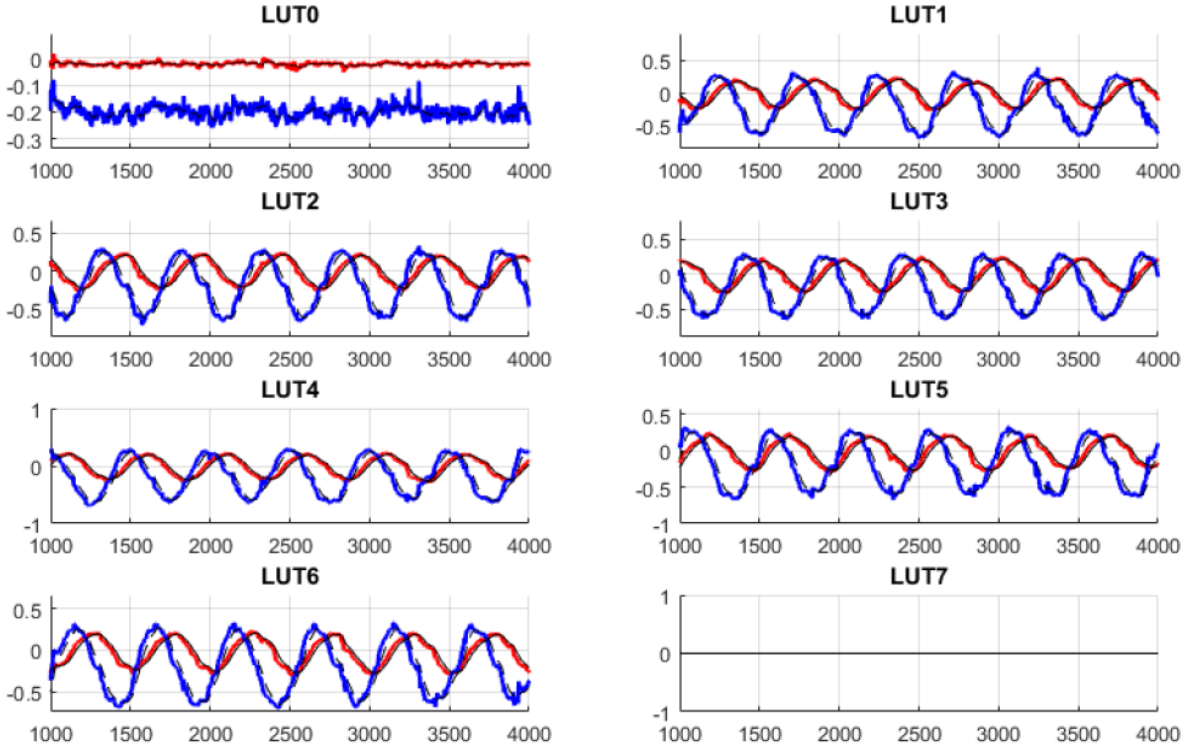

Fig 44: Current LUT reconstruction at a speed of 300rpm.

The zero-voltage current variations are almost constant: the amplitude of this vector depends only on the speed and the torque required to the motor, which are constant during the test. From the point of view of this single LUT, the frequency of update of this variation could be not so high in a constant speed operation.
Since the two zero vectors should produce the same variations, in the implementation of the code it is chosen to use only one of the two. The two vectors, in fact, correspond to the two short-circuit condition of the machine winding, when on the three terminals of the winding is imposed the maximum or the minimum voltage of the DC-bus. For this reason the look-up-table related to the current variation produced by $\overline{U}_7$ is empty (LUT7) and it is used only the one related to $\overline{U}_0$, which is equivalent.

A more interesting result is obtained for the six active vectors variations: these six change in a sinusoidal way during the rotation of the motor, since their expressions (1) depend on the d – q projections of the active voltage vectors. Since the speed is maintained constant during the test, the frequency of the sinusoidal wave is almost constant.
The expected behavior of the active variations is confirmed by the figure, which shows that the sinusoidal wave-form is reproduced with an acceptable accuracy for all the voltage vectors by the innovative reconstructive process. It is reminded that we are using only the current measures to reconstruct the system: the model-based approach for the current prediction guarantee a similar accuracy exploiting also the motor speed and position, its resistive and inductive parameters.
With the reconstructive process it is wondered to not support the scheme with additional anti-stagnation solutions in order to prevent the increment of the current ripple induced by the application of non optimal vectors. From this point of view the Fig 44 shows that the method should guarantee a correct estimation of the signs of all the variations.

4.2 The implementation of the improved Model Free scheme

As all the previous predictive control schemes considered in the thesis work, also the improved Model Free one is implemented in a similar way using DSPACE. The operations that are required every switching period to control the machine are executed in an interrupt that is repeated period by period.
Many parts of the interrupt are almost equal for the three schemes as the acquisition of the measures, the estimation of the current predictions or the evaluation of a certain cost function and the selection of the most suitable voltage vector. Unfortunately, the improved MF scheme requires a much longer time than the other two because of the reconstructive process. This process involves the necessity of identifying the sequence of three vectors with which the current LUT have to be updated and then the computations required for the reconstruction.
Since the time order of the current variations of the triplet is determinant to delete, step by step, the oldest element, the number of combinations of three vectors between seven voltage possibilities, without any repetition that have to be considered is equal to (considering also the 12 useless triplets):

$$D = \frac{n°_{vectors}!}{(n°_{vectors}-3)!} = \frac{7!}{4!} = 210 \qquad (1)$$

This number of combinations (1) is quite big if we consider that there is a time limitation for the interrupt, imposed by the length of the switching period. For this reason it is chosen at first a switching period equal to 200μs, even if the inverter could work at a frequency of commutation of 10kHz. An optimization of the code is anyway required since, with a non optimized code, it could be difficult also to conclude the execution in 200μs.
A common property of all the predictive schemes is, in fact, the following: if it is decreased the length of the switching period, the change of the rotor position in the same time is reduced and so the accuracy of the current predictions is further increased.
The necessity of evaluating all the combinations of triplets and of minimizing the time required for the identification of the triplet are the two aspect that are considered in the optimization of the code of the improved Model Free predictive scheme. It is presented now the solution found for the implementation of this scheme.

All the 210 combinations of current vectors are grouped using two criteria: the first is the type of triplet (between the ones listed in Chapter 4.1) and the second is the index of the first vector of the triplet. As a consequence, it has been created a specific matrix for each starting vector and each type of triplet:

- *cons3...[index]* for the three consecutive vectors;
- *opp2...[index]* for two opposite vectors and another active vector;
- *cons2_zero...[index]* for two consecutive vectors and the zero;
- *nopp2_zero...[index]* for two non opposite vectors and the zero;
- *noppncons*...[index] for three non consecutive and non opposite vectors.

The number of lines of these matrices depends on the number of triplet combinations of the specific group and so it changes depending on the type of triplet and on the first element. Each line of the matrices contains the indexes of the vectors that form one combination. All these matrices are fixed and they represent all the possible combinations that permits the reconstruction of four current LUT: the category of two opposite vectors and the zero is excluded.
Secondly, it is decided to introduce other empty vectors denominated with the same nomenclature used to define the matrices that contains all the triplet combinations: *flag_cons3...[index], flag_opp2... [index], flag_cons2zero...[index], flag_nopp2zero...[index]* and *flag_noppncons...[index]*.
Each line of these second vectors assumes the role of auxiliary flag for the vector combination that is contained in the same line of the previous matrices, in order to permit the identification of reconstructive combination.
Every switching period a new vector, characterized by an index *idx,* has to be considered in order to establish if it is possible to perform the reconstruction of four current LUT, which type of triplet has to be used and which current LUT can be updated.
The principle on which the implemented scheme is based is the following one: when the index *idx* is contained in one of the triplets listed in the lines of the matrices, the related auxiliary flag is incremented by one unit in the related line of the vectors. When in one line of the vectors it is reached the number three, it means that all the vectors that form the triplet have been applied and so the triplet could be used to reconstruct the current LUT. After the reconstruction process, the line of the vector of the exploited triplet is cleared: these lines can be considered as counters with a threshold value equal to three.
The simplest solution to implement the described method consists into considering all the 210 combinations of triplets and evaluate if the actual triplet composed by the last three different vectors is equal to one of them. This solution would be extremely long in fact every switching period 210 comparison should be done for each element: for this reason it is chosen a smart solution, that permits an inferior number of comparisons.
Other two flags are introduced in order to to permit a faster update of the vector auxiliary flags and a faster identification of the triplet, in particular these flags are called *flag#* and *act#*, where "#" represent the index of the voltage vector. Seven are the possible indexes, six for the active voltage vectors and one for the two zero vectors. It is reminded that only one of the two zero vectors ($\overline{U}_0$) is used in the implementation of the improved MF scheme.
The flag *flag#* represents the index of the most recent element of the triplet, the flag *act#* is used to further accelerate the update and then the identification: it is possible to create a simpler but longer process without the use of this second flag.
As a first passage of the code all the flags *flag#* related to the precedent switching periods are cleared in order to re-initialize the update process. On the other hand, the flags *act#* are not cleared: actually the *act#* used for the identification of the triplet in the precedent interval is already cleared after the conclusion of the identification of the vector sequence, at the end of the precedent switching period.
When the new vector *idx* is considered, the two flags *flag#* and *act#* related to the new index *idx* are increased by one unit. With the use of *flag#* it is reached a first optimization of the code: it permits, in

fact, to take into consideration only the triplets that contains the index "#" for the update of the auxiliary flags.
The number of triplets that are considered with this philter is reduced to 84, if the vector *idx* is active, and 72, if the last vector is the zero one. If the last vector is the zero, in fact, all the combinations of three consecutive vector, two opposite vectors and another active one and three non consecutive active vectors would not been considered. On the other hand an active vector could appear in all the types of triplets.
As a consequence, it is immediately evident that the process of update of the auxiliary flags has a different length, depending on the type of triplet: the use of the flag *act#* increases further more the difference of time required to conclude the operations of the interrupt. It is explained at first how these two flags interact in the phase of update of the auxiliary flags.
If the last vector applied is $\overline{U}_3$, we have to consider all the auxiliary flags related to the lines of the matrices that contains a combination with the index 3, found by *flag3*.
We consider in a first moment all the combinations where $\overline{U}_3$ is the first element. In the case of a *flag3,* the flags that have to be updated are the 28 combinations characterized by a 3 in the first position (the vectors are expressed with their index): (3;4;5), (3;5;4), (3;2;4), (3;4;2), (3;1;2), (3;2;1), (3;1;6), (3;6;1), (3;2;6), (3;6;2), (3;4;6), (3;6;4), (3;5;6), (3;6;5), (3;1;4), (3;4;1), (3;2;5), (3;5;2), (3;0;4), (3;4;0), (3;0;2), (3;2;0), (3;0;5), (3;5;0), (3;0;1), (3;1;0), (3;5;1), (3;1;5).
All these combinations require an update of the auxiliary flag but they are not taken into account for the identification of the reconstructive triplet, since $\overline{U}_3$ is the first vector and so they are all characterized by an auxiliary flag equal to 1.
Now we analyze the update of the auxiliary flags related to the combinations of triplets where $\overline{U}_3$ is not the first element: to perform this analysis it is supposed that $\overline{U}_1$ is the vector applied in the precedent switching interval. This fact implies that for the further update we have to exploit also the second flag *act1*.
Between all the triplets that contains $\overline{U}_3$, we have to increment now the related auxiliary flags of the triplets that can reach the amplitude of 2 or 3: one of these combinations could be produce a reconstruction of four current LUT.
The number of flags updated in this second phase is not constant but depends on the vector applied in the precedent interval:

- with an *act1* there are ten auxiliary flags that have to be update, in particular the ones related to the triplets (1;2;3), (1;3;2), (0;1;3), (0;3;1), (1;3;5), (1;5;3), (1;3;6), (1;6;3), (1;3;4), (1;4;3);
- with an *act2* there are ten auxiliary flags that have to be update, in particular the ones related to the triplets (2;3;4), (2;4;3), (2;1;3), (2;3;1), (2;3;5), (2;5;3), (2;3;6), (2;6;3), (2;0;3), (2;3;0);
- with an *act4* there are ten auxiliary flags that have to be update, in particular the ones related to the triplets (4;3;5), (4;5;3), (4;2;3), (4;3;2), (4;1;3), (4;3;1), (4;3;6), (4;6;3), (4;0;3), (4;3;0);
- with an *act5* there are ten auxiliary flags that have to be update, in particular the ones related to the triplets (5;3;4), (5;4;3), (5;2;3), (5;3;2), (5;3;6), (5;6;3), (5;0;3), (5;3;0), (1;3;5), (1;5;3);
- with an *act6* there are eight auxiliary flags that have to be update, in particular the ones related to the triplets (6;1;3), (6;3;1), (6;2;3), (6;3;2), (6;3;4), (6;4;3), (6;3;5), (6;5;3);
- with an *act0* there are eight auxiliary flags that have to be update, in particular the ones related to the triplets (0;2;3), (0;3;2), (0;3;4), (0;4;3), (0;1;3), (0;3;1), (0;3;5), (0;5;3).

In the current example, the number of updated in the second phase would be equal to ten.
Even if the auxiliary flags updated changes for different *flag#* and *act#* it is possible to generalize the fact that, for each active vector there are 28 auxiliary flags to update every switching interval, for the combinations where the vector is the first elements of the triplet. In addition, the number of updates required for the triplets where the *idx* vector occupies the second or the third position of the triplet are ten, for four of the six *act#*, and two for the two remaining *act#*.
Since the zero vector does not appear in all the triplets formed by only active vectors, the update of the auxiliary flags is faster. There are eight required updates when it is not the first element of the triplet and other 24 updates in the first phase.

It is noticed again that the time required for the update of the auxiliary flags is not constant: it is minimum in presence of a *flag0*, with only 32 updates, and maximum in case of a *flag#* related to an active vector and some particular *act#*, with 38 updates.
The result obtained with the proposed solution it is very interesting since 38 updates of the auxiliary flag substitutes the comparison between the actual triplet and 210 possible combinations.
A further acceleration of the auxiliary flags update is possible analyzing the triplets that are actually used in the control of the motor, at least in the most common operative conditions. Since some of the combinations are not so often used, it could be chosen to neglect some updates of the auxiliary flags and so to exclude some types of triplets from the reconstructive process.
In the implemented algorithm it is chosen to not exclude any combination of vectors in order to maximize the probability that a triplet can update the current LUT. Since the improved MF scheme does not use the application of non optimal vectors, the increment of the frequency of update reduce the possibility of the stagnation, without any decrease of the dynamic performances.
The separation of the process that permit to reconstruction of the system from the minimization of the cost function represent another advantage of the improved MF scheme.
After the update of the flags, it is needed the identification of the triplet in the correct temporal order: this process is very fast thanks again to the flags *flag#* and *act#*.
If the flag *act#* of the precedent vector is equal to the *flag#* of the new one, it is not necessary to look for a reconstructive triplet because it means that a voltage vector is applied twice and so it is impossible to reconstruct four current LUT.
If one of the auxiliary flags reaches the threshold value of three in the actual switching interval, it means that the vector *idx* is the last member of one of the combinations and so it is sufficient to analyze the combinations delimited by *flag#*. Since it is known also the precedent vector index, which is *act#*, the only triplets that are considered are the ones with the *flag#* vector as the last element and delimited also by *act#*: this two constrains permits the evaluation of only five triplets.
For example, when we have a *flag3* and an *act1* the only possible reconstructive triplets taken into account are: (1;2;3), (0;1;3), (1;5;3), (1;6;3), (1;4;3). When one of the auxiliary flag related to these five triplets is equal to three, it starts the phase of reconstruction of the current LUT.
Since we need to maintain the information of the time sequence with which the vectors of the triplet have been applied, the indexes of the vectors of the found triplet are saved in another vector *vett_seq*, respecting the temporal order of application. After the update and the identification of the ordered triplet, the flag *act#* of the old vector is cleared: this is the point from which the only not nil *act#* is the one of the most recent vector, that will assume the role of the old vector in the following interval.
Since, step by step, the oldest element of the triplet has to be removed, also all the auxiliary flags that contains this element are cleared. If the element is an active vector there are 56 flags that have to be cleared, if it is the zero vector there are 48 flags: also this process have different length depending on the specific vector.
When this phase of clearing of the flags ends, it is possible to loose the information of the time order and the number of combinations can be drastically reduced. It is obvious, in fact, that the triplets characterized by the indexes (1;2;3), (1;3;2), (2;1;3), (2;3;1), (3;1;2) and (3;2;1) are six combinations of the same three vectors and so the computations that are needed for the four reconstructions are exactly the same.
For this reason, after the clearing phase, the elements of the triplet are ordered on the basis of the indexes of the vectors instead of using the time criteria. Considering the previous example, this new order permits to associate to all the six combinations just one triplet, in particular (1;2;3).
At this point 26 different processes of reconstruction would be necessary for the 26 possible reconstructive triplets involved in the description of the Chapter 4.1: in order to compact the code, this number can be reduced exploiting the similarities between the triplets that belong to the same category.
If we consider the triplets (1;2;3) and (3;4;5) they are both triplets of the type three consecutive vectors and so the geometrical properties exploited in the reconstruction are the same, with a certain

phase shift. In particular, considering the geometrical roles, the vector $\overline{U}_3$ substitutes the role of $\overline{U}_1$, $\overline{U}_2$ is substituted by $\overline{U}_4$ and $\overline{U}_3$ by $\overline{U}_5$.
This peculiarity is justified by the fact that the two triplets are simply rotated of one hundred and twenty degrees and so the indexes of the vectors change but the disposition of the vectors in the $\alpha - \beta$ plane is maintained.
In order to translate this angular rotation in terms of vector indexes it is introduced a coefficient *scale*: this coefficient is equal to the minimum index of the elements of the triplet (which is always the first element, after the previous passage) decreased by one unit.
In the case of the triplet (3;4;5), *scale* is equal to 2, since the first vector of the triplet is $\overline{U}_3$ (Fig 45).

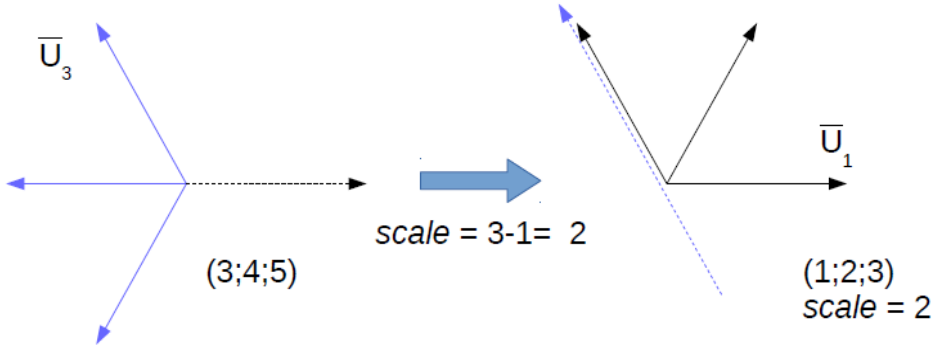

Fig 45: It is represented the computation of the parameter scale and its geometrical meaning.

All the indexes of the found triplet are decreased by a quantity equal to *scale* and the found triplet is associated to an equivalent one that contains the vector $\overline{U}_1$: the information of the relative position between the original triplet and the equivalent one is stored in the coefficient *scale*. The choice of $\overline{U}_1$ is simply a convention: with anyone of the active vectors could be realized a similar association.
If the triplet contains $\overline{U}_0$, it is not possible to apply the described method because the coefficient *scale* express an angular rotation between two active vectors and the current variations due to $\overline{U}_0$ are not influenced by the rotor position. As a consequence it is needed a specific solution for the association to an equivalent triplet when $\overline{U}_0$ is an element of the found triplet.
When this particular condition occurs, it is not taken into account the lowest index of the triplet, that would be obviously 0, but it is considered the second vector index of the triplet, so the intermediate one. The computation of the *scale* factor is performed with this second index and the result obtained has exactly the same geometrical meaning of the previous case.
In addition, the vector $\overline{U}_0$ is not considered in the change of the indexes due to the rotation from the original to the equivalent triplet: the reason of this peculiarity is again the fact that it does not depend on the rotor position.
With this coefficient it is possible to reduce the number of different reconstructive processes from 26 to just 14. In particular, the actual processes used are the ones that exploit the following equivalent triplets:

- (1;2;3), (1;2;6) and (1;5;6), in the category of three consecutive vectors;
- (1;2;4), (1;4;6), (1;2;5), (1;4;5), (1;3;6) and (1;3;4) in the category of two opposite vectors and another active vector;
- (0;1;2) and (0;1;6) in the category of two consecutive active vectors and the zero vector;
- (0;1;3) and (0;1;5) in the category of two non opposite and non consecutive active vectors and the zero;
- (1;3;5) in the category of three non opposite and non consecutive active vectors.

The last step before the update of the current LUT is the re-identification of the four current LUT that has to be updated. After the association of the equivalent triplet, in fact, we have changed the indexes of the triplet and so it is noticed that the updating LUT are not the ones complementary to the element of the auxiliary triplet. For this operation, in fact, we have to consider the original triplet, found by the auxiliary flag.
The current LUT are represented by two vectors, one for the d components of the current variations and another one for the q-components: the indexes of each line of the vectors are saved in the variables nominated *pos*.
Every switching period all these variables are initialized with an index that corresponds to the actual index of the vector line:

$$LUT_D[pos0; pos1; ....; pos6] = [LUT0; LUT1; ....; LUT6]$$

After the computation of the rotation factor *scale* related to the equivalent triplet, all the variables *pos* are incremented of a quantity equal to *scale* in order to restore the correct correspondence between the line of the LUT vectors and the original triplet found.
If a variable *pos* is greater than six, it means that the rotation between the equivalent and the original triplet is greater than 360°. In this condition the variable has to be decreased of six units in order to report the periodical property of the vectors also to the indexes.
It is presented, for example, the case of the previous triplet (3;4;5), associated to (1;2;3). Considering the associated triplet, the lines of the LUT that have to be updated are the ones whose variables *pos* are related to the vectors $\overline{U}_0$, $\overline{U}_4$, $\overline{U}_5$ and $\overline{U}_6$. With the use of the factor *scale*, which is equal to 2, it is possible to understand that the actual variations that could be refreshed are not the ones in the lines 1,5,6 and 7 but the ones in the lines 1,7,8 and 9. Since the last three positions are greater than six, they are decreased of an equivalent electromagnetic rotation and so they become 1,2 and 3, which are the actual lines that should be updated.
Finally, at this point it is possible to correctly update eight variations contained in the two vectors that represent the LUT. The two variations related to the most recent vector applied are updated at the beginning of the interrupt in order to exploit immediately the new measures for the reconstruction.

4.3 Measurement problems

Both the MFPCC schemes have in common the fact that the current predictions for the two future intervals are computed using only the current measures and neglecting all the other information of the model. It is evident that the accuracy and the precision of the current acquisitions are two of the most influencing parameters to guarantee high performances for the control scheme.
The problem of the accuracy of the measures could be not so relevant for the "forced" MFPCC scheme because, if a disturb occurs during the measurement phase, only one wrong current variation is stored. Neglecting the rotation of the machine in the interval, all the other variation maintain their accuracy: this is a direct consequence of the fact that there is only one update of the current LUT per switching period. From the point of view of the propagation of the measurement error, the forced Model Free scheme is more advantageous than the improved Model Free one.
In addition, even if a disturb induces the conditions for the beginning of the stagnation of one vector, the forced update after n_{old} switching period refreshes, sooner or later, all the variations because it readjusts their signs. Since the update is almost periodic, if the disturb is not periodic, it is not so likely that the error will affect also the next update and so it is possible to maintain the control of the motor.
In conclusion, in case of a forced MF scheme, a low accuracy of the measures generates a further increase of the current ripple but it does not compromise the stability of the scheme.
On the other hand, the improved MFPCC is much more influenced by a not accurate measurement, since a wrong acquisition compromise directly one current variation and, indirectly, the reconstructions of four other current variations. The correct knowledge of the reactions of the motor to the voltage vectors is kept only for the two oldest element of the triplet used for the reconstruction, the stagnation does not occur.
A so relevant change of the quantities that are used to describe the system increases significantly the difficulty of predicting the consequences of the disturb: the most optimistic consequence is an increase of the current ripple but, in some particular conditions, the stability of the control could be compromised. In this case, in fact, if all the d or q components have the same sign, the stagnation of one vector can not be stopped: the current update of the current LUT is interrupted if just one vector is applied.
In order to preserve the stability of the scheme, it is important, as a first improvement, to reduce the effects of the disturbs and optimize the accuracy of the measures.
A general solution that can be used to reduce the effects of the disturbs consists into filtering all the current variations that are updated in the LUT but the consequences of the filtering action have to be evaluated very carefully for the reconstruction. The filter, in fact, introduces a further delay in the reconstruction of the current LUT which cause an increase of the prediction error, driven by a higher position error. Unfortunately, the effects of the disturbs are at high speeds (the problem is analyzed in the following chapters) when the role of the position error is more relevant.
As a consequence, the solution implemented on the bench exploit the use of the filters to mitigate the effects of the disturb but their filtering action is very low (τ=0,001).
A second determinant aspect analyzed is the collocation of the current acquisition in the interrupt and the relative temporal position of this phase in the switching period of the inverter.
In the ideal case, the best collocation of the acquisition of the currents is the end or the beginning of the switching interval, when a new voltage vector is applied. These solutions permit to consider the whole variation of current due to the vector applied in the interval. On the other hand, if the acquisition is performed distant from this two instants, the measured variation comprehends the effects of two different voltage vectors.
Moreover, considering an ideal model of the system that comprehends the motor and the inverter, the two positions could be both used for the acquisition, because it is assumed that no disturbs can occur during the whole switching period.

In the real case, the first instants after the beginning of this period are characterized by the presence of the of current spikes due to the commutation of the states of the inverter. As a consequence of this, we can state that in this time interval there should not be performed the current acquisition. The amplitude of the spikes, in fact, can have the same order of magnitude of the current variations that we want to compute using the current measures.
Different solutions of this problem are proposed in literature, one of the more interesting is the one reported in [1]. This solution adopts a single measurement of current at the end of the switching period, so that it is possible to evaluate the whole variation of current in the period without being influenced by the spikes produced during the commutation.
Other solutions developed require two current acquisition every switching period: unfortunately a double acquisition increase significantly the time needed to execute the interrupt. Since the update of the flags, the individuation of the triplet and the reconstructions of the current variations require a quite long time it is preferred to reduce the length of the interrupt at least performing a single acquisition for each period.
A key-aspect of this solution consists in the fact that the time difference between the beginning of the acquisition and the end of the switching interval must be be long enough to conclude all the acquisition operations. If the operation is too long, in fact, it is possible to overcome the end of the switching period and so the solution becomes useless from the point of view of the elimination of the disturbs.
Concerning the relative position between the interrupt and the switching period, another aspect that has to be considered is related to the different time length that is needed to execute the interrupt itself. In the previous chapter (Chapter 4.2), in fact, it has been underlined several time that the number of flag updates changes between the different types of triplets.
The point is that, if the interrupt ends before a half of the switching period, it is possible to apply the voltage vector found by the minimization of the cost function in the interval (k+1)st. If this hypothesis is not verified, the control action has to be postponed of one interval: in stead of individuating the most suitable vector for the (k+1)st interval, it is evaluated the one for the (k+2)nd interval. Since the interrupt can have different time length, it is possible that sometimes it ends before the half of the period and sometimes after.
In order to standardize the time horizon for which the minimization of the cost function has to find the voltage vectors in all the switching periods, one of the two conditions has to be prevented.
With an optimized code as the one described in the previous chapter the time length of the interrupt is much shorter than 200μs, even shorter than 100μs: considering also the longest time required to the interrupt, it always ends before a half of the switching period. In this case it is possible to apply the voltage vector chosen in the interrupt directly in the (k+1)st interval.
If the code is not optimized or it is desired to exploit the maximum frequency of commutation of the inverter (10kHz), the problem previously described occurs. In these cases it is chosen to increment the time length of the interrupt in order to work always with a time horizon of two switching intervals. The solution is based on a controlled extension of the time length of the interrupt.
First of all, during the interrupt, it is timed the length of the process, since the standardization can be reached only with variable time increments.
At this point, the length of the interrupt is intentionally increased of an interval called "*remtime*" equal to the difference between the switching period reduced of a factor one tenth and the time required for the computations:

$$remtime = 0{,}8T_s - T_{computatuions} \Rightarrow T_{interrupt} = T_{computations} + remtime \quad (1)$$

In the following figure it is reported a scheme that represents the solution adopted: in particular it is highlighted the position of the different operation of the interrupt with the respect to the switching period. For sake of simplicity the interrupt is divided in three phases: the acquisition phase, the part

that comprehends all the computations described in the previous chapter (4.2) and the forced time extension *remtime*.

Fig 46: Relative position between the operations of the interrupt and the switching period

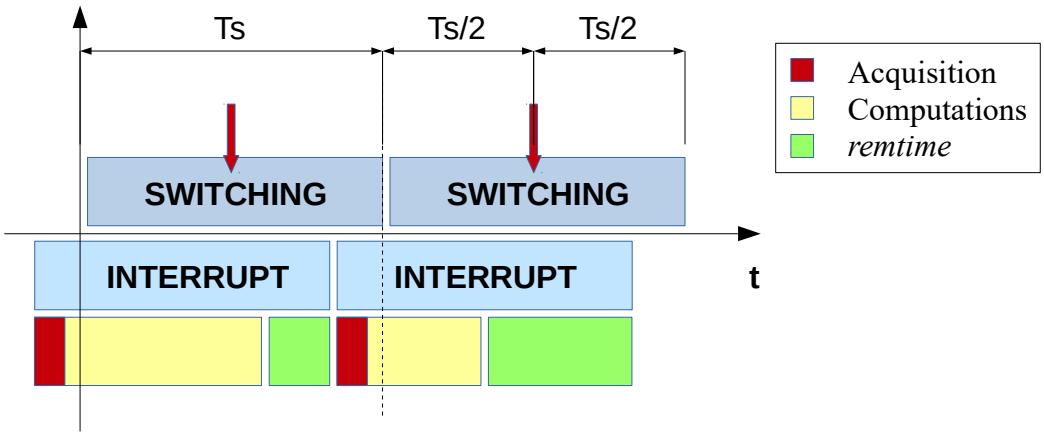

In the time difference between the starting of a new switching period and the beginning of the interrupt all the measurements are acquired. It is obvious that the anticipation of this phase introduces another error in the computation of the current variations. The acquisition, in fact, is intentionally performed with a safe distance from the switching and so the current differences are produced by the application of two vectors. Unfortunately this error can not be deleted because of the problem of the spikes. The shorter is the time required by the measure instruments to perform the acquisitions, the more accurate are the estimations of the current variations.
Since the acquisition phase has almost the same time length in all the intervals, the standardization of the length of the interrupt is obtained compensating the computations phase. With the forced increase of the interrupt length the vectors is always the one for the (k+2)nd interval, even if it could be applied before.
A third type of disturb that can be observed in the wave-form of the current is due to the configuration of the test bench, whose scheme is reported in the following figure (Fig 47).
The two electric machine in the bench are controlled separately by two different inverters: the slave one controls the REL motor under analysis and the master controls a Surface Permanent Magnet (SPM) motor, used to simulate different dynamic conditions, for example a load torque or a torque step.
Excluding the no-load tests, all the others require the use of both the machines and so the interaction between the two inverters can not be neglected.

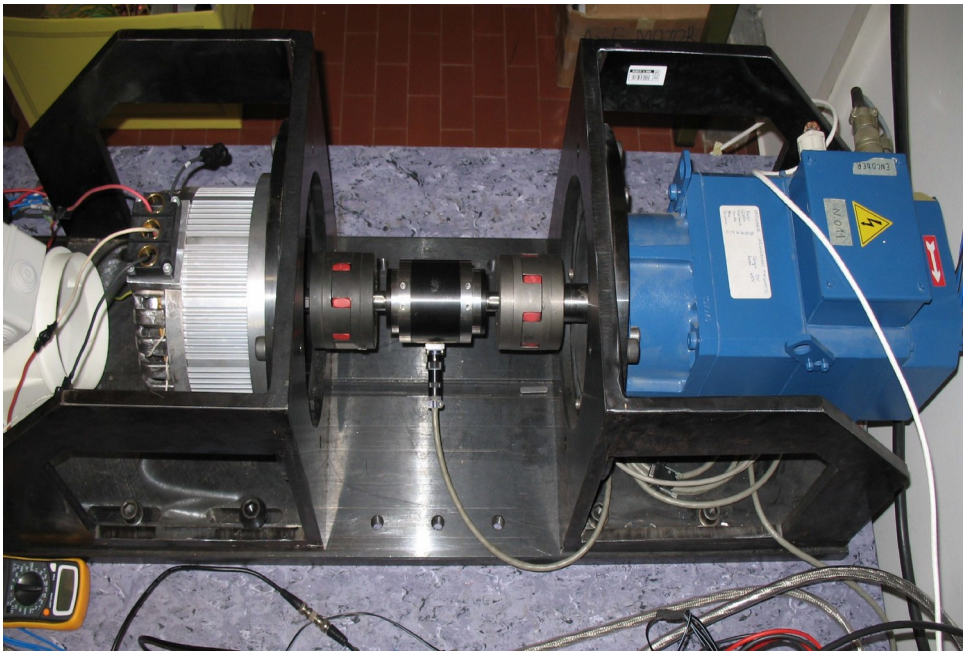

Fig 47: On the left it is installed the REL machine under analysis and on the right there is the SPM that permits to simulate different load conditions

Even if the nominal switching period of the converters are the same, there is a small difference between the two. This means that the beginning of the switching period of the master converter has not a fixed collocation in the switching period of the slave, that controls the REL motor, but it flows period by period.
Since the two inverters are not electromagnetically decoupled, the current spikes produced at the beginning of the switching period of the master affect the current measurements on both the motor winding.
With the solution of the synchronization of the current acquisition sufficiently far from the change of the states of the slave inverter, only the effects of one of the two switching disturbs are solved. The other disturb continues to affect the current measurements: fortunately, since its position is not fixed, it does not affect all the acquisition on the REL motor. This means that a further error could affect some reconstructions of the current LUT but, since the phenomena is not so frequent, the stability of the control scheme is not compromised.
A third phenomena that reduce the accuracy of the current measures is the presence of an omopolar disturb due to the change of the relative potential between the machine and the earth potential. Its amplitude depends on the configuration of the inverter switches and it is comprehended between zero and the voltage of the DC-bus.
A three-phase two levels inverter, in fact, permits to apply a voltage equal to zero or equal to the voltage of the DC bus to each phase of the three phase load connected, in this case the REL motor.
The different zero potential between two switching intervals in which are applied different voltage vectors induce an omopolar current variation that can be observed in the a-b-c reference system. Unfortunately, this disturb could compromise also the d – q quantities if it is used a non opportune measurement configuration.

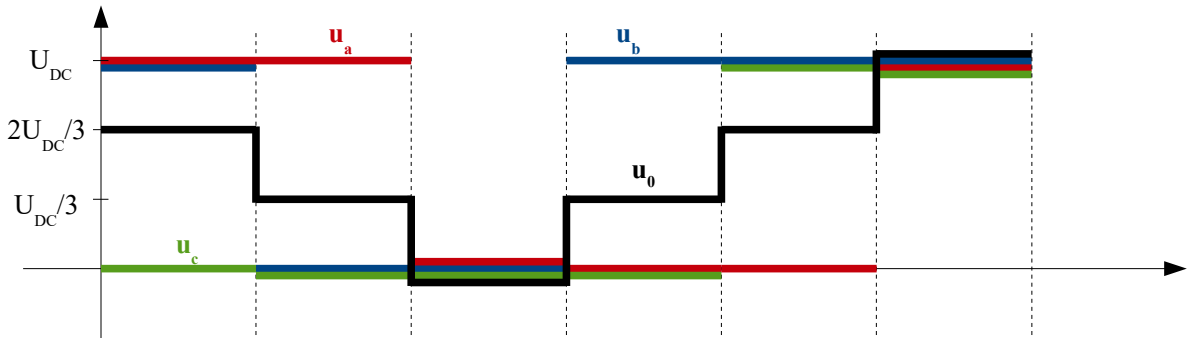

Fig 48 : Different amplitude of the zero potential of the motor for different configurations of the inverter switches.

The problem can be treated considering a three-phase unbalanced system u_a', u_b', u_c' and splitting the triplet in the balanced component u_a, u_b, u_c and the omopolar contribute u_0:

$$\begin{aligned} u'_a &= u_a + u_0 \\ u'_b &= u_b + u_0 \\ u'_c &= u_c + u_0 \end{aligned} \qquad \Rightarrow \qquad \begin{aligned} u_\alpha &= \frac{2}{3}\left(u'_a - \frac{1}{2}u'_b - \frac{1}{2}u'_c\right) = \frac{2}{3}\left(u_a - \frac{1}{2}u_b - \frac{1}{2}u_c\right) \\ u_\beta &= \frac{2}{3}\left(\frac{1}{2}u'_b - \frac{1}{2}u'_c\right) = \frac{2}{3}\left(\frac{1}{2}u_b - \frac{1}{2}u_c\right) \\ u_0 &= \frac{u'_a + u'_b + u'_c}{3} \end{aligned} \qquad (2)$$

The equations evidence that, after the application of the Clark's transformation, the omopolar term is intrinsically separated from the α – β component. As a consequence, in the α – β expression of the machine equations the current variation produced by the change of the motor's potential should not be observed. Since the omopolar component does not change also after the Park's transformation, the statement is valid also in the d – q system, where the control scheme works. This effect is obtained only if all the three current are measured because it is required a correct reconstruction of the zero component. In conclusion, a first method to delete the effects of the change of the motor's potential consists into performing three current acquisition every switching interval.
Another possibility to delete this effect is based on the measure of only two of the three currents and exploiting carefully the property of a three phase system. If it is chosen this solution, it is required a different configuration for the measurements. In this second case, in fact, it is compulsory to not use directly the measures of the three a-b-c components, since it is useless to eliminate the omopolar component:

$$\begin{aligned} u'_c &= -u'_a - u'_b = -u_a - u_b - 2\Delta u = -u_c - 2u_0 \\ u_\alpha &= \frac{2}{3}\left(u'_a - \frac{1}{2}u'_b - \frac{1}{2}u'_c\right) = \frac{2}{3}\left(u_a - \frac{1}{2}u_b - \frac{1}{2}u_c + \frac{3}{2}u_0\right) \\ u_\beta &= \frac{2}{3}\left(\frac{1}{2}u'_b - \frac{1}{2}u'_c\right) = \frac{2}{3}\left(\frac{1}{2}u_b - \frac{1}{2}u_c + \frac{3}{2}u_0\right) \end{aligned} \qquad (3)$$

The equations show that, if only two quantities are measured without considering the presence of the omopolar contribute, the zero component is maintained also after the α-β transformation and so it will appear also in the d – q equations, that are used to control the machine.
If only two currents measures are acquired, it is still possible to not propagate this component in the d – q system but with the acquisition of two (different) differences between two currents, for example $u'_a - u'_b$ and $u'_b - u'_c$. This process permit to compensate the two omopolar component that characterize a single quantity:

$$\begin{aligned} u'_a - u'_b &= u_a + \Delta u - u_b - \Delta u = u_a - u_b \\ u'_b - u'_c &= u_b + \Delta u - u_c - \Delta u = u_b - u_c \end{aligned} \tag{4}$$

From the second difference it is immediately evident that the β component will no more contain the zero component, in fact it depends only on the difference between u_b and u_c. With some manipulations of the expression of u_α it can be proved that also this second component does no more contain the omopolar component:

$$\begin{aligned} u_\alpha &= \frac{2}{3}\left(u'_a - \frac{1}{2}u'_b - \frac{1}{2}u'_c\right) = \frac{2}{3}\left(u'_a - u'_b + \frac{u'_b}{2} - \frac{u'_c}{2}\right) \Rightarrow \\ \Rightarrow \quad u_\alpha &= \frac{2}{3}\left(\left(u'_a - u'_b\right) + \frac{\left(u'_b - u'_c\right)}{2}\right) \end{aligned} \tag{5}$$

This analysis proves that only with a correct choice of the measurement configuration it is possible to remove the omopolar current disturbs due to change of the inverter's states. The solution adopted on the test bench is the one that exploit the acquisition of all the three currents, with any other elaborations of the measures.

4.4 Starting transient

A Model Free Predictive Control scheme always requires a solution for the initialization of the LUT: without the knowledge of the current variations the algorithm is not able to choose the first optimal vector that has to be applied to the winding of the motor.
Since it is not defined any model for the machine, at the beginning it can be considered as black-box, so with the initialization process we try to understand which is the output given by the motor to all the possible inputs. In this case, the input is represented by the application of one of the seven voltage vectors and the output are the two components of the current variation that it produces during a switching period.
The initialization of the scheme should guarantees two requirements: the first one is that at the end of the process all the seven current LUT have to be filled and the second one is the fact that, if it is possible, the rotor position should not change significantly during the process.
Two main solutions are found to initialize the scheme:

- a Model Based initialization;
- a specific initialization process that use only the measured current variations.

The first solution is based on the fact that the Model Based scheme does not need a support for the starting, since the current variations predicted depends on the amplitude of the voltage vectors and not only on the starting current. At the beginning the speed and the currents are zero, so the zero-components of the variations are nil, but the components due to the voltage vectors are predictable if the starting position is known.
As a consequence of this statement, it is possible to use a MB predictive control to choose the first vectors that has to be applied and, after a defined number of switching intervals, switch to the Model Free scheme. In this transient the predictions of the current are computed with the model and so this predictions are used also for the minimization of the cost function.
The effectiveness of this starting solution depends on the type of Model Free scheme adopted.
If we consider a MF scheme with the forced anti-stagnation algorithm, all the voltage vectors have to be applied at least once in order to full-fill the tables of the current variations. The number of step required to complete the knowledge of the seven vectors changes with the operative conditions and the characteristics of the motor.
We can suppose, for example, that a positive speed reference is imposed: at the beginning the torque required to the machine will be the maximum so that both the d and q component of the current start to increase. The most suitable vector able to increase these components changes with the rotor position. Since it is needed to initialize all the current LUT, it is possible to wait a whole electromagnetic period to be sure that all the vectors are applied once. Unfortunately, the time required to complete an entire rotation of the d-axis depends on the inertia of the machine and the load torque. As a consequence of this, it is very difficult to quantify the length of the initialization process in terms of switching intervals. In conclusion the solution that adopt the Model Based approach is not so suitable for this MF scheme.
If an improved Model Free scheme is used, the Model Based starting becomes more interesting. In this case it is required to apply only three voltage vectors, because all the other current variations can be evaluated thanks to the reconstructive process.
Also for this solution it is difficult to understand when the initialization is ended and it is possible to switch to the Model Free predictions, but the number of intervals required is much lower than the previous case. For the simulations performed on the bench, a number of step equal to 200 is selected but also a lower number can be chosen.
A common problem for the two MF schemes consists in the fact that the speed of the rotor increases during the initialization: if a wide angle is covered in this phase, the information of the rotor position can be lost.

In case of the forced anti-stagnation scheme, it could happen that at the end of the starting some vectors are already stagnant and so an updated is immediately required. In order to solve this problem a LUT could be built also for this scheme and so another complication has to be introduced. In case of the improved Model Free scheme, the continuous reconstruction of the LUT permits to keep updated all the current variations.
In conclusion the Model Based starting can be used but it suffers of many disadvantages, so that it is interesting to analyze the possibility of control the motor also during the starting transient without the knowledge of the model.
This second solution is based in the black-box approach so we impose the seven voltage vectors to the machine winding and we store the reactions, in term of current variations. If the seven vectors are applied in a row, the process is much faster then the previous one.
Since at the beginning the rotor speed is zero and the increase of the speed is quite slow with the respect to the switching period, the influence of the position error is almost negligible: if we are able to not move the d – q system, we can obtain a LUT very similar to the ideal one, where all the current variations are measured in the same position.
In order to not move the rotor, the torque that the motor generates due to the applied vectors must be close to zero. Since the torque depends on the product of the two current components, this goal can be achieved keeping the current equal to zero. For example, if the first vector imposed to the winding is $\overline{U}_2$, both the d and q current grows so a positive torque is produced and the d-axis starts to rotate. To compensate this torque and to not modify significantly the rotor position, the second vector that is imposed is $\overline{U}_5$, which should produce almost the opposite current variations and so a negative torque is produced: this torque brakes the previous acceleration.
This technique can be extended for all the other voltage vectors and so after the application of a certain voltage vector it is imposed its opposite. In the following figure it is reported the sequence of vectors used for the starting transient and the change of the speed, which is an indicator of the change of the rotor position.

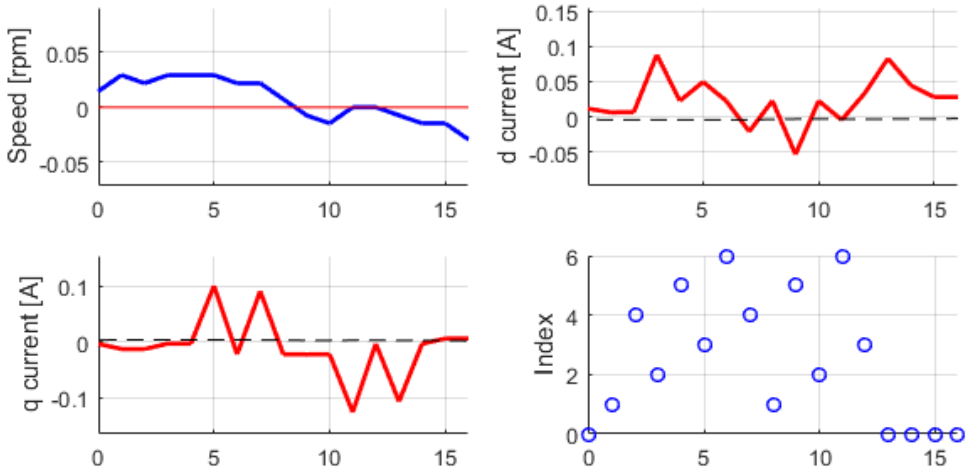

Fig 49: A zoom of the starting algorithm, it is evident the application of all the voltage vectors in order to initialize all the current LUT.

As the picture shows, in the implemented solution each vector is applied just once and so it is the fastest initialization that it is possible to implement using only the measured currents and not the reconstruction. Since the switching period is 200μs long, the process is extremely fast: the

modification of the rotor position is almost negligible during this transient, in fact the absolute amplitude of the speed is almost zero and the positive rotation is compensated by a negative rotation.
An obvious disadvantage of this solution is the fact that the time interval required for the initialization it is lost from the point of view of the speed control. On the other hand, for the MB scheme the initialization process is integrated with the speed dynamic.
Anyway, this second strategy is very interesting and it is suitable also for the forced anti-stagnation algorithm. Since all the variations are measured almost in the same rotor position, it is deleted the risk that some vectors are stagnant when the initialization phase is ended: all the signs of the current variations are correctly predicted.
The separation of the initialization phase from the dynamic of the motor it is not only a disadvantage because the durance of the phase is no more influenced by the operative conditions but it is defined only by the number of times that a vector is applied.
Finally it is noticed that this second approach is the only one that could be defined fully Model Free because it does not require the knowledge of the model of the machine from also for the initialization. This fact permits to simplify the implementation, since for the other case two control schemes are used.

4.5 Steady state operation

The novel approach used to predict the current variations is totally different than the one that is used by the Model Based scheme and so it is expected that its performances are influenced by different parameters.
From the analysis of the MB scheme, it has been understood that a first aspect to consider is the iron-saturation and so the increase of the load torque. More over, the study of the previous Model Free solution has shown that also the speed of the rotor is able to change significantly the performances, since the operating speed influences the periodicity of the repetition of the voltage vector sequence. The analysis is realized starting from a speed of 100rpm, a quite low speed compared to the nominal one, that is around 500rpm. At first it is studied the case of not saturated machine, so the load torque is set to 2Nm: Fig 50 reports the performances of the Model Based scheme, Fig 51 the performances of the Model Free scheme.

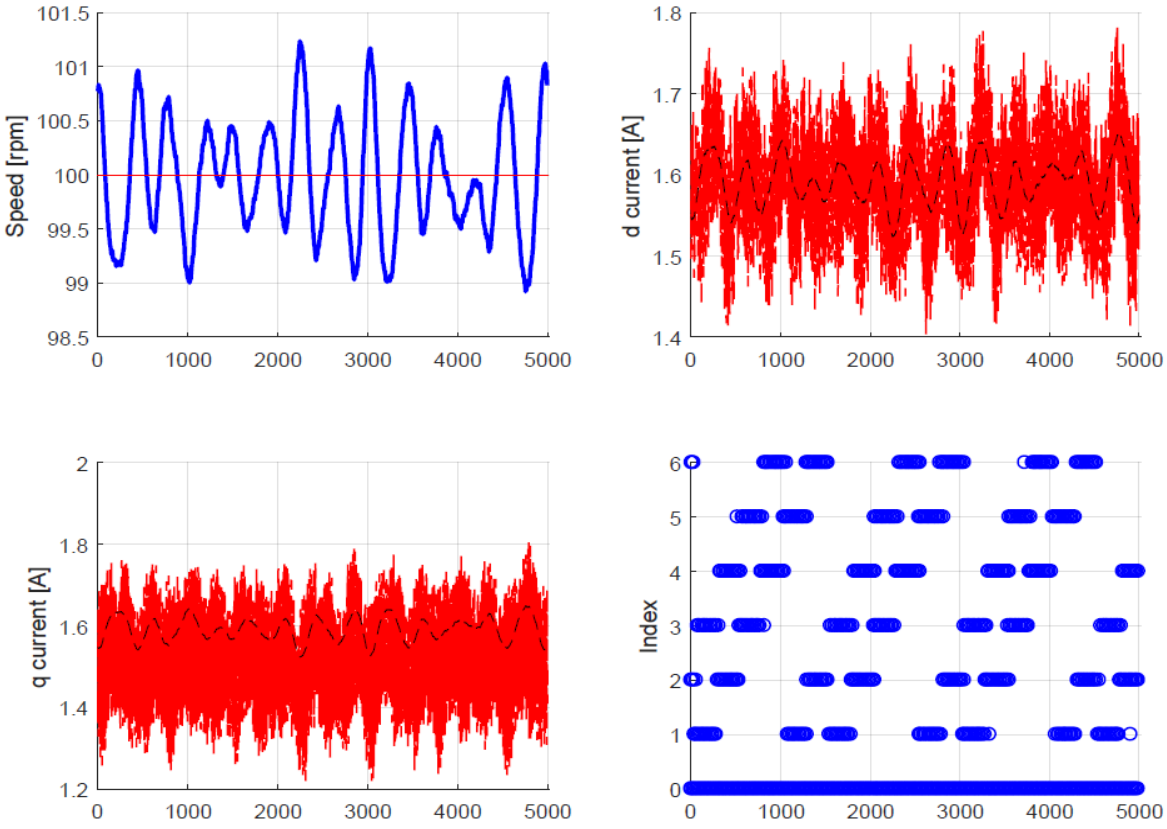

Fig 50: Performances obtained on the bench using the MB algorithm.

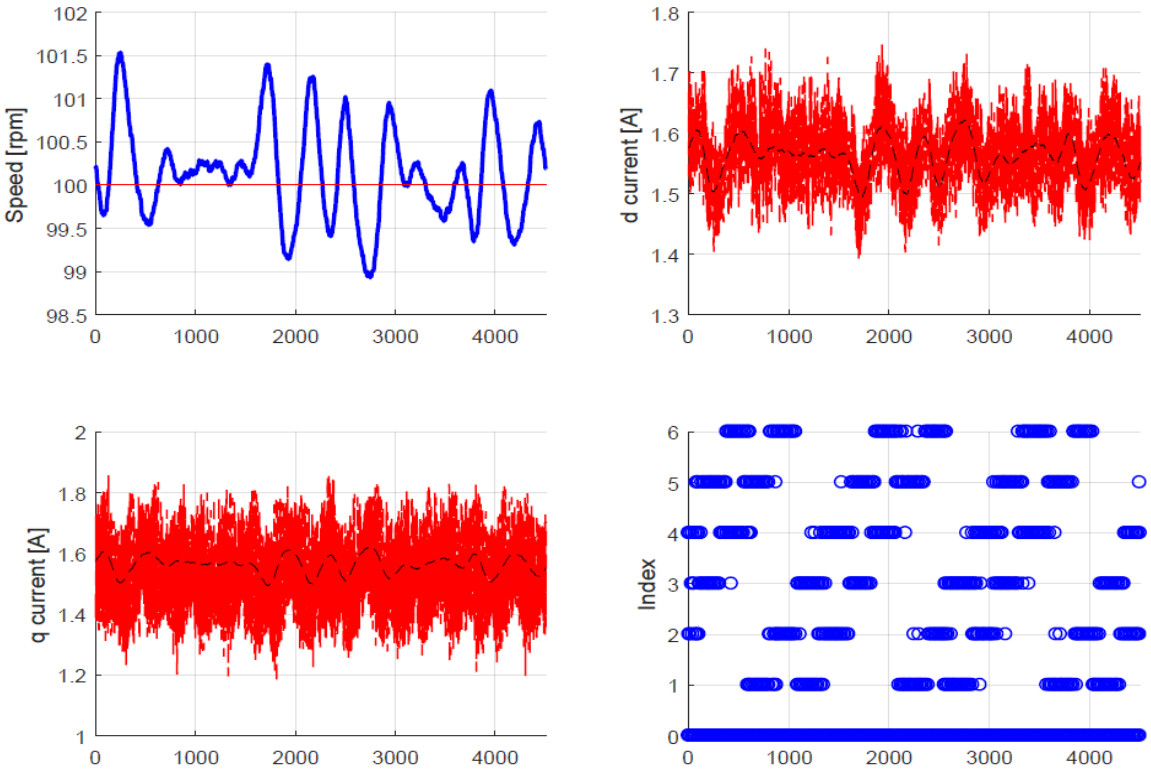

Fig 51: Performances obtained on the bench using the MF algorithm.

The conditions chosen for this simulations are very favorable for the Model Based scheme: iron saturation is almost not present. The consequence of this fact can be observed in the choice of the voltage vectors, which is reported in Fig 10, because the choice is almost the same of the ideal case.
The speed ripple and the current ripple that characterize this solution have the same same order of magnitude of the Model Based scheme. It is interesting to notice the fact that a low torque load requires a low amplitude of the currents so if some measure disturbs are still present they have the maximum weight in these conditions: this regime is one of the most critical for the Model Free scheme. The influence of this disturbs can be observed in the choice of the voltage vectors, which is a slightly different from the ideal case.
Anyway, the performances reached highlights that the reconstruction of the voltage vectors is an efficient solution to the stagnation. The delete of the forced update of the vectors permits to produce a current ripple that is almost the same of the Model Based. This result is very interesting if we consider that we are using only the measured current variations for the predictions: the MB, on the other hand, uses the speed, the motor parameters and the currents.
Even more interesting performances can be noticed if it is increased the load torque produced by the SPM motor to 12Nm: in the following figure it is reported the results obtained on the bench with the two schemes, in particular Fig 52 shows the results of the Model Based scheme and Fig 53 the results of the Model Free.

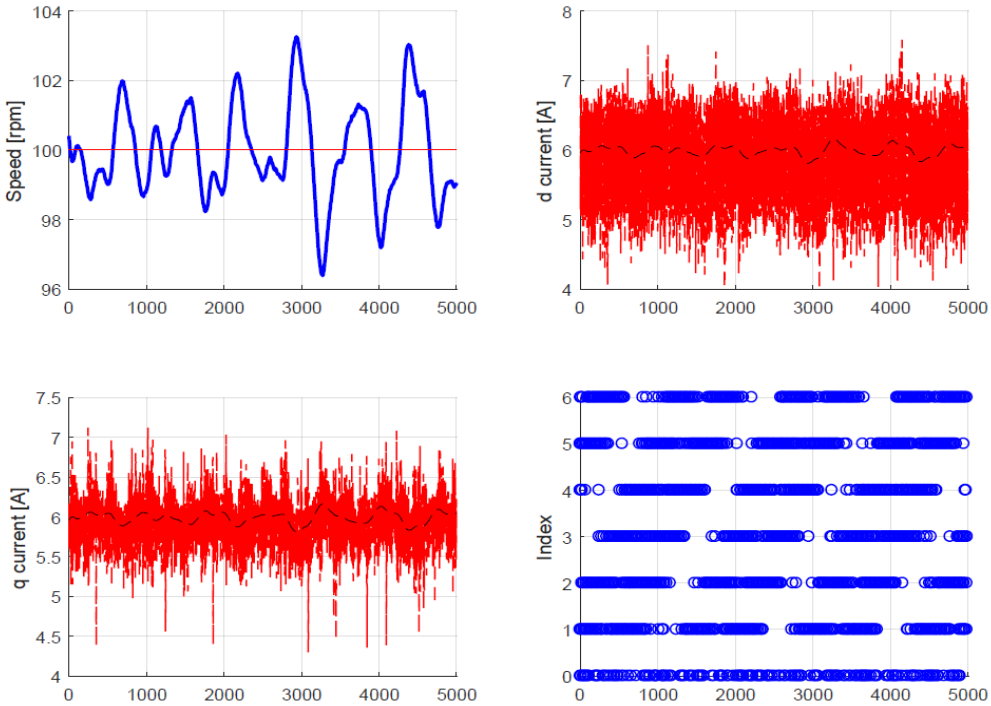

Fig 52: Performances obtained on the bench using the MB algorithm.

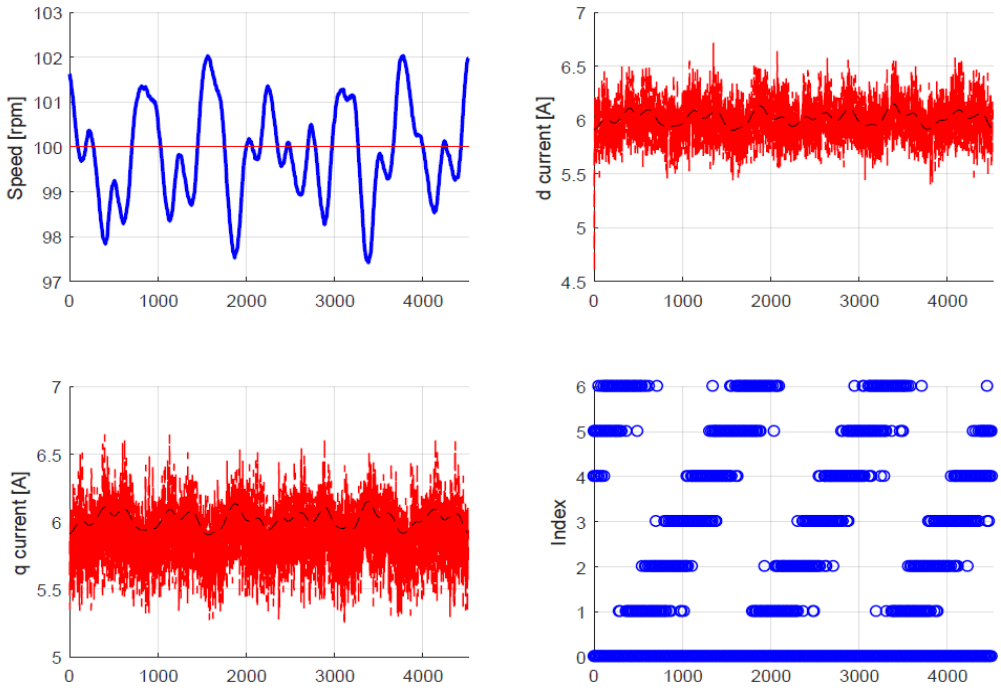

Fig 53: Performances obtained on the bench using the MF algorithm.

It is evident that the Model Based scheme begins to be affected by the prediction error due to the saturation, in fact the zero-voltage vector is applied with a much lower frequency and the sequence of

vectors is more difficult to identify. In addition, a significant increase of the current ripple is observed on the d-axis, the axis with the longer iron path for the magnetic flux and so the one whose reluctance changes more significantly. In the implemented scheme, in fact, it is used a convention of REL motor.
On the other hand, these operative conditions are not so critical for the Model Free scheme: it is confirmed that the MF solutions are more convenient in presence of saturation.
The more evident advantage gained with the Model Free approach is the reduction of the d-axis ripple, which becomes almost one half. A lower current ripple produces also a lower torque ripple and so a reduction of the speed ripple, that is even a bit lower than the ripple of the Model Based scheme. Anyway, it is difficult to observe a change of the speed ripple because the inertia of the motor helps to hide the torque oscillations.
In a previous analysis of the reconstructive process it has been observed that a good reconstruction of the variations is obtained only if the three vectors of the triplet are frequently updated. The study of the steady state operation of the Model Based scheme has evidenced the fact that a sequence of three vectors is always used for controlling the motor, both in case of saturated or not saturated machine. As a consequence of this, a constant speed operation guarantees a frequent update of a triplet of current variations: in particular one triplet of the same type is used every sixth of the electromagnetic period.
The prove of this accuracy is shown also from the sequence of vectors applied to the motor winding: a correct estimation of the variations reduces the ripple, so that the sequence observed is more similar to the ideal case.
Even if in the Model Free Predictive Control the model of the motor is not known, the performances in a saturated regime are higher than the Model Based, since it is not useful to adopt a wrong model of the machine.
In order to understand if the speed of the motor influences the performances of the scheme, it is chosen to perform some tests on the bench at a higher speed, in particular some tests are performed at 300rpm and 400 rpm. From these tests it is observed that there is a relationship between the speed and the performances obtained with the Model Free scheme, in particular they decrease with the increase of the speed.

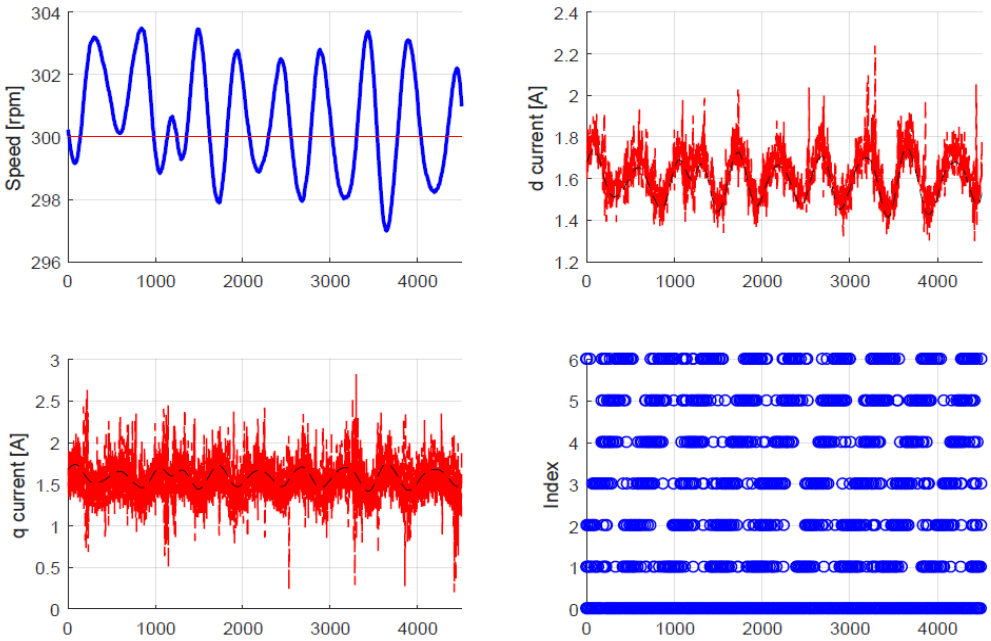

Fig 54

In the figure it is reported the case of a 300rpm speed and 2Nm load torque operation. In these conditions the choice of the voltage vectors is more similar to the behavior of the Model Based scheme in presence of iron-saturation: this means that there are some factors that reduce the accuracy of the estimations.
If we neglect the presence of the disturbs in the measurements, a first reason of this error is found in a more rapid change of the rotor position. The electromagnetic rotation of the voltage vectors covered in a switching period increases with the increase of the speed. As a consequence, the approximation of supposing the three current variations measured exactly in the same rotor position becomes rougher. The effects of the prediction error are evident in fact both the current and the speed ripple are increased.
The accuracy of the prediction is further decreased by a new kind of stagnation that occurs when only two voltage vectors are applied for a quite long period. When only two vectors are used, the reconstruction is blocked and so the information of the rotor position is lost: to understand why this fact happens, we have to analyze the process of the updating of the flags described in Chapter 4.2.
If a process of reconstruction of the current LUT is completed, all the auxiliary flags of the combinations that contain the oldest element of the triplet are cleared, so the counters are reset. As a consequence, starting from the following interval it is impossible to find new triplets between the combinations.
The angular error committed depends on the number of step for which only two vectors are used and the speed of the rotor: the time length of this stagnation multiplied by the motor speed gives the position error.
This stagnation is hidden also in the previous test where it is possible to observe several examples of these phenomena: a zoom of the 3800th and 3820th step permits to evidence the presence of this fact (Fig 54). All the stagnation that characterize this test are 20 or 30 step long, which means that the older vector is affected by a position of almost 5°:

$$\Delta\alpha_{me} = \frac{30\,T_s}{T_{me}} = \frac{30\,T_s n}{60\,p} = \frac{30*200*300}{120*10^6} = 5{,}4° \qquad (1)$$

From the point of view of the stability this fact should not cause problems because an error of only 5° is not able to compromise the predictions of the variations signs.

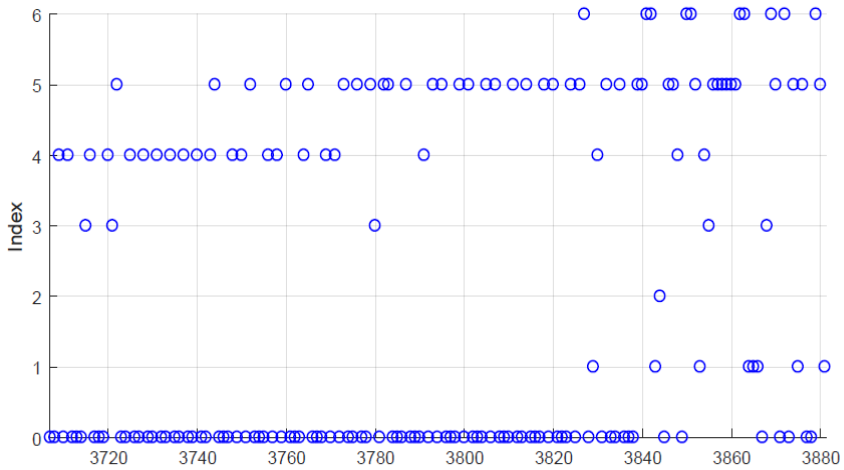

Fig 55: There are two evident stagnations in the figure, one that involves $\overline{U}_0$ and $\overline{U}_4$ and another that involves $\overline{U}_0$ and $\overline{U}_5$

When the torque required is quite high or the speed is reaching its nominal value, the position error becomes higher and a new stability problem occurs and a flux-weakening loop could be required to support the scheme.
This kind of instability is similar to the one that characterizes the Model Free scheme without an anti-stagnation support.
In order to understand the problem, we represent the discrete expressions of the two components of a current variation due to the application of a voltage vector (a convention of IPM is adopted):

$$\Delta i_{d,n}(t_k, t_{k-1}) = \frac{T_s}{L_d} u_{d,n}(t_k) + \frac{T_s}{L_d} \left(-R i_d(t_k) + \omega_{me} L_q i_q(t_k)\right) = \Delta i_d(u_n) + \Delta i_d(u_0) \quad (2)$$

$$\Delta i_{q,n}(t_k, t_{k-1}) = \frac{T_s}{L_q} u_{q,n}(t_k) + \frac{T_s}{L_q} \left(-R i_q(t_k) - \omega_{me} L_d i_d(t_k)\right) = \Delta i_q(u_n) + \Delta i_q(u_0) \quad (3)$$

For the analysis of this problem we are interested into studying the sign and the amplitude of the two when the speed ω_{me} is quite high, close to the nominal speed of the drive.
It has already been studied how the change of sign of $\Delta i_q(u_0)$ with the increase of the speed modifies the sequence of vector applied to the motor winding. The change of sign is caused by the different signs of the resistive contribution and the inductive one: i_d and i_q have opposite signs when the torque of the machine is positive because the machine works in the second quadrant of the i_d-i_q plane.
On the other hand, in the expression of $\Delta i_d(u_0)$ both the two contributions have the same sign so the amplitude of the $\Delta i_d(u_0)$ is always positive and much higher than the $\Delta i_q(u_0)$, for positive speeds.
A high amplitude of the zero-component shifts the mean value of all the active current variations, which have a sinusoidal wave-form.
If the peak value of the sinusoidal wave is lower than amplitude of the shift due to $\Delta i_d(u_0)$, the LUT that contains the d-current variations is filled only by positive values and so if a negative variation is required by the minimization of the cost function, no vector could satisfy the request. This condition of signs is very similar to the one that is observed in a simple MF scheme when a vector becomes stagnant.
In order to emphasis the shift caused by $\Delta i_d(u_0)$, it is possible to increase also the torque load: this permits a rise of the current so an amplification of the zero component, which depends on the speed and the current load.
In the following figure it is shown the reconstruction of the estimated current variations at a speed of 300rpm, but with a load torque of 12Nm. In particular, it is evident the shift of the active vector variation caused by the contribution of the zero-voltage vector: its amplitude is equal to 0,4A, which is very similar to the amplitude of the sinusoidal wave, that is almost 0,5A.
In the scheme implemented on the bench it is used the convention of a REL machine so the two axis are inverted and the problem occurs on the q-axis. Anyway, the problem consists in the fact that for one of the two axis all the current variations have the same signs: obviously the individuation of the axis depends on the convention adopted and the sign of the speed. The two quadrants where the motor can operate are in fact adiacent for both the conventions.

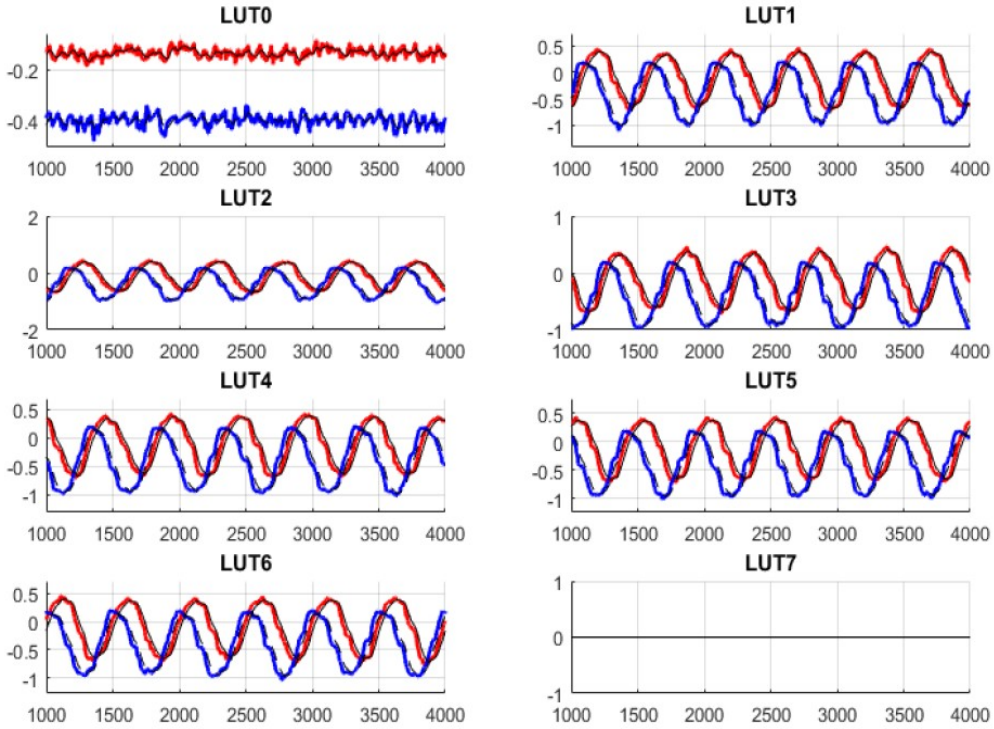

Fig 56: The red curves are the d-axis current LUT and the blue ones the q-axis current LUT.

The impossibility of finding a variation of the opposite sign cause the instability of the drive since it is not applied a vector able to bring the currents closer to their references but the vector that increase the less the error between the currents and their references. Since the same vector continues to be applied the current LUT are no more updated and the stagnation occurs: the phenomena is very similar to the one observed in a simple Model Free scheme. With the improved MF scheme, in fact, it is not directly solved the problem of the stagnation but it is wondered that at least three voltage vectors are sufficiently updated to permit an accurate reconstruction of the other current variations.
This phenomena can occurs both when the machine enters in the flux-weakening regime or when a disturb causes a wrong reconstruction of the LUT. Even if the influence of the disturbs in the current measurements has been reduced with the solutions previously described, some disturbs on the measured currents are still present.
If a convention of IPM is used to describe the motor, the two quadrants of the $i_d - i_q$ plane where the machine works are the second and the third (Fig 57), so the current i_d is negative for both the signs of the torque, on the contrary, i_q can assume both the signs, if the speed of the motor is assumed positive.
The nominal speed Ω_N of the drive can be estimated from the motor's equations, assuming a steady state, MTPA operation and neglecting the iron saturation:

$$\Omega_N = \frac{U_N \sqrt{2}}{p\, I_N \sqrt{L_d^2 + L_q^2}} \qquad (4)$$

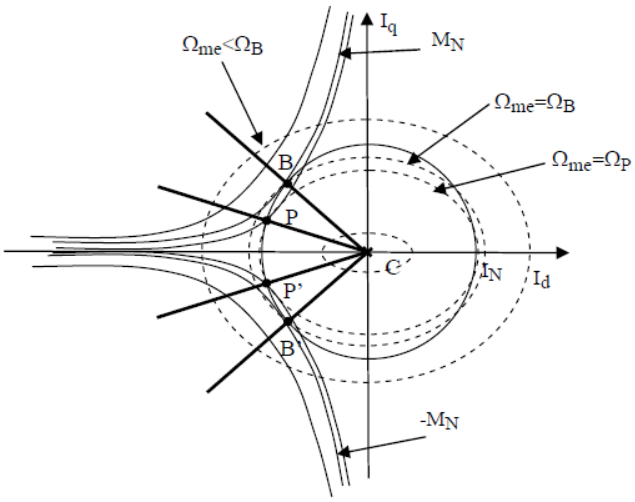

Fig 57: The figure represents the different regimes of the drive, in particular B represent the base point of the drive and P the beginning of the MTPV line

Since the hypothesis on which the formula is obtained are very strict, it is difficult to find precisely the amplitude of this speed because at least the influence of the inductive parameters of the motor is not negligible, as it has been noticed in the Chapter 2.4. The only two parameters that can be directly monitored are the limitation of the maximum amplitude of the current module (I_N) and the voltage module (U_N).
At first it is supposed to control the motor only in the MTPA part of it characteristic and so no voltage loop is used. If we try to overcome the nominal speed, at a certain speed it is found this condition:

$$u_d^2 + u_q^2 = \left(R\, i_d - \Omega_{me}\, L_q\, i_q\right)^2 + \left(R\, i_q + \Omega_{me}\, L_d\, i_d\right)^2 > U_{max}^2$$

where U_{max} is the maximum amplitude of the voltage module that the inverter can impose to the motor. This means that the amplitude of the voltage vectors generated by the inverter are no more able to compensate the resistive and the inductive drop in the motor and so it is impossible to further increase the current. If no disturbs afflict the measurements, when the voltage limitation is overcome, in the LUT it is impossible to find a vector that produces a positive variation of the current vector.
It is interesting to notice that this condition represents the beginning of the flux-weakening regime: this condition could be exploited in order to inserting a voltage-loop to extend the range of speed for which the motor can be controlled.
Unfortunately the same condition could occurs also if a disturb compromise a measure and the reconstruction of the voltage is not accurate.
In addition, several other approximation contributes to reduce the accuracy of the current variations reconstruction. All the variations, for example, are filtered in order to reduce the effects of the remaining current measures, but this action introduce a delay in the reconstruction of the seven LUT: the weight of the delay increases with the speed because of a faster change of the rotor position. Moreover, even the approximation of considering the position constant during the switching period becomes rougher. It is reminded that it is difficult to contract the length of this period under the threshold of 100-200μs, because of the high computational weight of the reconstruction process.
Another fact that can anticipate the critical condition is the stagnation of two vectors: if the current LUT are not updated it is possible that the positive q-axis peaks of the sinusoidal wave-form are cut.

If it is not used a voltage loop, the presence of seven current variations with the same signs causes often the instability previously described. Since there are many factors that can induce this condition, we can state that the occurrence of the stagnation is not completely prevented.
The forced anti-stagnation MF scheme is affected exactly by the same problems at high speeds but the different technique with which the current LUT are updated permits to reach different results.
First of all, the update of the current variations is realized only with measured currents: this avoid the propagation of the disturb in the seven current LUT.
If a disturb occurs during the current acquisition and all the variations on one of the two axis assume the same sign, the stagnation begins and it is applied the vector that produces the slower divergence of the current from its reference.
The forced anti-stagnation action guarantees a fast adjustment of the wrong current LUT. When it is used the strategy that exploits a variable choice of n_{old}, in fact, a low amplitude of n_{old} must be selected for high speed operations. In a period of n_{old} intervals all the variations are updated and so, if one of them have an opposite sign with the respect to the others, it is used to stop the divergence: the maximum length of a stagnation is fixed by the parameter n_{old}.
As a consequence, for this type of MF scheme the stability can be guaranteed also for higher speeds than the ones reached by the one characterized by the reconstruction of the LUT. With the improved MF solution, in fact, it is hazardous to overcome the speed of 400rpm, on the other hand, with the forced MF method it is possible to control the motor till 500rpm (Fig 58). Only with the second solution it is possible to cover almost all the operative conditions in which the MB scheme is able to control the machine.

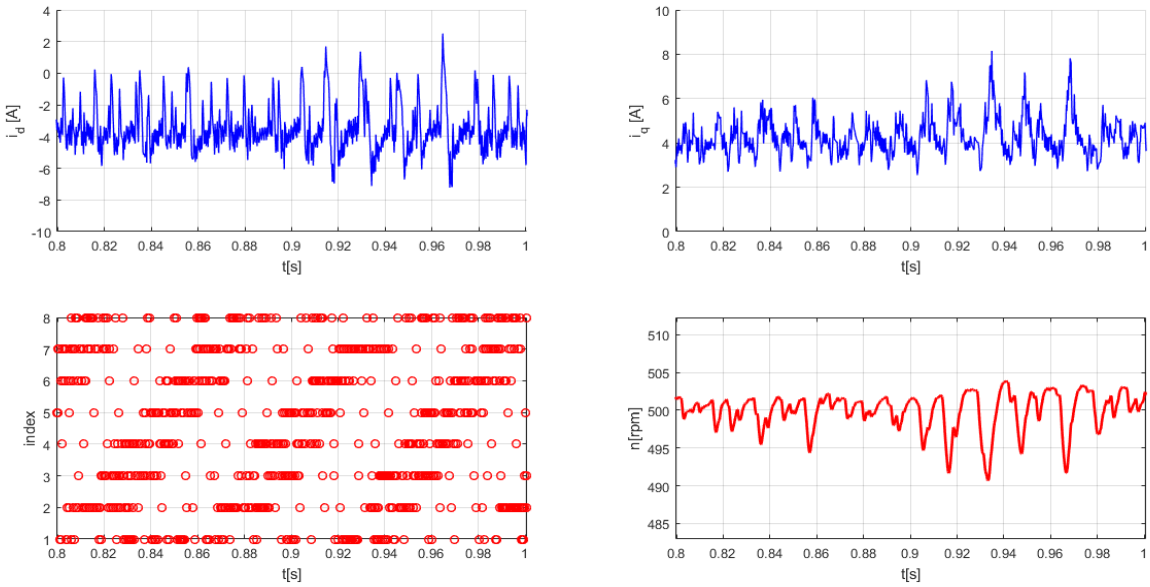

Fig 58

Since it is required a very frequent update of the current LUT in order to maintain the stability, many non optimal vectors has to be applied: this is the typical disadvantage that afflicts the forced anti-stagnation solution. As it is has been done for the low speed operations, it is interesting to look for other supporting conditions to increase the performances of the scheme.
In Fig 56 it is evident that already for a speed of 300rpm the q-current variations are significantly shifted by the zero current component: the shift is so high that, instant by instant, only one or two

variations are positive and their amplitude is also not so wide with the respect to the negative ones. It is evident that these two positive variations could play a key role in the increase of the performances of the schemes.
If the load torque and the operative speed are constant, the motor has to generates a constant torque and so the drive has to track two almost constant current references. As a consequence, the one or two voltage vectors that cause the positive q variations are always frequently updated, because they have to be used for the tracking of the q reference, when the q current is under its reference.
When one of the vector counter reaches its threshold value n_{old}, a stagnant voltage vector is forced to be applied. Because of the shift, this vector produces always a consistent decrease of the q current. The unused vectors, in fact, should be the ones that produce the highest reduction of the q current.
The effect of this variation could be not so negative, if the q current is higher than its references, on the other hand, it is totally negative if it would be needed a variation with an opposite sign. The occurrence of the second case contributes to amplify significantly the current ripple, as it is immediately observable in the previous figure. A so high current ripple compromises also the performances of the speed control of the rotor.
Since both the current reference and the measured current are known in the (k-1)st interval, the occurrence of the second update condition can be prevented introducing a simple check on the predictions.
Every time that a current LUT has to be updated and so the application of the relative voltage vector is forced, it is checked if at the end of the of the k(th) interval the predicted q current is under or over the reference. If the predicted current is over the reference, it means that it is required a negative q variation in the (k+1)st interval: since all the stagnant voltage vectors produce a variation with the same sign, the one whose counter has reached n_{old} can substitute the one chosen by the minimization of the cost function, without a significant increase of the current ripple. On the other hand, if the condition is not verified, the update is postponed to the following intervals.
The introduced condition does not compromise the stability until the nominal speed of the drive: the only two hypothesis on which this method is based are the presence of two variation with different signs and the fact that the positive variations are frequently updated. Unfortunately, when the nominal speed is overcome, all the q variations are negative and so it is no more possible to increase the q current. Since the first hypothesis is no more valid, the stagnation occurs and the control of the motor is lost.
This solution should permit a decrease of the ripple without the utilization of any parameter of the motor and so it can be considered still a Model Free scheme. Both this solution and the one found for the low speed operation are not completely model free because all the considerations on the amplitude of the components of the two current variations are based on the machine equations.
In the following figure it is reported a simulation in the same operative conditions of the one reported in Fig 58 but, in this second one, it is exploited the condition just described, as a support to the simple use of a low amplitude of n_{old}.

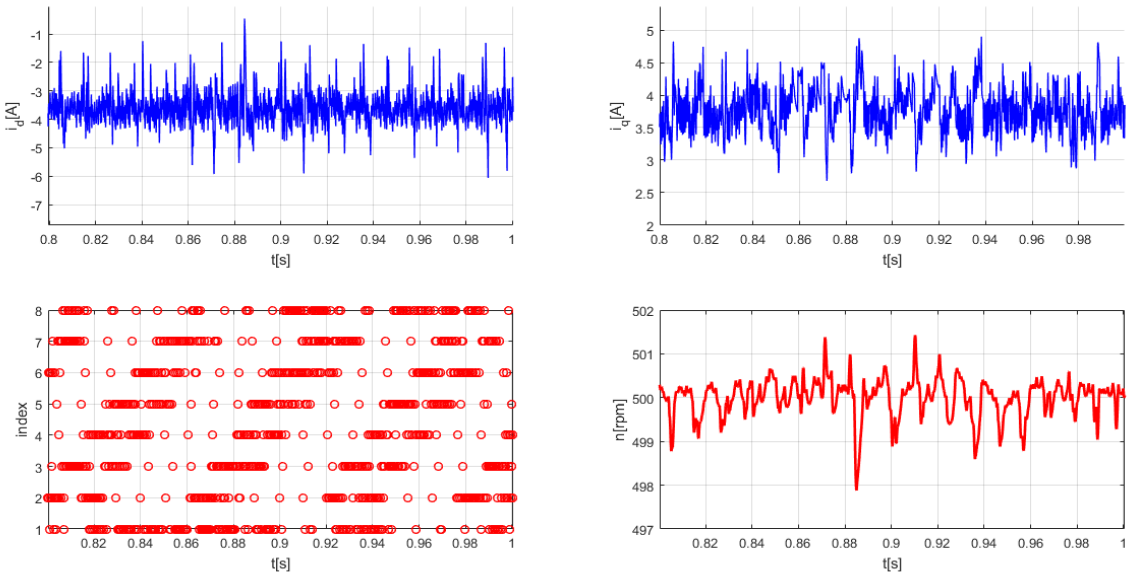

Fig 59

Even if there are no significant changes of the chosen voltage vectors, the results obtained with this solution are extremely interesting. Since the condition is obtained from the optimization of the q-axis reference tracking, the most evident improvement is reached on this axis, with a reduction of the current ripple of almost one half. In addition, the reduction of the q-axis ripple generates indirectly a reduction of the current ripple on the other one. This unexpected result is due probably to the utilization an inferior number of vectors to maintain not so wide the ripple on the q axis.
If the q-current is closer to its reference, in the minimization of the cost function the weight of the d-axis current error is increased. As a consequence of this, more vectors are used to optimize the tracking of the d-reference.
From the point of view of the speed ripple, both the solutions are characterized by good performances: the relative ripple in both the cases is much lower than the one observed in case of a low speed operation. The introduction of the condition for the q current represents, anyway, a consistent improvement, with which it is obtained a further reduction of the speed ripple of a factor higher than one half.
It is interesting to notice the fact that the condition on the relative position between the k(th) current ad its reference could be adopted also in a wider range of operative condition. A shift in the q current variations is always present when the speed is positive and the load brakes the rotation of the motor. The decrease of the current ripple for lower speeds is obviously not so significant, since the shift has an amplitude that is directly proportional to the speed.
In addition, the exploiting of the shift due to the zero variation for the improvement of the performances of the forced anti-stagnation MF scheme requires a continuous monitoring of the signs of the speed and of the currents. The axis on which the shift is more relevant depends on the sign of the load torque and on the verse of the rotations
In the following table are reported all the possible combinations obtainable by the machine equations, with a convention of a REL motor. With this convention, the d-axis is identified with the one on which flows the greater part of the magnetic flux, so the d and q axis are inverted.

ω_{me}	M_{brake}	$-R\,i_d$	$-R\,i_q$	$+\omega_{me} L_q\, i_q$	$-\omega_{me} L_d\, i_d$	Shift
> 0	> 0	< 0	< 0	> 0	< 0	q-axis
> 0	< 0	> 0	< 0	> 0	> 0	d-axis
< 0	> 0	> 0	< 0	< 0	< 0	q-axis
< 0	< 0	< 0	< 0	< 0	> 0	d-axis

Table 4: Zero shift

When the load torque opposes the rotation of the motor, the shift characterizes the q axis, on the other hand when the load accelerate the rotor the shift characterizes the other axis.
Since the computational weight of the forced anti-stagnation MF scheme is not so high, the evaluation of these simple sign conditions could be done in order to increase the performances of the scheme. This action permits to obtain a partial compensation of the current ripple that still affects the scheme but it is not a definitive solution because of the necessity of a forced update for the stability.
The condition that amplifies the effectiveness of this method is the presence of a consistent zero component on one of the two components of the current variations. In a low speed operation this hypothesis is not verified and so the improved forced update behaves almost as the simple forced update. The current tracking is characterized by the typical current ripple that afflicts this regime, that is studied in Chapter 3.3. For this range of speed the solution that exploits a smart use of the zero vector produce more relevant results.
Even if we neglect the solutions found to improve the performances for specific operative conditions, the forced MF scheme represents the most interesting MF solution from the point of view of the stability. The key factor that guarantees this property is the continuous check of the situation of the each current variation directly on the motor winding every n_{old} intervals.
This is the only found method able to take into account correctly the information of the change of the rotor position and to solve directly the problem of the stagnation.
On the other hand, the approach used for the improved Model Free scheme is not based on the resolution of the problem of the stagnation but, in same way, it is more similar to the Model Based approach. The reconstruction, in fact, is obtained exploiting the mathematical properties that relates the seven current variations, even if any motor parameter is involved in the reconstruction process.
In the MB scheme, the change of the rotor position in every switching period is taken into account in the estimation of the voltage component of the current variation, on the contrary it is totally ignored in the case of the improved MF scheme.
As a consequence of this fact, nothing can stop the stagnation of one vector after the first update of the current LUT: this is another reason that explain the higher sensitivity of the improved MF scheme to the stability.

4.6 Dynamic performances

The steady-state performances of the improved Model Free scheme are different in different operative conditions, because of the determinant influence of the rotor speed and the torque load. In a dynamic operation both these two parameters change so it is expected that the acceleration or deceleration transient can be influenced too.
The first kind of test performed on the machine is a speed ramp: the parameters that influence this transient are the amplitude of the ramp and its time length and, obviously, the load torque that brakes the motor.
From the previous analysis of the constant speed operation, it is expected that the phenomena that can compromise the stability of the control scheme during these transients are the two observed, so the presence of disturbs in the current acquisition and the construction of seven current LUT with all the current variations characterized by the same sign for one of the two axis.
These considerations suggests that the motor should not have problems in the tracking of speed ramps characterized by a low amplitude, eventual stability problems should occur only for higher final speeds.
On the other hand, the time length of the ramp is a parameter whose effects should be observed in the fast ramps. In these conditions, in fact, it is interesting to verify if the behavior of the cost function's minimization on the two axis is different in presence of a big error between the currents and their references. Because of the considerations made in the Chapter 2.2, in fact, it has been chosen a function that does not compensate the anisotropy of the REL motor, so it should be analyzed if this fact creates stability problems.
It is considered, at first, the influence of the ramp amplitude on the performances of the scheme. For this the purpose it is presented a comparison between the behavior that characterizes the improved Model Free method (Fig 60) and the one of the Model Based (Fig 61). As a first case, it is considered a ramp of 100rpm and 0,5s long characterized by the presence of a braking load torque of 5Nm.

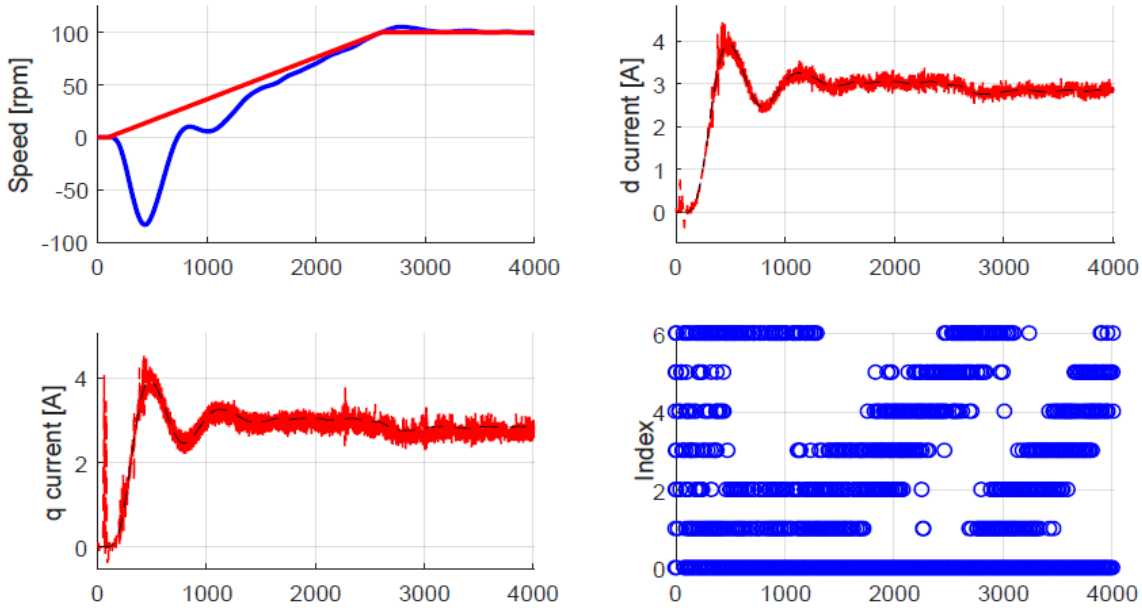

Fig 60: Performances of the improved MF scheme

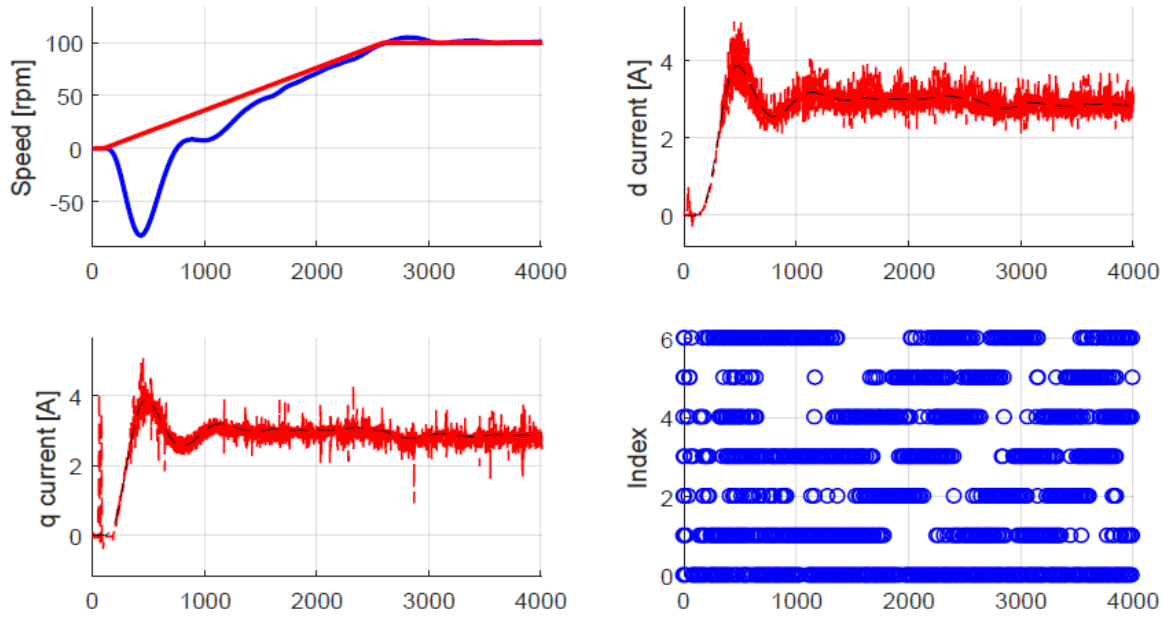

Fig 61: Performances of the Model Based scheme

The capability of keeping the speed reference depends essentially on the characteristic of the motor, in particular its inertia, and the two parameters of the PI controller inserted the speed loop, which is the same for the two cases. As a consequence, the two speed profiles obtained with the different schemes are very similar.
During the ramp a significant torque is required to accelerate the motor and so the effects of the iron saturation are observable from the first instants, even if the load torque is not so high. A prove of this fact is found in the almost random utilization of the voltage vectors by the MB scheme in the first 3000 switching periods, which represents the accelerating part of the transient.
To obtain a definitive prove of this fact, it is needed an analysis of the prediction error that afflict the two solutions. Instead of adopting an instantaneous approach to represent the error and plotting its amplitude for each switching period, as it is done in the Chapter 2.4, it is possible to introduce two integral square errors, denominated ISE, one for each axis. These parameters are computed as the sum of the square of all the prediction errors committed in every interval:

$$ISE_d = \sum_{test} (i_d - i_{d,pred})^2 \qquad (1)$$

$$ISE_q = \sum_{test} (i_q - i_{q,pred})^2 \qquad (2)$$

Even if the relative weight of the error with the respect to the amplitude of the current variation is lost, these two parameters are very effective to compare the performances of different schemes. Since in the implemented scheme it is adopted a convention of REL machine, the axis that is more strongly influenced by the presence of the iron saturation and the consequent change of the relative inductance is the d one.
In the case of the speed ramp previously described, the difference between the parameters ISE between the schemes on both the axis is consistent (Fig 62): the improved MF scheme offers a more accurate description of the system. A so high difference between the two solutions further proves the presence of an error in the model exploited by the MB technique for the estimation of the current variations, caused by the iron saturation. Without the adoption of an adaptive mode for the MB

scheme, in fact, it is impossible to take in consideration the variation of the motor inductive parameters.

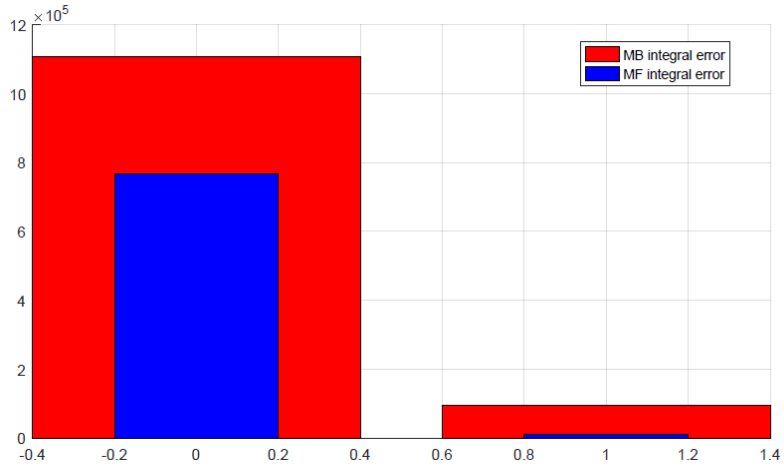

Fig 62: The first two bars represent the integral square error ISE on the d axis, the second two the error on the q axis

As in the case of the steady state operation, one of the most evident effects of the prediction error is the increase of the current ripple in the tracking of the references: in the ramp under analysis the difference is particularly evident on the d-axis. On the other hand, on the q-axis the improvement of the accuracy of the current predictions is not so effective, since the integral error ISE_q that characterize the MB scheme is already not so wide (second bars of the Fig 62).
This permits also to understand that the correlation between the prediction error and the current ripple is not so obvious. In fact, even if the relative reduction of the integral prediction error on the q-axis is greater than on the other, there are no significant positive effects on the q-reference tracking. The amplitude of the ripple, in fact, remains almost the same, it is obtained only the elimination of some current spikes.
As a consequence, a further increase of the accuracy would not guarantee a better tracking on the q axis, since the amplitude of the ripple is close to the minimum permitted by the seven current variations.
A non negligible integral error is still present on the d-axis: it is impossible to eliminate the effects of all the approximations introduced to build the reconstructive process. The weight of the simplifying hypothesis are, anyway, lower than the utilization of a not accurate d – q model of the motor. This fact is proved also by the change of the sequence of vector
From the constant speed analysis of the drive, it is expected that the increase of the amplitude of the ramp could compromise the stability of the scheme, if it is reached the critical situation in which all the current variations have the same signs.
In order to analyze if this phenomena could occur, the amplitude of the ramp is increased from 100rpm to 300rpm and then to 400rpm, keeping the same load torque and the same durance of the ramp. At first it is considered the behavior of the Model Based scheme, in order to evidence the differences with the respect to the previous ramp: it is commented only the test with an amplitude of 400rpm, since for the other one the considerations are similar to the ones made for the 100rpm ramp.
As the Fig 63 shows, also this transient is not problematic for the Model Based scheme and the considerations that we can make are the same of the previous test in term of the presence of the iron saturation and of a significant current ripple, especially on the d-axis. In the last part of the tests, when

it is reached the final speed, it is evident the reduction of the frequency of application of the zero vector: this represents another prove of the presence of the prediction error.
One of the most interesting advantage of the Model Based solution is the fact that, even if the prediction error is very high, the control continues to be maintained also in the most difficult transients.

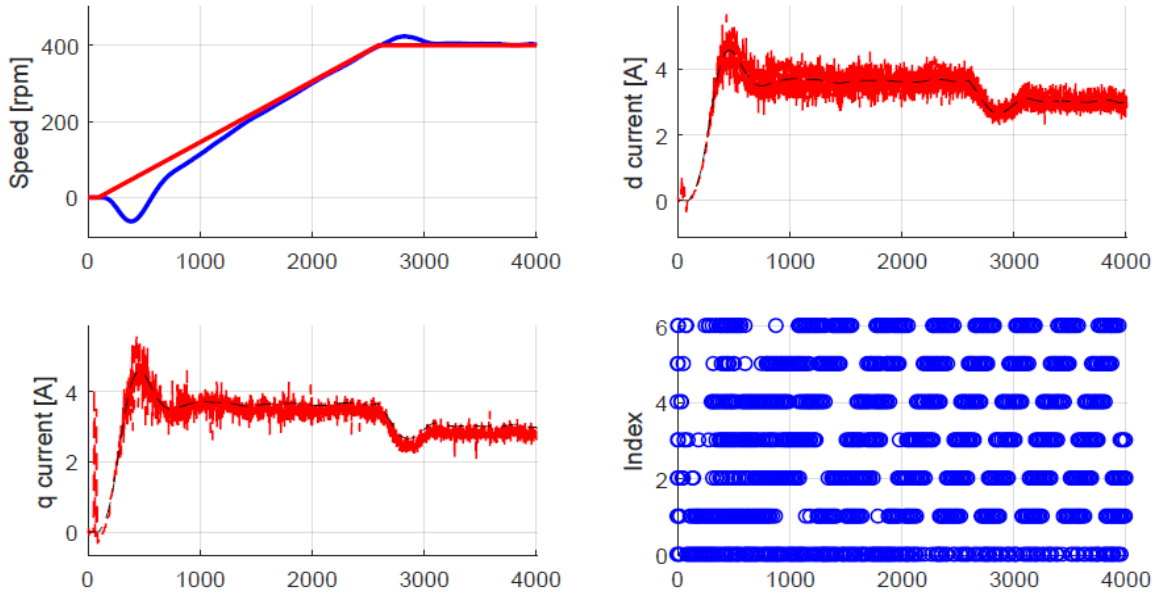

Fig 63

Since no voltage loop is introduced in the MB scheme and the speed tracking is maintained, the limit of the nominal speed of the drive is not overcome. If the approximations introduced for the reconstruction process are not so rough, also the improved Model Free scheme should be able to control the motor.
An alternative way to understand if this condition is reached consists into reconstructing the seven LUT with the measured current, as it is done by the improved MF scheme, but controlling the machine using the Model Based approach (Fig 64). With this strategy it is possible to monitor their wave-form even if the reconstructive process is not directly involved in the control of the motor. From the point of view of the stability it is sufficient to reconstruct the amplitude of the current variations on the axis that is characterized by the higher zero component.
In the figure reported it is evident the change of the amplitude of the shift produced by the zero current variation and the progressive reduction of the peaks of the sinusoidal wave-form. These peaks permit, anyway, to guarantee always the presence, at least, of one positive variation: this is the reason why the q-axis tracking does not present any problem for the MB technique.
Another important information obtained from the reconstruction is the influence of the disturbs that afflicts the current acquisitions. The sinusoidal wave-form are, in fact, is characterized by several spikes or flat parts.
From the point of view of the MB scheme, these disturbs together with the adoption of a wrong model of the motor contribute to the reduction of the accuracy in the current predictions. A sinusoidal form is intrinsically guaranteed by the voltage component of the variations.
If the motor is controlled with the improved MF method, the situation is totally different since the variations are directly used to the control without any other elaboration, except the filtering.

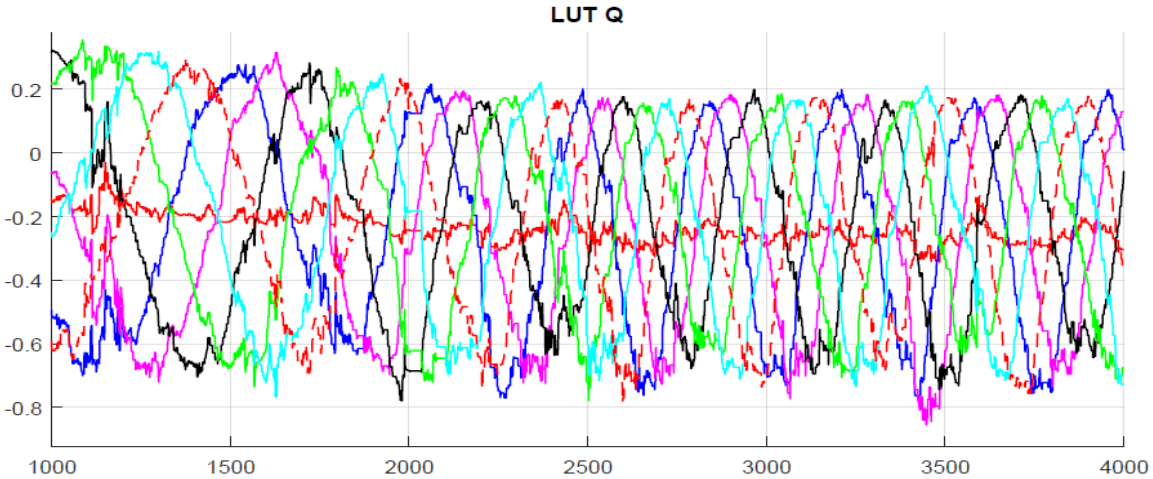

Fig 64: The seven curves represents the reconstruction of the q-axis current LUT. The zero zero variation can be easily recognized since it is the only one characterized by a non sinusoidal profile.

Because of all the considerations made it is expected that also the improved Model Free scheme should be able to track a speed ramp with an amplitude of 400rpm. Unfortunately, in the tests performed on the bench it has never been obtained a correct tracking of the ramp: the Fig 65 represents one of the failed tests.
In the first part of the ramp the behavior of the improved MF scheme is very similar to the one manifested in the 100rpm ramp. Also in this case it is reached a consistent decrease of the current ripple, with the respect to the MB solution thanks to a more accurate evaluation of the current variations. The reduction of the prediction is again particularly evident on the d-axis: the instantaneous prediction error is decreased of a factor higher than one half.
The amplitude chosen for the ramp appears as a border line value from the point of view of the stability, in fact the control is lost almost at the end of the transient. Actually, with a zoom of the time window in which the control is lost, it is possible to understand that the undesired decrease of the speed begins just before the conclusion of the ramp.

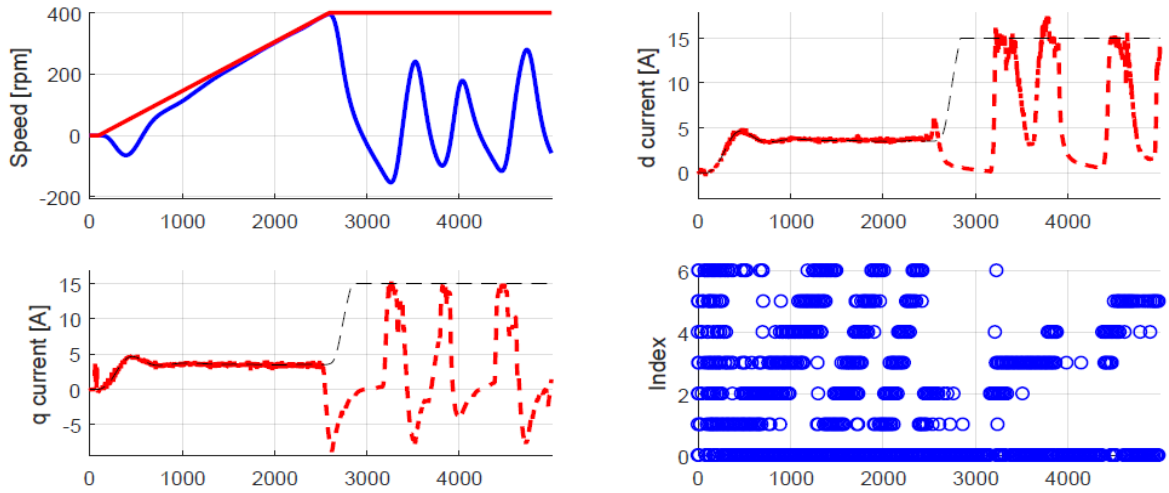

Fig 65: Stability problems caused by a too high amplitude of the speed ramp.

It is reminded that the essential difference between the improved MF scheme and the Model Based one is the use of the model to estimate the current predictions. With the support of the model it is intrinsically taken into consideration that, if the motor is rotating, all the intervals are characterized by a different electromagnetic configuration. On the other hand, with the improved MF scheme the system is described in a discontinuous way. In all the intervals in which it is not possible to reconstruct the current LUT, the electromagnetic configuration is considered the same of the previous one.
It has been proved that this approach is more accurate than the utilization of a wrong model: a higher precision is unfortunately not a positive fact from the point of view of the stability,
Since the control action is based on the reconstruction of the current variations, the origin of the instability has to be found in the current LUT. In particular we focus the attention on the analysis of the moments when the control is lost (Fig 66): as for the previous figures in blue it is reported the q component of the variations and in red the d ones.

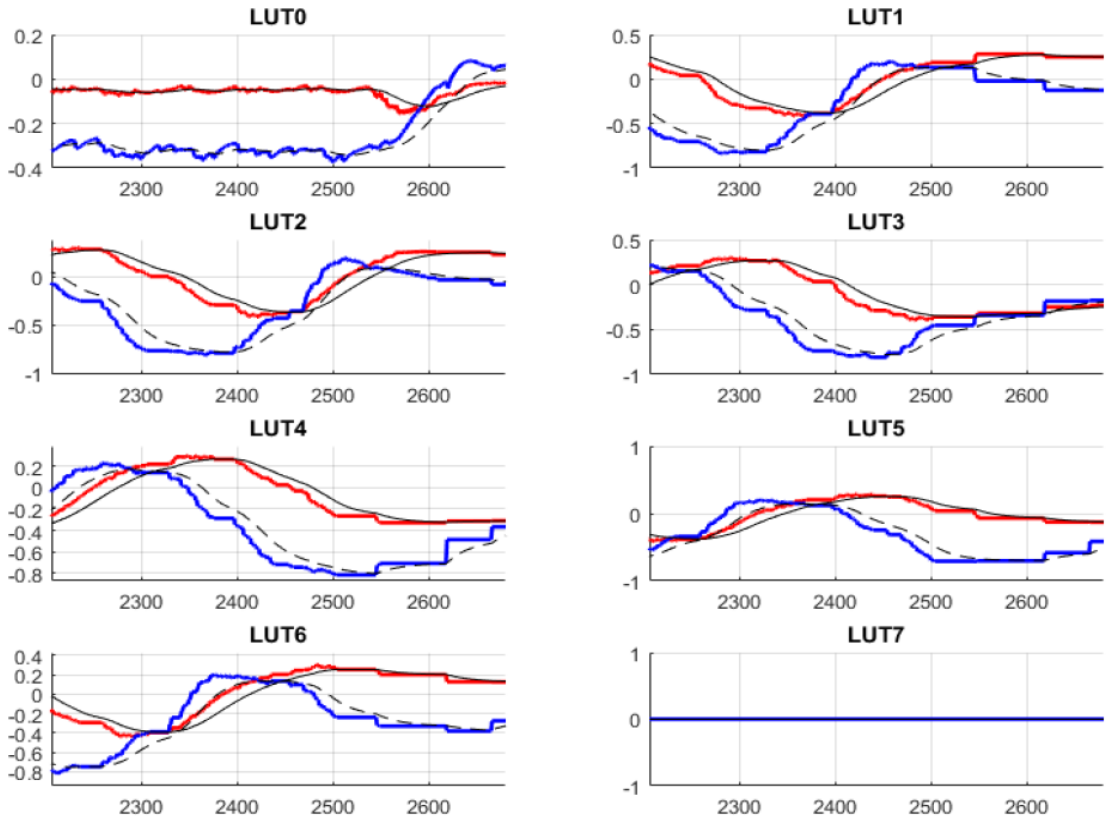

Fig 66: Reconstruction of the current LUT: the stagnations are particularly evident since they generate horizontal segments in the sinusoidal wave-form.

As it has been observed for the high speed operation, also for the for this speed ramp it is possible to notice the phenomena of the stagnation of two vectors that create the flat part of the current LUT. The origin of this stagnation is found in the change of the vector sequence used to control the machine. Even if the sequence appears similar to the one that is observed in the ideal case, there is an essential difference.
In the analysis performed in Chapter 2.3, after the triplet $\overline{U}_1$, $\overline{U}_5$, $\overline{U}_0$ it is applied the triplet formed by $\overline{U}_2$, $\overline{U}_6$, $\overline{U}_0$ and then there is another triplet that contains $\overline{U}_1$: there is an interruption in the application of the vector $\overline{U}_1$ in which it is applied a different triplet. On the contrary, in the ramp this interruption

is not observed, probably because the presence of the prediction error makes the change of triplet less evident. This phenomena is observable, obviously, for all the vectors.
Almost in the middle of this long interval in which a vector is applied it can occur a very particular condition. If the amplitude of the two component of the zero current variation is compensated by an active vector, only two vectors are used to track the two current references.
When the stagnation is not so long, for example the one just before the step 2400, its effects are only local and the sinusoidal wave-form is maintained: the problems start when the stagnation are longer and close one to the other, after the step 2500. In these instants, in fact, $\overline{U}_0$ and $\overline{U}_2$ can control the motor without the needing of a third variation and so two quite long stagnations begin. At the end of the first stagnation the amplitude of the current variation related to $\overline{U}_3$ is still negative, even if in a couple of switching intervals it should substitute the role of $\overline{U}_2$.
During the second stagnation, another fact contributes to the beginning of the instability. Since the speed ramp is almost finished, it is no more needed an acceleration of the motor, so the torque produced by the motor is decreased. Because of the formula reported in the Chapter 2.2, the two current references are both reduced in their absolute value. As a consequence, the amplitude of the zero component start to decrease.
This fact permits a further durance of the stagnation in fact $\overline{U}_3$ is not correctly estimated and the reduction of the q-variation induced by $\overline{U}_0$ extends the time interval in which $\Delta i_q(\overline{U}_2)$ is positive.
Since all the current variations are influenced by the zero one, the five current LUT, that are not updated, are affected by a significant prediction error. At the end of the second stagnation, in particular in the step 2622, the same sign characterize all the q-current variations.
The fact that all the variations are negative is again not due to the overcoming of the nominal speed and the beginning of the flux-weakening regime, but it is a consequence of a not enough frequent update of the current LUT. From the analysis of the prediction error in every all the intervals (Fig 67) it is evident the correlation between the peaks of this error and the end of a stagnation. During the repetition of two vectors the error is inferior than the 10%, because the applied vectors are continuously updated. Only at the end of the stagnation it it possible to understand which is the error that afflict the other variations. In the test under consideration, for example, the highest error is committed close to the step 2550, when $\overline{U}_1$ is applied: after a stagnation of $\overline{U}_0$ and $\overline{U}_2$ fifty intervals long, in fact, $\overline{U}_1$ does no more produce a positive q-axis variation, but an almost nil variation (Fig 66).

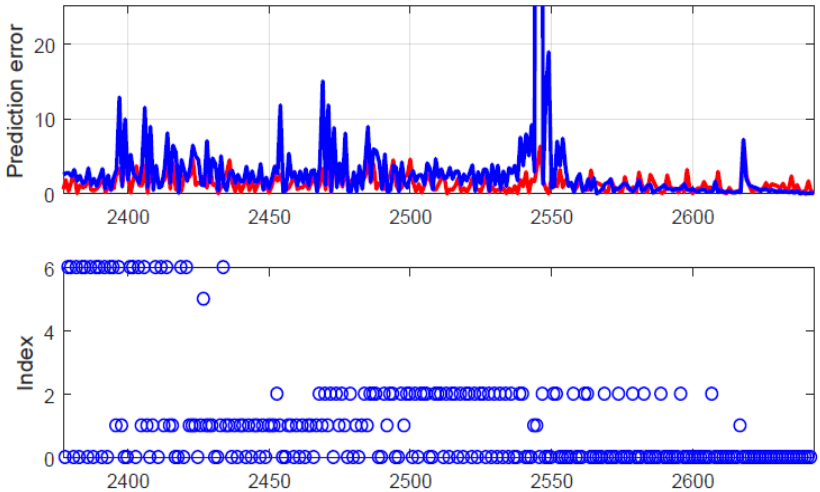

Fig 67: In the first figure the red line represents the d-axis error and the blue line the q-axis error

A forced update of the current LUT should be used to preserve the stability of the scheme: in this way it is prevented the stop of the reconstruction.
The second parameter of the ramp taken into consideration is its time length. In all the tests presented up to now, the length is set equal to 0,5s: it is interesting to analyze how the drive responds when this length is reduced. For this purpose the previous tests are repeated at first with a length of 0,25s and then of 5ms.
The main difference between these tests and the first ones is the fact that the speed ramp becomes too fast to be tracked by the drive and so the actual speed is quite distant from its reference, especially in the case of a length of 5ms. On the other hand, from the point of view of the stability, this change is not so relevant: the ramps with an amplitude of 100rpm and 300rpm are successfully performed and from the one with the amplitude of 400rpm the problem of the stability occurs. In the case of the 0,25s long ramp the loss of the control happens in correspondence of a long stagnation in which the zero current variation is changing, as for the 0,5s long ramp: this further proves the fact that this phenomena should be prevented.
In conclusion the analysis of the steady state and dynamic performances of the drive it is deduced that the improved MF scheme proposed is not suitable to control the machine in the high speeds regimes. After a speed of around 400rpm the occurrence of the stagnation of two vectors together with all the approximations introduced to build the scheme do not guarantee the stability.
Another transient considered in the comparison of the two predictive schemes is the torque step. Since the control of the motor is not always guaranteed over the 400rpm, the comparison is realized only for lower speeds, in particular 50rpm, 100rpm and 300rpm. The amplitude of the torque step is increased from 2Nm to 12Nm in order to consider different iron-saturation conditions of the lamination.

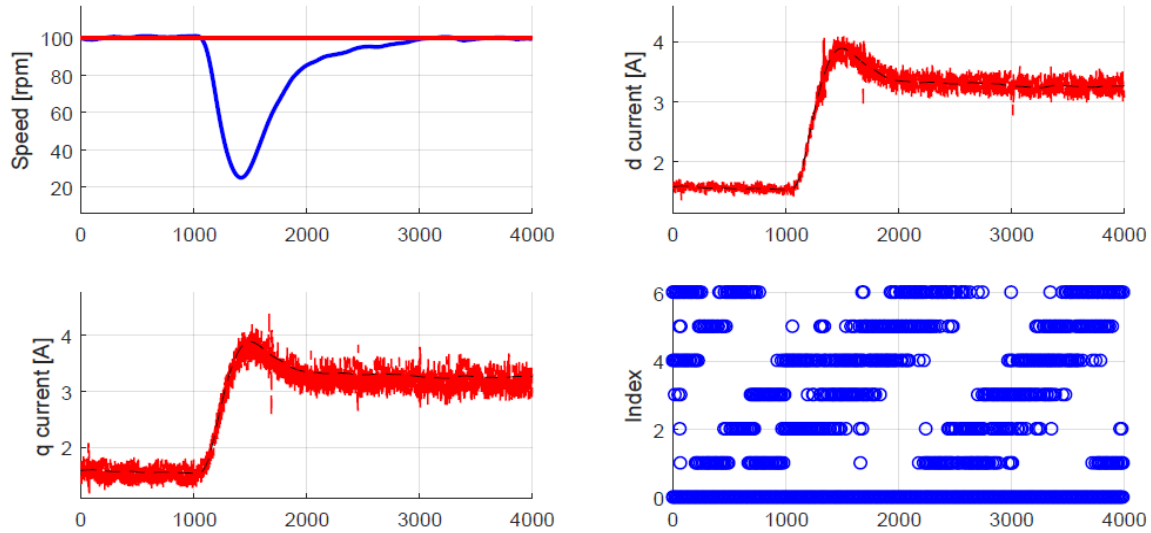

Fig 68: Performances of the improved MF scheme in a 6Nm wide torque step at a speed of 100rpm

After the application of the step, the speed of the motor starts to decrease (Fig 68): the capability of the system to react to the step depends on the inertia of the motor and on the parameters of the PI controller of the speed loop.
The fall of the speed and the change of the torque required from the motor causes a consistent modification of the zero current variation and so the update of the current LUT should be quite frequent to maintain an accurate knowledge of the system. As for the speed ramps, the stability problems could occur in case of the presence of the stagnations.

In order to quantify the accuracy in the description of the scheme, it is possible to compare the integral square error (ISE) committed by the improved MF method and by the MB method in the previous test. Instead of considering the entire time length of the test, the error is computed from the beginning of the torque step: this permit to neglect the error produced in the constant speed operation that precede the step.

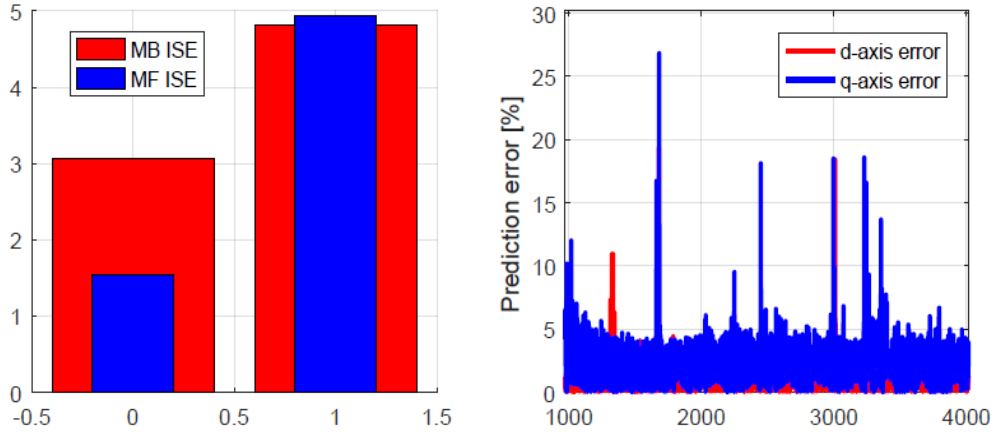

Fig 69:On the right are represented the two components of the ISE, on the left the it is reported the prediction error committed with the improved MF scheme interval by interval.

The comparison (Fig 69) reveals that the improved MF scheme guarantee a consistent decrease of the error only on the d-axis, so the solutions are comparable. From a step's amplitude of 8Nm the error committed by the MB scheme due to the change of the inductive parameter becomes more relevant and the improve MF solution guarantees a more accurate description on both the axis.
If we consider the instantaneous prediction error it is evident that the main contribute to the ISE is not given by beginning of the torque step. In the first part of the transient, in fact, it is committed an error close to the 10%, whereas the peaks of the error are reached later and they are probably caused by some disturbs in the current acquisition, since during all the test is not observed any long stagnation. The presence of a stagnation, anyway, would not be so problematic, because the position error requires a quite big number of switching intervals to assume a relevant amplitude for this range of speed.
As for all the speed ramps or the constant speed operation, the performances of the improved MF scheme decrease with the rise of the speed also for the torque steps. Despite this, no significant problems are observed for all torque steps at 300rpm, from the point of view of the stability.
In these tests it is observed again the phenomena of the stagnation induced by the repetitive application of two voltage vectors, even if they are not observed in the Simulink simulations. It is reminded that the simulations do not take into account many aspects, for example the presence of the current disturbs that are the main contribute of the prediction error in the previous test.
The relation between the ends of a stagnation and the peaks of the prediction error is even more evident (Fig 70), unfortunately no solution has been tested to prevent this phenomena.

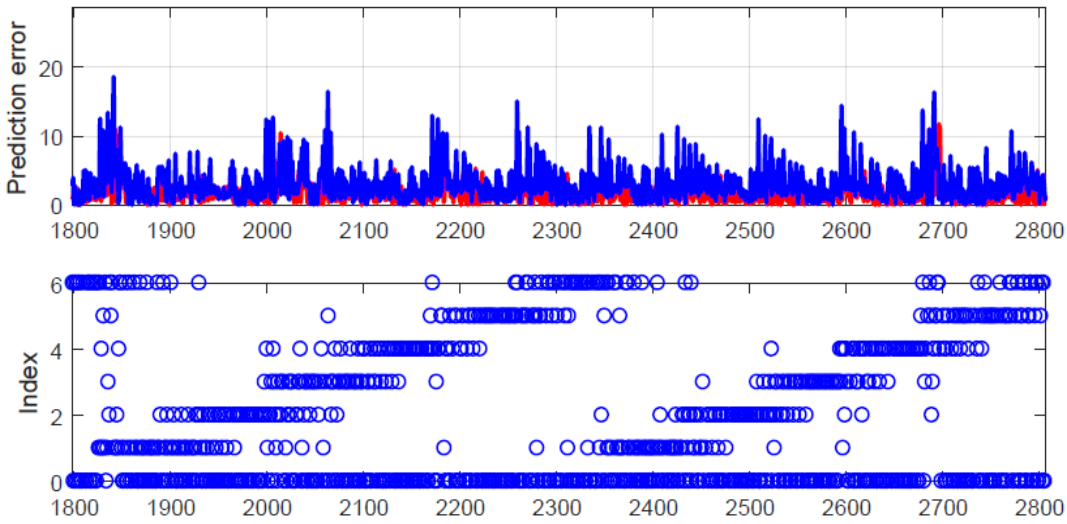

Fig 70: The two figures are related to a torque step with an amplitude of 6Nm performed at 300rpm

4.7 Possible upgrades of the Model Predictive scheme

Both the Model Free Predictive drives that we have analyzed ignore completely the system that are controlled, in fact they do not use equation of the motor. More over, the only quantities used to compute the current predictions are the d – q currents of the motor. These two aspects are the consequences of the Model Free approach: the control is based only on the reactions of the system, in this case the REL motor, to a certain input.
One of the most relevant disadvantages of this approach is the instability caused by the approximation introduced to compute the predictions: we suppose that all the current variations are measured in the switching interval. This fact introduces some intrinsic errors in the reconstruction due to the fact that the position of the rotor is not considered used by the control scheme.
In order to overcome these stability problems, it is possible to build a new control scheme that use all the information that are known of the system, like the rotor position and the model of the machine.
First of all, the rotor position it is already measured in the two actual schemes to perform the speed control. This quantity can be used to improve the scheme, without the introduction of other measuring instruments.
Secondly, since the system under analysis is well known because it is a reluctance motor: it is possible to describe it with the machine equations in some particular conditions. When the saturation occurs, the Model Free approach could support the model and guarantee more precise values of the motor parameters.
From the analysis of the d – q machine equations it is possible to understand how the Model Free approach can support the Model Based predictions:

$$\Delta i_{d,n}(t_k, t_{k-1}) = \frac{T_s}{L_d} u_{d,n}(t_k) + \frac{T_s}{L_d} \left(-R i_d(t_k) + \omega_{me} L_q i_q(t_k)\right) = \Delta i_d(u_n) + \Delta i_d(u_0) \quad (1)$$

$$\Delta i_{q,n}(t_k, t_{k-1}) = \frac{T_s}{L_q} u_{q,n}(t_k) + \frac{T_s}{L_q} \left(-R i_q(t_k) - \omega_{me} L_d i_d(t_k)\right) = \Delta i_q(u_n) + \Delta i_q(u_0) \quad (2)$$

The zero-component of both the variations are highly influenced by the change of the operative conditions, in particular the inductance and the resistance of the winding. It is evident that the Model Based prediction of these two components should not be used.
During the analysis of the Model Free schemes, it has been observed the fact that the zero voltage vectors is applied very frequently, when the current predictions are precise. Under the hypothesis of high accuracy of the predictions, the model estimation of the zero-component can be substituted by the last measured variation.
Another aspect that support this substitution is the fact that the two zero-variations do not depend on the rotor position, so even if a short stagnation occurs, the amplitude of the two components should not be influenced.
On the other hand, a quantity able to decrease the accuracy of the predictions is the change of the current components i_d and i_q. These two components remain almost constant during a constant speed operation but they quickly change during a transient like a torque step or a speed step. In order to overcome this limit is possible to adopt the same concept of the forced anti-stagnation: when the zero-vector is not applied for a defined number of switching intervals, it is applied overcoming the minimization of the cost function.
At this point, it has been detected an efficient way to keep update the zero-components but we have still not used the information given by the model of the motor or the knowledge of the rotor position: from this point of view, a Model Free approach is used.
The active part of the current variations are influenced by different parameters, in particular the d - q components of the inductance and the rotor position.
In order to solve completely the problem of the stagnation, the active components of the voltage vectors should be estimated using the model of the REL motor and the knowledge of the rotor position:

$$u_{d,k+1} = \frac{2}{3} U_{dc} \cos\left(\theta_{me,k+1} + n\frac{2}{3}\pi\right) \quad (3)$$

$$u_{q,k+1} = \frac{2}{3} U_{dc} \sin\left(\theta_{me,k+1} + n\frac{2}{3}\pi\right) \quad (4)$$

For the prediction of the rotor position at the (k+1)st interval it can be used the same formula presented for the Model Based scheme, which is quite precise, as it has already been noticed.
Unfortunately, the active components of the current vectors are influenced also by the inductive parameter of the motor L_d and L_q, which are highly dependent on the iron-saturation. If a high accuracy is required, this aspect can not be neglected.
An adaptive approach should be used for the inductance estimation and so the actual current variations produced by the seven voltage vectors: this represents a second support of the Model Free approach to the predictions.
The most precise knowledge of the inductance can be extracted from the (k-1)st interval, in particular using the last measured current variation and the last zero-variations, which is supposed frequently updated. Two possible expressions of the inductances can be obtained by the machine's equations:

$$L_{d,k-1} \approx \frac{T_s \frac{2}{3} U_{dc} \cos(\theta_{me,k-1})}{\Delta i_{d,k-1} - \Delta i_d(u_0)} \quad (5)$$

$$L_{q,k-1} \approx \frac{T_s \frac{2}{3} U_{dc} \sin(\theta_{me,k-1})}{\Delta i_{q,k-1} - \Delta i_q(u_0)} \quad (6)$$

With these two equations it is possible to refresh the amplitude of the inductances every time that an active vector is applied, a condition that frequently occurs in all the dynamic tests performed on the motor.
The prefect equivalence between the inductance amplitude and their expression is reached only when both the active current variations and the zero ones: a condition impossible to verify. As a consequence of this, also the accuracy of the active variations are influenced by the update frequency of the zero-vector. A forced anti-stagnation of this vector is suggested also by the analysis of the active components.
The estimated current components for the n-th voltage vector are predicted as:

$$\Delta i_{d,n}(t_k, t_{k-1}) = \frac{T_s}{L_{d,k-1}} u_{d,n}(t_k) + \Delta i_d(u_0) \quad (7)$$

$$\Delta i_{q,n}(t_k, t_{k-1}) = \frac{T_s}{L_{q,k-1}} u_{d,n}(t_k) + \Delta i_d(u_0) \quad (8)$$

A similar computation is repeated also for the (k+2)nd interval in order to choose the vector that minimize a given cost function, as for all the other predictive schemes.
In conclusion, the presented upgrade is a hybrid configuration that tries to use the advantages of both the control schemes, in particular the adaptive property of the Model Free approach, to estimate the parameters of the motor, and the equation of the machine to correctly evaluate the change of the variations with the rotor position. These two properties should reduce the influence of the iron-saturation on the drive performances and guarantee the stability for all the possible dynamic transient.
Another field in which the model free approach could be adopted is the Model Predictive Hysterisis Current Control (MPHCC) [4]. In particular, the model based algorithm used to estimate the current predictions could be substituted by the current variations directly measured on the motor.
The integration of the MF approach to other scheme is particularly interesting because it is wondered to find a scheme able to intrinsically eliminate the problem of the stagnation and to guarantee the stability for a wide range of operative conditions. From this point of view the appeal of the MPHCC consists in the possibility of exploiting different criteria to track the current references.
Some simulations have been performed for this scheme in case of not so high speed and they suggest that an intrinsic anti-stagnation could be generated by a double error in the evaluation of the signs of the current variations. In case of higher speeds also this predictive scheme manifests stability problems.
A more detailed analysis of this scheme should permit the understanding of the limits of this solution and other possible upgrades.

4.8 Appendix: The Simulink model

The scheme is further complicated with the respect to the forced MF one because of the introduction of the reconstructive process. For this reason, the Simulink model is characterized by a new Matlab function dedicated to the reconstruction of the current LUT.
Since the method used for the evaluation of the current prediction and the choice of the voltage vector is the same of a simple MF scheme, it is possible to exploit a configuration similar to the one described in the Chapter 3.5. The only difference is represented by the update of the current variations which is realized in separately in the new Matlab function.

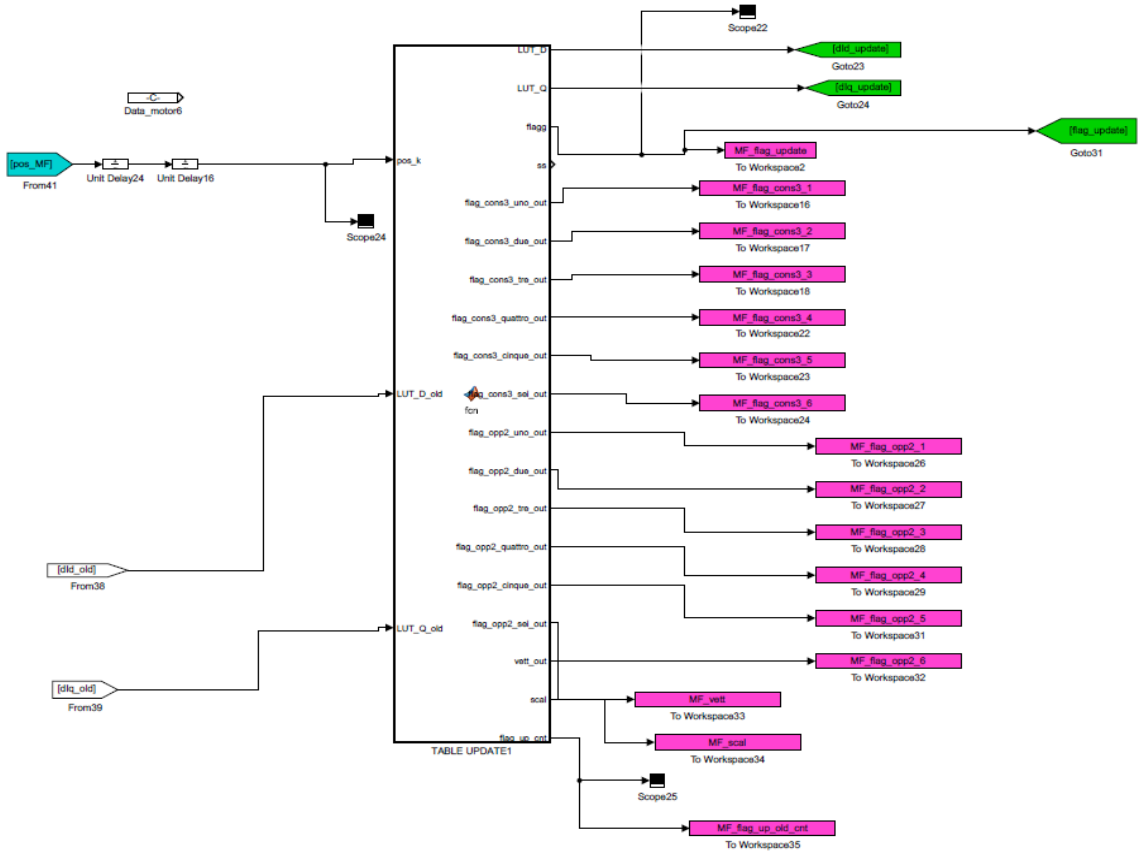

Fig 71

5 A voltage loop for the flux weakening operation

5.1 Description of the voltage loop

In the previous chapter it has been noticed that a voltage loop should be introduced not only for the flux weakening operation but also to solve the instability that occurs in case of high speeds (lower than the nominal) and high load torque.
It is not necessary to estimate the nominal speed of the motor to detect the condition in which the flux weakening is required, since it is possible to exploit the monitoring of the current variation signs, as it is proposed in the previous chapter. When all the q components of the variations assume the same sign, the control of the motor could already be lost so the real flux weakening operation is anticipated. The anticipation is obtained comparing the amplitude of the current variations with a constant instead of the zero.
The control scheme adopted for the flux weakening operation is the one described in [5] and represented in the following figure.

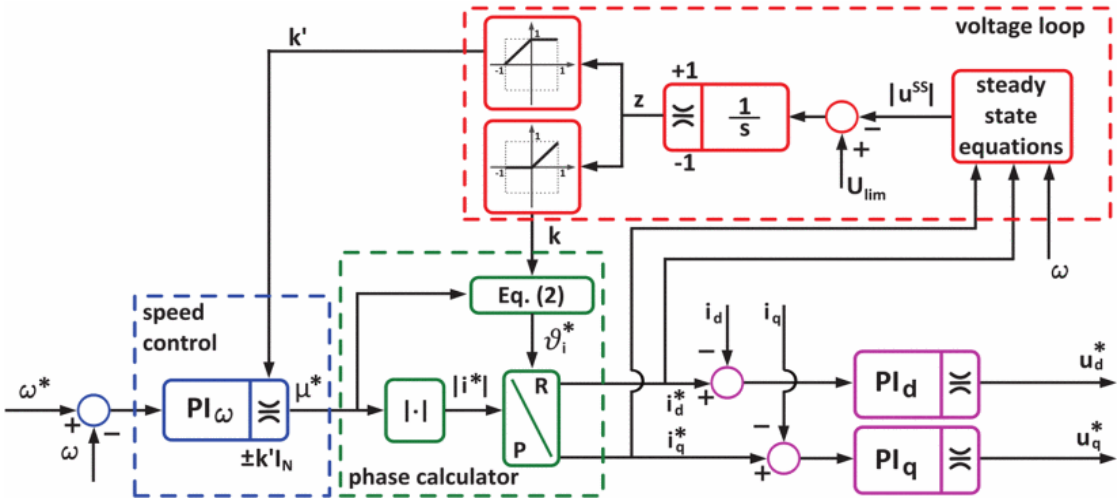

Fig 72: Scheme proposed in [5]

The speed loop is very similar to the previous one in fact the reference speed is compared with the actual and the error is the input of a PI controller. For this loop it is convenient to express the reference current components in a polar system: μ^* represents the module of the vector and ω its argument. In this case, the current module is not limited only by the nominal current I_N but it has two variable constrains $\pm\mu_{lim}$:

$$\mu_{lim} = \pm k' I_N \qquad (1)$$

The parameter *k'* permits the reduction of the current amplitude when the voltage limit is overcome and so it comes from the voltage loop.
In case of a REL machine, the arguments that characterize the MTPA and MTPV are two constants because the two relatives trajectories (represented in Fig 57) are the two straight lines defined by the expressions:

$$MTPA: \quad i_q = \pm i_d \qquad MTPV: \quad i_q = \pm \frac{L_d}{L_q} i_d \qquad (2)$$

Similarly to the module, also the argument ϑ is influenced by the voltage loop since it depends on the parameter *k*:

$$\theta = k\,\theta_{MTPA} + (1-k)\,\theta_{MTPV} \qquad (3)$$

where ϑ_{MTPA} and ϑ_{MTPV} are the distances between the working point and the two operating lines.
The parameter *k* is introduced in order to rotate the point of work of the drive between the two operating lines, if the nominal point is overcome. When *k* is equal to one the working point is on the MTPA trajectory, vice versa when *k* is equal to 0 the point is on the flux weakening area.
In order to compute these two parameters that directly define the current reference, a third parameter *z* is introduced. The amplitude of *z* has an upper constrain 1 and a lower constrain -1 (line 3497-3498 of the next figure).
There are two possible expressions to compute α and β, depending on the sign of *z*:

$$z > 0 \qquad \alpha = 1 \wedge \beta = z \qquad (4)$$

$$z < 0 \qquad \alpha = 1+z \wedge \beta = 0 \qquad (5)$$

If the first condition is verified and *z* = 1, the point of work stays on the MTPA trajectory because in the expression (3) it is deleted the angular contribute of ϑ_{MTPV} and the maximum is current is limited by the nominal value I_N. The same condition comprehends also the working points between the MTPA line and the MTPV line, since the movement between the two trajectories is obtained with the variable amplitude of *k* (or *z*).
On the other hand, when the second condition is verified, the point of work is on the MTPV line in fact the argument of the current (3) $\vartheta=\vartheta_{MTPV}$. In this case the voltage limit imposes a reduction of the module of the current, obtained with the reduction of the parameter *k'*, because $1+z < 1$.
Every switching period a counter called *count_cycle* is increased by one unit.
If it is verified the flux weakening condition and so the signs of the q currents (in case of positive speed), the flag *flag_vl_mf* is maintained equal to zero, while in the opposite case it is increased of one unit. For the sake of the stability, the intervention of the voltage loop is anticipated by the introduction of a safety coefficient *thr*: the q-currents are compared with *thr* and not with the zero in order to completely eliminate the possibility of obtain seven LUT with the same sign.
A second counter *count_flag* is increased every iteration of the quantity *flag_vl_mf* and so it represents the number of iteration in which the flux weakening condition is not verified starting from the same instant of *count_cycle.*
When the counter *count_cycle* reaches the value *N_cycle*, it is checked which is the amplitude of the counter *count_flag*, in particular with the respect to the number of cycles *N_cycle*.
If the condition of flux weakening is never verified, we would obtain a *count_flag*=*N_cycle* and so we need to move the working point closer to the MTPA line. Since the MTPA operation is characterized by a positive *z*, the parameter *z* itself is increased by a certain positive increment, indicated with *dz_vl*.
On the other hand, when it is found exactly an opposite situation and so a counter *count_flag* equal to zero, it is needed to move the operating point in the area of the flux weakening regime, where the parameter *z* has a negative sign. As a consequence, the actual *z* is decreased of the same quantity *dz_vl*.
Both the rise and the decrease of *z* is stopped when the upper or the lower limit are overcome: in these two conditions *z* could not be modified and it remains respectively equal to 1 and -1.

```
3461                if (vl_mf){
3462                    LUTs_up=1; MB_mode_flt=10.0;
3463                    count_cycle += 1;
3464                    if (LUT_Q_up[0]> -thr &&  LUT_Q_up[1]> -thr &&  LUT_Q_up[2]> -thr
                        &&  LUT_Q_up[3]> -thr &&  LUT_Q_up[4]> -thr &&  LUT_Q_up[5]> -thr
                        &&  LUT_Q_up[6]> -thr  ||
3465                        LUT_Q_up[0]< thr &&  LUT_Q_up[1]< thr &&  LUT_Q_up[2]< thr &&
                            LUT_Q_up[3]< thr &&  LUT_Q_up[4]< thr &&  LUT_Q_up[5]< thr &&
                            LUT_Q_up[6]< thr  )
3466                    {
3467                        flag_vl_mf =0;
3468                    }
3469                    else flag_vl_mf =1;
3470
3471                    count_flag += flag_vl_mf;
3472
3473                    if (count_cycle == N_cycle)             // ogni N_cycle istanti
3474                    {
3475                        if (count_flag == N_cycle)          // se trovo N_cycle volte
                            consecutive rispettata la condizione di convergenza: aumento z_fw
3476                        {
3477                            z_vl += dz_vl;
3478                        }
3479                        else
3480                        {
3481                            if (count_flag == 0)            // se per N_cycle volte
                                consecutive non trovo vettori che rispettano la condizione:
                                diminuisco z_fw
3482                            {
3483                            z_vl -= dz_vl;
3484                            }
3485                        }
3486                        count_cycle=0;
3487                        count_flag=0;
3488                    }
3489
3490                    if (LUT_D_up[0]== 0.0 &&  LUT_D_up[1]== 0.0 &&  LUT_D_up[2]== 0.0
                        &&  LUT_D_up[3]== 0.0 &&  LUT_D_up[4]== 0.0 &&  LUT_D_up[5]== 0.0
                        &&  LUT_D_up[6]== 0.0)
3491                    {
3492                        z_vl=1; count_flag= N_cycle;
3493                    }
3494                    if (rpm_m_ref<300.0){z_vl=1; count_flag= N_cycle; } // DA
                        SOSTITUIRE! EVITARE FW INIZIALE (??)
3495
3496
3497                    if (z_vl >= 1.0)  z_vl=1.0;
3498                    if (z_vl <= -1.0) z_vl=-1.0;
3499
3500                    if (z_vl>=0.0){alpha_vl=1.0;  beta_vl=z_vl;}
3501                    else {alpha_vl=1.0+z_vl; beta_vl=0.0;}
3502
3503
3504                        tempoo += TC;
3505                        rpm_m_ref=1000.0/2.0*tempoo;
3506                        if (rpm_m_ref>1000.0) {rpm_m_ref=1000.0;}
3507
3508                }
3509                else {MB_mode_flt=0.0; indice = index_min(J_cost); rpm_m_ref=0.0;
                    tempoo=0.0; torque_ref=0.0;}
```

Fig 73: z_vl corresponds to *z*, *alpha_vl* to *k'* and *beta_vl* to *k*

The last situation that can occur is the case of a *count_flag* that assume an intermediate value between 0 and *N_cycle*. When this condition occurs, the working point is maintained in the same position and so *z* is not modified.

5.2 Effects of the voltage loop on the current predictions

It is reminded that the aim of the introduction of the voltage loop is the resolution of the instability observed for the high speed operation: the instability, in fact, is not due to the overcoming of the nominal speed but to the several hypothesis on which the reconstructive process is based. The introduction of a voltage-loop in the scheme can modify the behavior of the motor also in other conditions.
For the sake of coherence with the measures performed on the bench, the convention adopted in this chapter for the motor is the convention of a REL machine. As a consequence of this choice, the axis that suffers the problem of the current variations signs is the q-axis.
With this convention the reciprocal position between the MTPA and MTPV lines is inverted, with the respect to the IPM one. In particular, the angular coefficient of the MTPV line is higher than the one of the MTPA line.
The configuration of the bench permits to motor the engine at idle till 1000rpm thanks to the SPM machine driven by the master inverter. Withe the SPM motor the REL machine is accelerated over the nominal speed, in order to analyze the changes in the reconstruction of the current LUT.

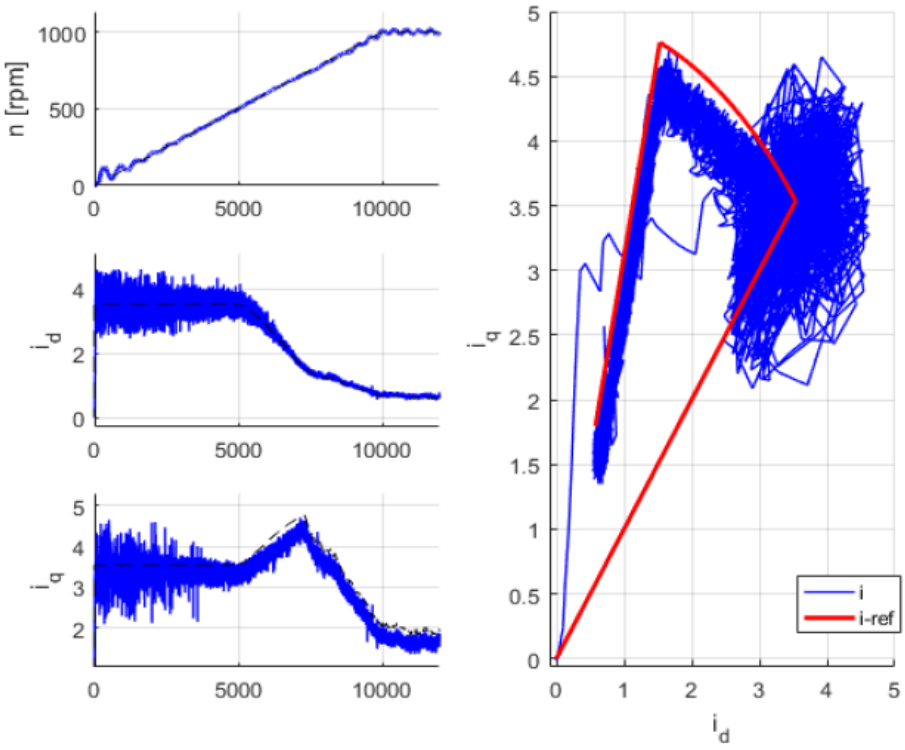

Fig 74: Rotation between from the MTPA line to the MTPV line.

This test permits, first of all, to identify the actual nominal speed, which results almost 500rpm: the theoretical formula exploits the parameters of the motor, that are not constant. The amplitude is extrapolated from the change of relative amplitude of the two current components (Fig 74) caused by the beginning of the rotation from the MTPA line to the MTPV line.
In the rotation between the two lines it is noticed that the nominal current is never reached because of the parameter *thr* that anticipate the action of the voltage loop. When the MTPV line is reached the

argument of the operative current points do not change significantly but the current module decreases because of the decrease of the parameter α.
Since the stability of the MFPCC scheme is due essentially to the sign of the predicted current variations, it is needed to understand which is the effect of the rotation of the operative line on the q-axis current variations. In the following figure it is reported the amplitude of the positive part of the seven q-axis LUT during the flux weakening operation.

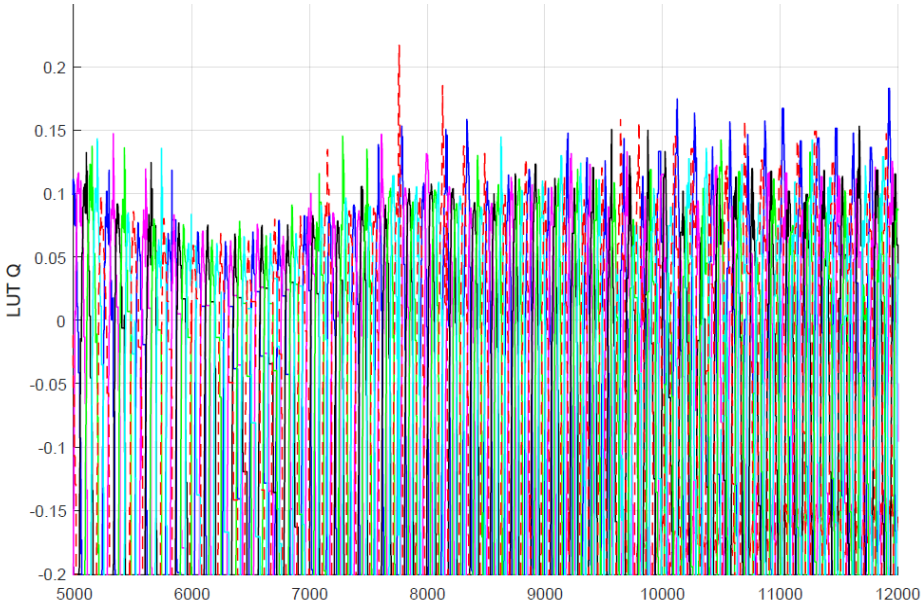

Fig 75: Positive part of the d-axis current LUT.

Thanks to the voltage loop, for all the speeds it is always possible to find a positive q-current variation and this should guarantee the stability of the MF scheme. The two parameters α and β generated by the voltage loop, in fact, acts directly in the expression the Δi_q:

$$\Delta i_{q,n} = \frac{T_s}{L_q} u_{q,n} + \frac{T_s}{L_q} \left(-R i_q - \omega_{me} L_d i_d\right) = \Delta i_q(u_n) + \Delta i_q(u_0)$$

$$i = i_d^2 + i_q^2 = \alpha I_N \qquad i_d = i \cos(\omega(\beta)) \quad \wedge \quad i_d = i \sin(\omega(\beta))$$

A first reduction of the shift due to the zero component $\Delta i_q(u_0)$ is caused by the decrease of the current module generated by the parameter α, that reduce the current limit. This fact permits a decrease of both the contributes that compose $\Delta i_q(u_0)$.
In addition, the relative weight of the zero variation, that depends on the rotor speed, is further reduced by the rotation of the operative line in the direction of the MTPV trajectory, which is caused by the parameter β.
This test shows that the current LUT built during a flux weakening operation should permit the control of the motor and should also solve the instability observed before the overcoming of the nominal speed. The introduction of the constant *thr* prevent the possibility that all the q current LUT assume the same sign and so the minimization of the cost function should always be able to find a vector that reduce both the components of the current error.

An intrinsic disadvantage of the use of the voltage loop to solve the problem of the instability is the fact that the flux weakening of the machine could reduce the torque also in case of speed minor than the nominal one. When the current disturbs or the stagnation of two vectors anticipate the conditions on the current LUT signs, the voltage loop starts to rotate the working point from the MTPA line to the MTPV one.
The adoption of a voltage-loop, anyway, prevents only the construction of current LUT with the same signs but it does not solve the origin of this fact, which is the position error that continues to afflict the improved MF scheme. As a consequence, a further improvement in the MF approach to the estimation of the current variation could be the utilization of the rotor position, which is already measured.

6 Conclusion

The thesis work is focus on the study of the Model Free Predictive control schemes, in order to find some possible solutions to the stagnation problem and, secondly, to increase their dynamic performances in different operative conditions.
The analysis of the MB scheme has permitted to understand that for a predictive algorithm the role of the cost function is determinant in the selection of the voltage vectors applied to the motor. For a REL motor, it is convenient to find an expression that interacts properly with the electromagnetic anisotropy. In particular, two solutions are found to obtain a more balanced behavior on the two axis: the adoption of a second order expression of the current error and the compensation of the anisotropy with the measurement of the ratio between the two different d – q components of the machine's inductance. In a model free approach, it is not convenient the compensation of the inductances since it requires an estimation of their amplitude, which are not constant.
Another interesting result obtained with this analysis consists in the fact that the behavior of the control scheme has been changed working only on the expression of the cost function, without any modification of the process of the current prediction. This is a relevant result from the point of view of the individuation of alternative anti-stagnation algorithms for the MF predictive schemes.
A second analysis on the MB scheme has permitted the comprehension of the criteria used for the selection of the voltage vectors in a steady state regime, for different ranges of speed and load torque. The control scheme adopts commonly three different voltage vectors in every sixth of the electromagnetic period to control the REL motor. Even if the elements of the triplets could change in different conditions of iron saturation, the utilization of, at least, three different vectors validate the hypothesis on which it is based the improved MF scheme. In fact, a frequent update of three different current variations is a hypothesis required to reconstruct the current LUT with a high accuracy.
Moreover, it is observed that the change of the criteria on which the vectors are chosen is the origin of the decrease of the performances of the scheme in presence of iron saturation. When the model of the machine is not known with a sufficient precision, the minimization of the cost function is no more able to find the optimal vector, since the estimations of the current predictions are affected by a significant prediction error. In this condition the number of vectors used in each sixth of the period increases, because there is a continuous compensation of the wrong current estimations.
In order to overcome the problems that characterize the MB scheme, two different solutions are proposed: a model free approach for the estimation of the current predictions and an improved MB scheme.
The second solution exploits a different utilization of the current measures to update the values of the motor inductances step by step. In the thesis work it is decided to focus the attention on the possibilities offered by the first solution.
As a first point of the MF scheme analysis, it is demonstrated that the problem of the stagnation of the voltage vectors is an intrinsic consequence of this kind of approach and it is the effective origin of the instability that is observed also in literature [1]. The problem is a consequence of a wrong estimation of the signs of the current variations, caused by the periodical criteria with which the vectors are chosen. A model free approach for the predictions, in fact, does not consider the change of the rotor position between two different switching intervals. The conclusion of this analysis is the evidence that a Model Free Predictive control should always be supported by an anti-stagnation algorithm to maintain the stability.
Three main solutions are considered in the thesis for the resolution of the problem: a forced update anti-stagnation algorithm, the utilization of a smart cost function and, in particular, an improved MF predictive solution.

The solution based on a forced anti-stagnation is a technique already considered in literature [2]. Exploiting the study of the steady state behavior of the MB scheme, it is possible to optimize the anti-stagnation action.
As a first improvement, it is found an optimal range for choosing the frequency of update for each speed of the rotor. This is obtained, in particular, adopting a variable amplitude of the threshold value n_{old} of the counter that quantify the number of intervals for which a vector is not applied. Other solutions are found for specific range of operative speed.
In case of a low speed operation, it is possible to exploit the low amplitude of the zero vector variation in order to further reduce the current ripple: this solution can be superimposed to the optimal choice of n_{old}. In case of a high speed operation, the stability of the scheme can be improved introducing a further constrain on the signs of the variations that substitute the optimum vector selected by the minimization of the cost function.
As an alternative to the utilization of external constrains, it is discussed also the possibility of work with a cost function that intrinsically solve the stagnation. This property is obtained introducing in the cost function also the indicators of the age of the vectors. In this field it should be interesting the research of other expressions for the cost function, trying to involve also other parameters to preserve the dynamic performances of the scheme for different speeds. Since the stability depends on the rotor speed, the speed itself could be one of the parameter to take into consideration for the modification of the cost function.
Both these two methods involve the application of non optimal vectors to guarantee the stability of the scheme are characterized by a higher current ripple with the respect to the Model Based scheme: this is the reason why a novel approach has been studied.
In the thesis it has been demonstrated that it is possible to reconstruct four of the seven current variations starting from the knowledge of just three variations: this strategy introduce the novel possibility of update indirectly the current LUT. It is no more required a by-passing of the minimization of the cost function.
Secondly, it has been proposed a possible implementation of this technique. In order reduce the time length of the interrupt, it has been optimized the phase of update of the flags used for the individuation of the reconstructive triplet.
A further optimization of the code should permit a reduction of the execution time and so the rise of the switching frequency: a higher frequency guarantees a reduction of the prediction error related to the change of the rotor position in the interval. On of the possible solutions to reach this goal is the exclusion of all the unused combinations of triplets, but it appears very difficult to prove their effective uselessness in all the possible transients.
The refreshing of many current variations in just one interval requires a higher attention on the current measurements. For this reason, it has been chosen the most convenient instant of the switching period to perform the current acquisitions and the omopolar disturbs are deleted in the d – q system with the measurement of all the three current. In addition, to further decrease the effects of the disturbs, all the variations are filtered before the substitution of the old ones. All these solutions used to improve the accuracy of the measures are essential form the point of view of the stability.
This different MF approach permits to keep updated the current LUT in the majority of the dynamic tests performed, in particular in all the steady state tests, speed ramps and torques steps characterized by a speed inferior than 400rpm.
Both the simulations and the tests realized with this predictive scheme manifests comparable performances to the ones realized with the Model Based scheme, in case of not so high speed and load torques. When the saturation affects the accuracy of the model of the motor, the MF scheme is commonly characterized by an even lower current ripple and speed ripple. As a consequence, the MF approach, that need an inferior number of input parameters for the current prediction, could describe the system even with a higher accuracy than one that exploit the d – q model of the REL machine. The only quantity used by the improved MF scheme to estimate the predictions is, in fact, the motor

current. On the other hand with the MB method are needed also the rotor speed and position, the resistance and the inductance of the stator winding and the voltage of the DC-bus of the inverter.
Unfortunately, the improved MF scheme still suffers of stability problems, in particular for high operative speeds. In these cases, the combined effects of a high zero variation component, the non nil length of the switching period, the remaining disturbs during the current acquisition and the presence of the stagnation of two vectors compromise the reconstruction of the current variations. When the signs of all the current variations are the same, the stagnation begins, as in the case of a MF scheme without any anti-stagnation solution. Since any forced anti-stagnation criteria is used to anticipate the update of the current LUT, when the stagnation begins, it is difficult to interrupt it. The reconstructive process, in fact, is not based on the direct elimination of the stagnations, but it is created to permit a more accurate model free description of the system: the resolution of the problem for low speeds is one of the consequences of this fact. In conclusion, the main difference between a simple MF scheme and the improved one is the fact that it is needed the update of only three current variations, instead of all the seven.
The instability still observed at quite high speed could be solved with different techniques: with the support of a forced anti-stagnation process or with the introduction a voltage loop for the flux weakening operation. In the first case, the update of the current variations is guaranteed by the application of unused vectors, in the second case the stagnation should be prevented by the continuous presence of variations with opposite signs. Unfortunately, the criteria chosen for the individuation of the flux weakening regime (the sign of the current variation) is verified also in other conditions, as a consequence of current disturbs or prediction errors.
Actually, one of the most relevant weak point of all these Model Free solutions is the fact that they not exploit information of the rotor position for the predictions, even if it is measured in both the MF schemes. As a consequence of this statement, a further upgrade of the improved Model Free scheme could be the integration of the rotor position in the evaluation of the current predictions. This upgrade could be another method to prevent the instability due to the stagnation. In case of the adoption of a smart cost-function, the rotor position could be used to give an intrinsic anti-stagnation to a simple MF scheme.
In conclusion the improved Model Free scheme represents an advantageous alternative to the Model Based one, in all the conditions in which it does not manifest the instability.

Bibliography

[1] C. K. Lin, T. H. Liu, J. Yu, L. C. Fu, and C. F. Hsiao, "Model-free predictive current control for interior permanent-magnet synchronous motor drives based on current difference detection technique", *IEEE Transactions on Industrial Electronics*, vol. 61, no. 2, pp. 6667-681, Feb 2014

[2] C. K. Lin, J. Yu, Y. S. Lai, and H. C. Yu, "Improved model-free predictive current control for synchronous reluctance motor drives, *IEEE Transactions on Industrial Electronics*, vol. 63, no. 6, pp. 3942-3953, June 2016

[3] H. A. Young, M. A. Perez, and J. Rodriguez, "Analysis of finite-control-set model predictive current control with the model parameter mismatch in a three-phase inverter", *IEEE Transactions on Industrial Electronics*, vol. 63, no. 5, pp. 3100-3107, May 2016

[4] D. Da Rù, M. Morandin, S. Bolognani, and M. Castiello, "Model Predictive Hysteresis Current Control for wide speed operation of a Synchronous Reluctance machine drive", IECON 2016-42nd Annual Conference of the IEEE Industrial Electronics Society, 2016

[5] V. Manzolini, D. Da Rù, and S. Bolognani, "A new control strategy for high efficiency wide speed range synchronous reluctance motor drives", 2017 IEEE International Electric Machines and Drives Conference (IEMDC), 2017

[6] P. Cortes, J. Rodriguez, C. Silva, and A. Flores, "Delay compensation in model predictive current control of a three-phase inverter", *IEEE Transactions on Industrial Electronics*, vol. 59, no. 2, pp. 1323-1325, Feb 2012

[7] S. Bolognani, Appunti del corso di "Azionamenti elettrici", 2016

“Si ringrazia particolarmente:

I miei genitori, mia sorella e mio fratello per il sostegno totale che ho ricevuto nel corso di questi anni e per i valori che mi hanno trasmesso, che mi hanno aiutato a raggiungere questo traguardo.

Un grazie a tutti gli amici con cui ho avuto il piacere di condividere quest’esperienza per tutti i momenti felici trascorsi insieme e per tutto ciò che mi hanno insegnato.”